

JULIUS—MAXIMILIANS—UNIVERSITÄT WÜRZBURG

Institut für Theoretische Physik und Astronomie
Theoretische Physik II



A Supersymmetric Higgsless Model Of Electroweak Symmetry Breaking

Diploma thesis

by

Karoline Köpp

Supervised by Prof. Dr. Thorsten Ohl

31. 03. 2009

Zusammenfassung

Die vorliegende Diplomarbeit beschäftigt sich mit einem supersymmetrischen higgslosen Modell mit einer gekrümmten Extradimension. In Modellen mit kompakten zusätzlichen räumlichen Dimensionen kann die elektroschwache Eichsymmetrie ohne ein Higgs-Feld, wie es vom Standardmodell der Elementarteilchenphysik vorhergesagt wird, durch Randbedingungen gebrochen werden. Die Erforschung dieser Modellen stellt daher einen alternativen Zugang zum Verständnis der elektroschwachen Symmetriebrechung dar, deren zugrundeliegender Mechanismus bisher experimentell noch nicht bestimmt werden konnte.

Modelle mit einem exponentiell gekrümmten Randall-Sundrum Raumzeithintergrund, haben sich in den vergangenen Jahren als besonders vielversprechend erwiesen. In einer Erweiterung [1] des ursprünglichen Modells [2] werden gekrümmte Extradimensionen mit Supersymmetrie (SUSY) verbunden. Der Schwerpunkt dieser Arbeit liegt auf der Untersuchung einer neuen und vergleichsweise sanften Art der SUSY-Brechung auf einer getrennten infraroten „Brane“ in der neuen Dimension.

Die Arbeit ist wie folgt aufgebaut: Zunächst werden in Kapitel eins und zwei die notwendigen Grundlagen zu Extradimensionen und Supersymmetrie besprochen, um das Modell im dritten Kapitel einführen zu können. Der Aufbau des Modells auf zwei „back-to-back“ Intervallen und das resultierende Massenspektrum bilden den Ausgangspunkt für alle weiteren Untersuchungen. Die konkrete Wahl der Randbedingungen und Modellparameter wird in den anschließenden Kapiteln vier und fünf für den Eich- und den Materiesektor getrennt diskutiert und konkret begründet. Wir untersuchen die Kaluza-Klein Wellenfunktionen und geben Näherungslösungen für die leichtesten Moden des Spektrums an. Zusätzlich zu den Standardmodellteilchen (mit Ausnahme des Higgs) enthält unser Modell supersymmetrische Teilchen. In unserem Setup ist das Neutralino mit einer Masse von 80 – 95 GeV das leichtesteste supersymmetrische Teilchen (LSP). Als Folge der SUSY Brechung auf einer separaten infraroten Brane sind im Materiesektor supersymmetrische Teilchen mit geringeren Massen als der typischen Skala der Kaluza-Klein-Anregungen von ungefähr 1 TeV möglich. Prinzipiell könnten daher auch die Sneutrinos als alternative LSP Kandidaten dienen.

In Kapitel sechs berechnen wir die elektroschwachen Präzisionsobservablen S und T und weisen nach, dass realistische Werte für diese Parameter im Rahmen unseres Modells möglich sind. In extradimensionalen Modellen ist die Masse eines Teilchens mit einer geometrischen Interpretation verbunden. Konkret bestimmt die Krümmung der Kaluza-Klein Wellenfunktion in dem zusätzlichen räumlichen Intervall die Masse eines Teilchens. Um das schwere Top Quark zu reproduzieren, müssen sich die Kaluza-Klein Funktionen der dritten Quarkgeneration stark von denen der leichten Fermionen unterscheiden, was effektiv zu einer Abweichung der Kopplung führt. Im siebten Kapitel gehen wir auf dieses sogenannte $Zb_l\bar{b}_l$ Problem ein. Es lässt sich lösen, indem man die dritte Quarkgeneration in eine erweiterte Repräsentation der $SU(2)$ einbettet, sodass die Kopplung durch Symmetrien geschützt ist. In Kapitel acht untersuchen wir die Eignung des Neutralino LSP als Kandidat für dunkle Materie. Wir finden, dass die Reliktdichte sehr empfindlich von der Neutralinomasse abhängt und mit dem experimentell bestimmten Wert nur für Neutralinos kurz oberhalb der W -Masse reproduziert werden kann. Als Abschluss diskutieren wir im neunten Kapitel mögliche Collidersignaturen des skalaren Σ_0 Teilchens.

Contents

Introduction	1
1 Extra dimensions	3
1.1 Motivation	3
1.2 Flat extra dimensions	3
1.2.1 Kaluza-Klein decomposition	3
1.2.2 Nonrenormalizability	4
1.2.3 Fields in extra dimensions	4
1.3 Boundary conditions	6
1.3.1 Coupled boundary conditions	6
1.3.2 Brane localized terms	7
1.4 Warped extra dimensions	7
1.4.1 The Randall-Sundrum metric	8
1.4.2 Warped spacetime	8
1.4.3 Spinor fields in warped space	10
1.4.4 Gauge fields in warped space	11
1.4.5 Scalar fields in warped space	11
2 Supersymmetry in 5D warped space	13
2.1 A brief introduction to 4D SUSY	13
2.1.1 Supersymmetric algebra	13
2.1.2 Superfields	14
2.1.3 SUSY Lagrangian	16
2.2 Supersymmetry in extra dimensions	18
2.2.1 Flat 5D SUSY	18
2.2.2 Warped 5D SUSY	19
3 The model	21
3.1 Principles	21
3.1.1 Higgsless electroweak symmetry breaking	21
3.1.2 Unitarity in higgsless models	22
3.1.3 SUSY breaking on a new IR brane	22
3.1.4 Two AdS ₅ Slices	23
3.1.5 Twisted Boundary Conditions	24
3.2 Setup	25
3.2.1 The Lagrangian	25
3.2.2 Field content	26
3.2.3 Boundary conditions	27
4 Gauge sector	30
4.1 Boundary conditions	30
4.1.1 Boundary conditions at the UV and the EWSB brane	30
4.1.2 SUSY breaking	31
4.1.3 Brane kinetic terms	32

4.2	Mass spectrum	32
4.2.1	Bosonic Kaluza-Klein wave functions	32
4.2.2	Gauge boson and chargino masses	33
4.2.3	Neutralino masses	34
4.3	Interactions	37
4.3.1	Gaugino interactions with gauge bosons	37
4.3.2	Neutralino interactions with matter	40
5	Fermions and sfermions	42
5.1	Implementation	42
5.2	Matter	42
5.2.1	Massless fermions	43
5.2.2	Massive fermions via Dirac mass terms	44
5.2.3	Mass splitting	45
5.2.4	Neutrinos	45
5.3	Smatter	46
5.3.1	Charged sfermions	46
5.3.2	Sneutrinos	48
5.4	Discussion of the spectrum	48
6	Electroweak precision observables	52
6.1	The Peskin-Takeuchi parameters S and T	52
6.2	Oblique corrections in the standard model	53
6.3	Tree level calculation of S and T parameter	55
6.4	Results	57
6.4.1	The S parameter without a brane kinetic term	57
6.4.2	The S parameter with a brane kinetic term	58
6.4.3	The T parameter	59
6.5	Discussion	61
7	The $Zb_l\bar{b}_l$ problem	63
7.1	Origin of the $Zb_l\bar{b}_l$ problem	63
7.2	An alternative representation of custodial symmetry	65
8	Dark matter	68
8.1	Calculation of the relic density	68
8.1.1	Annihilation	69
8.1.2	Coannihilation	70
8.2	Neutralino dark matter in our model	70
8.2.1	Annihilation	71
8.2.2	Coannihilation	73
9	Outlook: Collider signatures of a neutral scalar field	76
	Conclusion	81
A	Notation, conventions and abbreviations	83
A.1	Notations and conventions	83
A.2	Definitions and abbreviations	84

B	Fields	86
B.1	Overview	86
B.2	Gauge bosons	88
C	Boundary conditions	90
C.1	Boundary conditions for the two brane model	90
C.1.1	Boundary conditions for top and bottom quark in the enlarged representation	92
	Bibliography	93

Introduction

The standard model of elementary particles has certainly earned its current status by its astonishing experimental success. It has predicted W and Z bosons as well as gluons, the top and the charm quark before these particles were experimentally observed. Also, it is in agreement with remarkable accuracy with almost all presently available data. Including the hitherto experimentally unconfirmed Higgs boson, electroweak symmetry breaking is realized with the minimal additional field content of one scalar Higgs.

Despite the success of the standard model, there are strong indications that it is not complete. In particular, it offers no explanation for dark matter. Non-relativistic dark matter is by indirect experiments confirmed to contribute to the total energy density of the universe about four times more than ordinary baryonic matter. Another limitation is the still unanswered question for the mechanism of electroweak symmetry breaking (EWSB).

Obviously, there is the need for experimental evidence of the presence of the predicted Higgs boson. If a Higgs boson exists, it most probably will be detected at the LHC. However, the standard model mechanism is problematic to some extent. The catch phrase here is “hierarchy problem”: It is known that in order to incorporate gravity, physics at energy scales of the order of 10^{19} GeV has to be included into a complete theory. The problem is that a standard model Higgs field acquires quantum corrections which are quadratically divergent with the cutoff scale. If that cutoff is at the Planck scale, an incredibly finetuned counterterm would be required to keep it below the upper bound of $m_H = 1$ TeV, which is necessary to insure unitarity.

The problems of many theorists to accept an unexplained finetuning over nineteen digits is reflected by the number of alternative suggestions for EWSB mechanisms. Examples are large extra dimensions [3], Randall-Sundrum models [4], little Higgs [5], fat Higgs [6] and gauge extensions of the Minimal Supersymmetric Standard Model (MSSM) [7]. All these models feature a light Higgs field. Supersymmetry (SUSY) stands out for the mathematical significance of its algebra. The supersymmetric algebra is the only graded Lie algebra consistent with relativistic quantum field theory [8].

A more radical idea is, instead of taming quantum corrections, to completely abandon the concept of an elementary Higgs field breaking electroweak symmetry. The earliest representative of this class of models are technicolor (TC) [9] and its extensions (ETC) [10]. However, these models suffer from severe phenomenological problems concerning the realization of fermion masses and flavor changing neutral currents. A further completely higgsless approach to EWSB are extra dimensions. Especially models of warped extra dimensions with underlying Randall-Sundrum metric [4] have come into the focus of interest within the last years. The five dimensional spacetime with one compact extra dimension proposed by the authors of [4] is a slice of AdS_5 , which is on one hand a possible solution to Einstein equations with a cosmological constant and on the other hand interesting in the context of the AdS/CFT correspondence. The setup is such that the theory is weakly coupled and Kaluza-Klein excitations appear at scales within the reach of the LHC. The model is nonrenormalizable, but valid up to about 10 TeV. Electroweak symmetry can be broken by boundary conditions without a Higgs field in a way that preserves unitarity [11].

A first model including a matter sector with a realistic fermion spectrum, has been proposed in [2]. Combining higgsless EWSB with one of the most elegant idea of mathematical physics, a supersymmetric extension of the warped higgsless model was proposed in [1]. The main motivation was to furnish the model with a viable dark matter candidate. The nature of dark

matter is among the most pressing questions of elementary particle physics.

The non-trivial supersymmetric extension to 5D was realized with the minimal additional particle content. Analogous to electroweak symmetry breaking, SUSY breaking is done by boundary conditions. First calculations of LHC signals of this model have been carried out in [12]. However, the SUSY breaking in [1, 12] is located at the high energy brane which is a rather brute-force method. Moreover it is entangled with the $SU(2)_R \times U(1)_X \rightarrow U(1)_Y$ breaking, also located at the UV brane.

In this work, we want to test a more systematic way of supersymmetry breaking by constructing the model upon two AdS_5 slices. We have to introduce a couple of new parameters, but it turns out that most of these parameters, apart from the fermion localizations in the second interval, are either equivalent to parameters of the original setup with a single AdS_5 slice, or else unimportant for physical observables considered in this work.

The structure of this diploma thesis is as follows: We start by introducing extra dimensional field theory in chapter one and proceed to Supersymmetry in extra dimensions in the second chapter. These chapters focus on the concepts necessary for the extended supersymmetric higgsless model which will be presented in chapter three. Chapter four and five are dedicated to a detailed discussion of the gauge and the matter sector, explaining the assignment of boundary conditions and the mass spectrum of the model. We investigate the electroweak precision observables S and T in chapter six and show that our model passes these first tests of validity. In the following chapter we discuss the $Zb_l\bar{b}_l$ problem and a possible solution. In chapter eight we investigate the neutralino as possible dark matter candidate. Further on we discuss a possible light scalar particle Σ_0 appearing in the supersymmetric spectrum. We conclude this work summarizing our results.

1 Extra dimensions

In this chapter, we will discuss extra dimensions. Starting with the flat case, we will then proceed to warped extra dimensions, which are the foundation of the model investigated in this thesis.

1.1 Motivation

Kaluza and Klein were considering the possibility of extra dimensions already in 1921 [13] and 1926 [14]. This was only a couple of years after the centuries old concept of three dimensional Newtonian space had been replaced by the four dimensional Minkowski spacetime. Their main motivation was to unify electromagnetism with gravity. Later on, in the context of string theory, extra dimensions¹ entered the game again. In our case, extra dimensions are of interest because on one hand they can solve the problem of hierarchy and scales in a very elegant way [4]. On the other hand, they give a direct geometrical interpretation of quantities like mass and couplings, which in the 4D picture are merely parameters.

Obviously, if extra dimensions are present, they must be different from the four we observe. The reason why they are hidden could be for example that they are finite and sufficiently small to lie beyond the so far experimentally accessible energy range. Whether or not the presence of extra dimensions would be detectable does not only depend on the size of the extra dimension. For example, one could allow only a few particles to travel along the additional dimension.

Randall and Sundrum introduced an exponentially curved extra dimension in [4] and showed how the exponential can be used for explaining widely separated energy scales quite naturally.

In the following sections, we will discuss, using simple examples, the features of extra dimensions and the field theoretical approach to them.

1.2 Flat extra dimensions

Let us start with an additional flat spacetime coordinate confined to an interval $[0, \pi R]$. The new coordinate is embedded by defining

$$(x^\mu, y) = x^M \in \mathbb{R}^4 \times [0, \pi R], \quad (1.1)$$

where M runs over $0, 1, 2, 3, 5$. The flat 5D metric with one additional spacelike dimension reads $\eta_{MN} = \text{diag}(1, -1, -1, -1, -1)$. We will use $\mu, \nu = 0, 1, 2, 3$ when referring to 4D Lorenz indices.

1.2.1 Kaluza-Klein decomposition

Any field $\phi(x, y)$ is now a function of all 5 dimensions. We make the ansatz:

$$\phi(x, y) = \sum_{n=0}^{\infty} \phi^n(x) f^n(y), \quad (1.2)$$

¹And at least six of them.

because we know from Fourier analysis that, due to the compact interval, the y -dependence can be described by a complete, countably infinite tower of linearly independent functions $f^n(y)$. In the context of extra dimensions, the Fourier approach is called Kaluza-Klein (KK) decomposition. Throughout this work, we will refer to the $f^n(y)$ as KK functions. The 4D fields $\phi^n(x)$ will be called coefficient functions. The explicit form of the KK functions on the compact interval can be determined by the dynamics and boundary conditions on the branes which are limiting the extra dimension.

1.2.2 Nonrenormalizability

In five dimensions, the action reads $S = \int dx^5 \mathcal{L}$ instead of $S = \int dx^4 \mathcal{L}$. Therefore the 5D fields necessarily have a mass dimension $1/2$ higher than 4D fields. Consequently, operators which are renormalizable in four dimension become non-renormalizable in higher dimensions. To give an example, the familiar interaction $\bar{\Psi}A\Psi$ is of mass dimension 4 in the 4D theory but of dimension $5\ 1/2$ in the 5D theory. It has to be multiplied with $\Lambda_c^{-1/2}$, where Λ_c defines the relevant scale and is of mass dimension one. Therefore, the interaction is non-renormalizable.

In the following we will mostly integrate over the fifth dimension and consider the resulting effective 4D theory. In this picture, the resulting infinite tower of Fourier modes leads to an infinite number of corrections which cannot be absorbed with a finite number of counterterms. Thus, an extra dimensional model cannot describe the complete physics but has to be interpreted as an effective theory, valid only below a cutoff scale Λ_c .

1.2.3 Fields in extra dimensions

The generalization of the Lagrangian to 5D is straightforward. In the case of scalar fields, the derivatives ∂_μ are replaced by ∂_M . In the following, we will start with the simplest example of a scalar field and afterwards discuss gauge fields in a flat compact extra dimension. The treatment of spinor fields will be postponed until warped extra dimensions have been discussed.

Scalar field

The free action of a scalar field in 5D is

$$S = \frac{1}{2} \int d^4x \int_0^{\pi R} dy \partial_M \phi \partial^M \phi. \quad (1.3)$$

Using the KK expansion (1.2) and integration by parts, this can be written as

$$S = \frac{1}{2} \sum_{m,n} \int d^4x \left[\partial_\mu \phi^m \partial^\mu \phi^n \underbrace{\int_0^{\pi R} f^m f^n dy}_{\mathcal{Z}_{mn}} - \phi^m \phi^n \underbrace{\int_0^{\pi R} f^n \partial_5 \partial_5 f^m dy}_{\mathcal{M}_{mn}} + \phi^n \phi^m \cdot \underbrace{[f^m \partial_5 f^n]_0^{\pi R}}_{\mathcal{B}_{mn}} \right]. \quad (1.4)$$

We see that the scalar field, which is massless in the 5D picture, obtains a mass term \mathcal{M}_{nm} when integration over the extra dimension is performed. We define the operator $\hat{O} := \partial_5^2$ and choose the f^n to be orthogonal eigenfunctions satisfying

$$\hat{O} f^n = -m_n^2 f^n. \quad (1.5)$$

Canonical normalization is then obtained by rescaling the already orthogonal eigenfunctions such that

$$\mathcal{Z}_{mn} = \delta_{mn}.$$

Brane localized terms \mathcal{B} , arising from integration by parts, will modify the 5D dynamics via the equations of motion (e.o.m.) on the boundaries. To make the action (1.4) independent of these terms, it is necessary to choose boundary conditions such that \mathcal{B}_{mn} vanishes for all m, n . In this case we say the boundary conditions are compatible with the variation of the action.

Once compatible boundary conditions on both ends of the interval have been imposed, the differential equation (1.5) can be solved leading to the explicit expressions for the tower of KK functions.

Gauge field

For gauge fields some specific subtleties regarding gauge fixing arise, which are worthwhile to discuss. We will at first constrain ourselves to the abelian case. The generalization to the non-abelian case is straightforward. In five dimensions, the gauge action can be rewritten as

$$S_{4D} = -\frac{1}{4} \int d^4x F_{\mu\nu} F^{\mu\nu} \quad \rightarrow \quad S_{5D} = -\frac{1}{4} \int d^5x F_{MN} F^{MN}. \quad (1.6)$$

For brevity we used $\int d^5x$ instead of the more explicit $\int d^4x \int_0^{\pi R} dy$.

Due to the extra dimension, the 5D vector field gains an additional component A_5 . The KK expansion reads:

$$\begin{aligned} A_\mu(x, y) &= \sum_n A_\mu^n(x) f^n(y) \\ A_5(x, y) &= \sum_k A_5^k(x) g^k(y) \end{aligned} \quad (1.7)$$

To expand the parts containing this additional field we rewrite the action as

$$S = -\frac{1}{4} \int d^5x (F_{\mu\nu} F^{\mu\nu} + 2\partial_\mu A_5 \partial_\mu A^5 + 2\partial_5 A_\mu \partial^5 A^\mu - 4\partial_5 A^\mu \partial^\mu A^5). \quad (1.8)$$

Variation with respect to A_5 leads to the equation of motion

$$\square A_5^k(x) \cdot g^k(y) - \partial_\mu A^{\mu, k}(x) \cdot \partial_5 f^k(y) = 0, \quad (1.9)$$

where we have used the separation ansatz of (1.2) and orthogonality of the mass eigenfunctions. In order to satisfy this equation, we require

$$\partial_5 f^k(y) = g^k(y). \quad (1.10)$$

As f^k and g^k are both eigenfunctions to \hat{O} , it is straightforward to show that their eigenvalue spectrum is identical. In the case of $m_n = 0$, either $f^k(y)$ or $g^k(y)$ vanishes, while the other takes a constant value.

To avoid the last term in (1.8) which mixes A_μ and A_5 , we choose the gauge fixing:

$$\mathcal{L}_{gf} = -\frac{1}{2\xi} (\partial_\mu A^\mu + \xi \partial_5 A^5)^2 \quad (1.11)$$

Since the extra dimension is compact and the Minkowski space is not, in principle there is no symmetry under 5D Lorentz transformations. This is also reflected in the different KK

expansions. So we lose nothing by choosing a gauge fixing term where the fifth component of the gauge fields is explicitly treated in a different way than the other four. As combined action of (1.8) and (1.11) we finally obtain

$$\begin{aligned}
 S &= \int d^5x \left[\frac{1}{2} A_\mu \left(\square g^{\mu\nu} - \left(1 - \frac{1}{\xi}\right) \partial^\mu \partial^\nu - \partial_5 \partial_5 \eta^{\mu\nu} \right) A_\nu - \frac{1}{2} A_5 \left(\square - \xi \partial_5 \partial_5 \right) A_5 \right] \\
 &= \int d^5x \sum_n \left[\frac{1}{2} A_\mu^n \left((\square + m_n^2) \eta^{\mu\nu} - \left(1 - \frac{1}{\xi}\right) \partial^\mu \partial^\nu \right) A_\nu^n \right. \\
 &\quad \left. - \sum_k \frac{1}{2} A_5^k \left(\square + \xi \tilde{m}_k^2 \right) A_5^k \right],
 \end{aligned} \tag{1.12}$$

where we have assumed canonical normalization and vanishing boundary action. We identify this as the action of a tower of vector fields A_μ^n with masses m_n and another tower of scalar fields A_5^n with masses $\sqrt{\xi} \tilde{m}_k$. As we have discussed above, $m_n = \tilde{m}_n$ is satisfied because the gauge fields are connected by equations of motion. Thus, the unphysical part in the gauge propagator of A_μ cancels with the scalar contribution of A_5 , analogous to the cancellations with the Goldstone bosons in the SM.

1.3 Boundary conditions

In extra dimensional models the masses of 4D fields stem, like in (1.4), from integrals over ∂_5 derivatives which we name \mathcal{M} . Therefore, masses are determined by the form of the KK functions, which in turn are fixed by imposing boundary conditions. In particular, massless fields require $\mathcal{M} = 0$ and therefore have flat KK wave functions.

First of all, boundary conditions should of course be chosen to be compatible with the symmetries imposed on the Lagrangian for physical reasons. Additionally, the conditions have to be assigned in a way that the boundary action term, stemming from integration by parts, vanishes in the variation. As can be seen in (1.4), the resulting boundary action \mathcal{B} is of the general form $f \partial_5 f$. For a single field the simplest solution is to impose either

$$\begin{array}{ll}
 \text{a Neumann} & \partial_5 f(y)|_{y=0, \pi R} = 0 \\
 \text{or a Dirichlet} & f(y)|_{y=0, \pi R} = 0
 \end{array}$$

boundary condition. In the case of Dirichlet boundary conditions the flat KK functions of massless fields have to be zero in the entire extradimensional interval such that the corresponding field is removed from the theory. In contrast, Neumann boundary conditions allow massless solutions.

1.3.1 Coupled boundary conditions

In the case of coupled boundary conditions only the sum of boundary action terms has to vanish and not the individual parts. Assume for instance that symmetries allow a coupled boundary condition:

$$A_L - A_R|_{y=y_0} = 0 \tag{1.13}$$

As the boundary condition has to be satisfied at all spacetime points x^μ , the coefficient functions have to be identical

$$A_L^{(k)}(x) = A_R^{(k)}(x) =: A^{(k)}(x), \tag{1.14}$$

and (1.13) reduces to the condition

$$f_R^{(k)}(y_0) = f_L^{(k)}(y_0). \tag{1.15}$$

The brane localized action from integration by parts is:

$$\begin{aligned} \mathcal{B} &= A_L \partial_5 A_L + A_R \partial_5 A_R \stackrel{(1.14)}{=} A^2(x) \left(f_L(y_0) f'_L(y_0) + f_R(y_0) f'_R(y_0) \right) \\ &\stackrel{(1.15)}{=} A^2(x) f_L(y_0) \left(f'_L(y_0) + f'_R(y_0) \right) \end{aligned} \quad (1.16)$$

To make it vanish, the second boundary condition on that brane has to be $f'_L(y_0) = -f'_R(y_0)$. A very elegant method for solving a system of fields coupled by boundary conditions at an arbitrary number of branes, using a matrix mechanism, has been developed by A. Knochel [15].

In the case of fields connected by equations of motion (e.o.m.), like e. g. $A_\mu = A_\mu(x)f(y)$ and $A_5 = A_5(x)g(y)$, the boundary conditions for one field automatically determine the boundary conditions for the other field. As we have discussed, $\partial_5 f^k(y) = g^k(y)$ is required by the e.o.m. for all y . So when we assign a Neumann boundary condition to a A_μ field, for consistency A_5 has to be assigned a Dirichlet boundary condition and vice versa.

1.3.2 Brane localized terms

A possibility to modify boundary conditions and therefore the corresponding mass spectrum and couplings are brane localized terms. These are additional local contributions to the Lagrangian added at $y = y_0$, where y_0 is the position of a brane limiting the extradimensional interval. Generally one distinguishes between localized mass terms of the form

$$\mathcal{L}_{y_0, \text{mass}} = \frac{1}{2} M_{ij} \phi_i \phi_j \delta(y - y_0)$$

and kinetic terms with the structure

$$\mathcal{L}_{y_0, \text{kin}} = \kappa \partial_\mu \phi \partial^\mu \phi \delta(y - y_0).$$

In the e.o.m., localized terms lead to an additional contribution proportional to $\delta(y - y_0)$. This causes a discontinuity of either ϕ or ϕ' , thus modifying either the Dirichlet or the Neumann boundary condition.

1.4 Warped extra dimensions

After this warm-up, let us proceed to warped extra dimensions. It turns out that models of warped extra dimensions have attractive phenomenological properties that flat extra dimensions cannot provide.

As before in the case of flat extra dimensions, the Lorentz indices running over 0, 1, 2, 3, 5 will be named M, N and the ones going 0, 1, 2, 3 are named μ, ν . To distinguish warped and flat objects it will be sufficient to explicitly refer to the warped Randall-Sundrum metric as g_{MN} and to the flat 5D Minkowski metric as η_{MN} . The corresponding 4×4 subtensors are $g_{\mu\nu}$ and $\eta_{\mu\nu}$. Similarly, we will denote the warped Dirac matrices $\hat{\gamma}^M$ ($\hat{\gamma}^\mu$) and the flat ones γ^M (γ^μ).

1.4.1 The Randall-Sundrum metric

The most promising realization of a warped space known today was proposed by Randall and Sundrum in 1999 [4]. They introduced an exponentially curved background metric:

$$g_{MN} = \begin{pmatrix} e^{-2Rky} & 0 & 0 & 0 & 0 \\ 0 & -e^{-2Rky} & 0 & 0 & 0 \\ 0 & 0 & -e^{-2Rky} & 0 & 0 \\ 0 & 0 & 0 & -e^{-2Rky} & 0 \\ 0 & 0 & 0 & 0 & -R^2 \end{pmatrix} \quad (1.17)$$

The parameter k denotes the curvature and Rk the size of the extra dimension. The exponential is the key to solve the problem of widely separated scales. A Planck scale mass of $M_{\text{pl}} \approx 10^{19}$ GeV, located at $y = 0$, will be weighted by a factor of $e^{-Rk\pi}$ at the other end of the extradimensional interval, $y = \pi$. So, when $Rk\pi$ is chosen appropriately ($Rk\pi \approx 37$), the Planck mass parameter is “redshifted” to the TeV scale. The warped spacetime described by (1.17) is a slice of AdS_5 . Randall and Sundrum showed that such a slice with two branes and suitable cosmological constants is a solution to Einstein equations with a cosmological constant in 5D. The AdS_5 slice is especially interesting because of the AdS/CFT correspondence [16]. The correspondence establishes a relation between the Randall-Sundrum (RS) extradimensional setup and conformal field theories, where symmetry is dynamically broken by strong interaction.

1.4.2 Warped spacetime

For clarity, in this subsection we will introduce additional Lorentz indices a, b running over $0, 1, 2, 3, 5$. While the Riemann indices M, N denote the warped spacetime coordinates, a, b explicitly refer to flat coordinates.

When leaving the usual flat spacetime, we need to define what is meant by covariant derivative in curved spacetime and generally understand how the underlying metric affects the fields living on it. On an arbitrary manifold, one can define a tangent space at each point spanned by orthonormal vectors.

In general, it is not possible to compare vectors at two points of the manifold, because they are elements of two different tangent spaces. To define the covariant derivative, one requires a map which defines the connection between corresponding tangential spaces. The generators of the parallel transport of a vector from one spacetime point to another are the Christoffel symbols Γ_{MN}^P . Using the Christoffel symbols, one can define the covariant derivative of a vector A_N by

$$D_M A_N \equiv \partial_M A_N - \Gamma_{MN}^P A_P, \quad (1.18)$$

where, in addition to the usual $\partial_M A_N$, we take parallel transport into account as well. Parallel transport has to fulfill metricity:

$$D_M g_{NP} = \partial_M g_{NP} - \Gamma_{MN}^Q g_{QP} - \Gamma_{MP}^Q g_{NQ} = 0 \quad (1.19)$$

It also has to be symmetric, i.e. torsion-free:

$$\Gamma_{MN}^P - \Gamma_{NM}^P = 0 \quad (1.20)$$

These two requirements lead to the recipe how the Christoffel symbols are derived from the metric, given by

$$\Gamma_{MN}^P \equiv \frac{1}{2} g^{PL} (\partial_M g_{NL} + \partial_N g_{ML} - \partial_L g_{MN}). \quad (1.21)$$

To be in agreement with general relativity, our theory needs to be invariant under general coordinate transformations (diffeomorphisms). Thus, we need to quantify how diffeomorphisms act on the fields. This is trivial for scalar fields and we also know that the behavior of vector fields under a general coordinate transformation is described by the usual Jacobian. It is not so intuitive to define how spinor fields transform.

However, since our spacetime locally has Minkowski metric, we can go into the local Lorentz-frame, where we are familiar with spinors. We define as orthogonal basis vectors the vielbeins e_N^a . These connect the local Minkowski metric η_{ab} with the warped metric tensor g_{MN} through

$$g_{MN} = \eta_{ab} e_N^a e_M^b. \quad (1.22)$$

Note that this expression is invariant under local Lorentz transformations acting on a, b . Now, a spinor should be independent of the specific choice of the local Lorentz-frame. This is equivalent to requiring local gauge invariance, and so the covariant derivative reads

$$D_M \Psi_i = \partial_M \Psi_i + \omega_{M i}^j \Psi_j. \quad (1.23)$$

The gauge field for the Lorentz group, ω_M , is called the spin connection. As in the case of the Christoffel symbol, consistency arguments determine how it is derived from the underlying metric. By requiring

$$D_M e_N^a = \partial_M e_N^a + \Gamma_{MN}^L e_L^a + \omega_{M b}^a e_N^b = 0, \quad (1.24)$$

we find

$$\omega_{M b}^a = e_N^a e_b^P \Gamma_{MP}^N - (\partial_M e_N^a) e_b^N. \quad (1.25)$$

We see that in flat spacetime, where the vielbeins e_N^a are constant, the spin connection vanishes. One can check that

$$D_M \gamma_{ij}^N = \partial_M \gamma_{ij}^N + \Gamma_{ML}^N \gamma_{ij}^L + \omega_{M i}^k \gamma_{kj}^N + \omega_{M j}^k \gamma_{ik}^N = 0 \quad (1.26)$$

is satisfied.

The $\omega_{M ij}$ carrying spinor indices are related to the $\omega_{M ab}$ via the Lorentz generators by

$$\omega_{M ij} = -\frac{i}{4} \omega_{M ab} \Lambda_{ij}^{ab} = -\frac{i}{4} \omega_{M ab} \frac{i}{2} [\gamma^a, \gamma^b]_{ij}. \quad (1.27)$$

In the case of the RS metric (1.17) we use μ, ν and an explicit fifth coordinate. The only nonvanishing Christoffel symbols are

$$\Gamma_{\mu\nu}^5 = -\frac{k}{R} g_{\mu\nu} \quad \text{and} \quad \Gamma_{5\nu}^\mu = \Gamma_{\mu 5}^\nu = -Rk \delta_N^M. \quad (1.28)$$

The fünfbeins are given by

$$e_\mu^a = e^{-Rky} \delta_\mu^a, \quad e_{\bar{5}}^5 = R, \quad (1.29)$$

$$e_a^\mu = e^{Rky} \delta_a^\mu, \quad e_{\bar{5}}^5 = 1/R, \quad (1.30)$$

where we have denoted the index of the flat fifth component with a bar. There are two non-vanishing spin connection coefficients

$$\omega_{\mu \bar{5} a} = -\omega_{\mu a \bar{5}} = k e^{-Rky} \eta_{\mu\nu} \delta_a^\nu, \quad (1.31)$$

hence the spin connection corresponding to the Randall-Sundrum metric is

$$\omega_{\mu ij} = -\frac{1}{8} k e^{-Rky} \eta_{\mu\nu} \delta_a^\nu ([\gamma^{\bar{5}}, \gamma^a]_{ij} - [\gamma^a, \gamma^{\bar{5}}]_{ij}) = \frac{1}{2} k e^{-Rky} \eta_{\mu\nu} \gamma^{\bar{5}} \gamma^a. \quad (1.32)$$

1.4.3 Spinor fields in warped space

Fermions in five dimensional spacetime form representations of the 5D Lorentz group. The smallest irreducible representation is a Dirac fermion with four components, while in the usual 4 dimensions the smallest representation of the 4D Lorentz group is a Weyl fermion with two components. The 5D action of a fermion is:

$$S = \int dx^5 \sqrt{g} \left[\frac{i}{2} (\bar{\Psi} \hat{\gamma}^M (D_M \Psi) - (D_M \bar{\Psi}) \hat{\gamma}^M \Psi) - M_{\text{bulk}} \bar{\Psi} \Psi \right] \quad (1.33)$$

To make the action diffeomorphism-invariant, it always has to be equipped with a factor $\sqrt{g} := \sqrt{\det g}$ which is $\sqrt{g} = R e^{-4Rky}$ for the RS metric.

It can be checked using (1.19) and (1.26), that by performing integration by parts we can rewrite (1.33) as

$$S = \int dx^5 \sqrt{g} \bar{\Psi} [i \hat{\gamma}^M D_M - M_{\text{bulk}}] \Psi + \underbrace{\left[\int dx^4 \sqrt{g} \bar{\Psi} \hat{\gamma}^M \Psi \right]_0^\pi}_{\mathcal{B}}. \quad (1.34)$$

With

$$\bar{\Psi} \hat{\gamma}^M D_M \Psi = \bar{\Psi} \left[e^{Rky} \gamma^\mu \partial_\mu + \gamma^5 \frac{\partial_5 - 2Rk}{R} \right] \Psi \quad (1.35)$$

and expressing the bulk mass in units of the RS curvature $c := M_{\text{bulk}}/k$, the fermionic action up to boundary terms is:

$$\int dx^5 \sqrt{g} \bar{\Psi} \left[i e^{Rky} \gamma^\mu \partial_\mu + \frac{1}{R} \begin{pmatrix} -\partial_5 + (2-c)Rk & \\ & \partial_5 - (2+c)Rk \end{pmatrix} \right] \Psi \quad (1.36)$$

Writing $\Psi = (\eta, \bar{\chi})^T$ in components, we obtain the equations of motion

$$\begin{aligned} -e^{Rky} i \bar{\sigma}^\mu \partial_\mu \eta + \frac{\partial_5 - (2+c)Rk}{R} \bar{\chi} &= 0 \\ \text{and} \quad -e^{Rky} i \sigma^\mu \partial_\mu \bar{\chi} + \frac{-\partial_5 + (2-c)Rk}{R} \eta &= 0. \end{aligned} \quad (1.37)$$

Using KK decomposition

$$\Psi = \begin{pmatrix} \sum_n \eta^n(x) f_\eta^n(y) \\ \sum_n \bar{\chi}^n(x) f_\chi^n(y) \end{pmatrix}$$

and the 4D e.o.m.

$$\begin{aligned} i \bar{\sigma}^\mu \partial_\mu \eta^n - m_n \bar{\chi}^n &= 0, \\ i \sigma^\mu \partial_\mu \bar{\chi}^n - m_n \eta^n &= 0, \end{aligned} \quad (1.38)$$

this leads to the coupled equations for the KK functions:

$$\begin{aligned} -e^{Rky} m_n f_\eta^n + \frac{1}{R} (\partial_5 - (2+c)Rk) f_\chi^n &= 0 \\ -e^{Rky} m_n f_\chi^n + \frac{1}{R} (-\partial_5 + (2-c)Rk) f_\eta^n &= 0 \end{aligned} \quad (1.39)$$

Writing down the derivatives of (1.39) and plugging in the equations themselves again, one obtains the decoupled differential equations

$$\begin{aligned} \left(\frac{\partial_5^2}{R^2} - 5k \frac{\partial_5}{R} + (m_n^2 e^{2Rky} - (c^2 + c - 6)k^2) \right) f_\eta^n &= 0, \\ \left(\frac{\partial_5^2}{R^2} - 5k \frac{\partial_5}{R} + (m_n^2 e^{2Rky} - (c^2 - c - 6)k^2) \right) f_\chi^n &= 0. \end{aligned} \quad (1.40)$$

The solutions are

$$\begin{aligned} f_\eta^n(y) &= e^{5Rky/2} \left[a_n J_{c+1/2} \left(\frac{m_n}{k} e^{Rky} \right) + b_n Y_{c+1/2} \left(\frac{m_n}{k} e^{Rky} \right) \right], \\ f_\chi^n(y) &= e^{5Rky/2} \left[a_n J_{c-1/2} \left(\frac{m_n}{k} e^{Rky} \right) + b_n Y_{c-1/2} \left(\frac{m_n}{k} e^{Rky} \right) \right] \end{aligned} \quad (1.41)$$

where J_i and Y_i are the Bessel functions.

1.4.4 Gauge fields in warped space

In warped spacetime, the action (1.8) is replaced by

$$\begin{aligned} S &= \int dx^5 \sqrt{g} \left[-\frac{1}{4} g^{MN} g^{OP} F_{MO} F_{NP} \right] \\ &= \int dx^5 R \left[-\frac{1}{4} \eta^{\mu\nu} \eta^{\omega\rho} F_{\mu\omega} F_{\nu\rho} + \frac{1}{2R^2} e^{-2Rky} \eta^{\mu\nu} F_{\mu 5} F_{\nu 5} \right] \end{aligned} \quad (1.42)$$

and the gauge fixing (1.11) in warped space reads

$$S_{gf} = - \int dx^5 \frac{R}{2\xi} \left(\eta^{\mu\nu} \partial_\mu A_\nu - \xi \frac{e^{-2Rky}}{R} (\partial_5 - 2Rk) A_5 \right)^2. \quad (1.43)$$

By variation we obtain the equation of motion:

$$\square A_\mu - \left(1 - \frac{1}{\xi} \right) \partial_\mu \partial_\nu A^\nu - \frac{e^{-2Rky}}{R^2} (\partial_5 - 2Rk) \partial_5 A_\mu = 0. \quad (1.44)$$

Making use of the KK decomposition (1.7) and the usual 4D e.o.m.

$$\square A_{\mu,n} - \left(1 - \frac{1}{\xi} \right) \partial_\mu \partial_\nu A_n^\nu = -m_n^2 A_{\mu,n}, \quad (1.45)$$

we end up with the differential equation

$$\frac{e^{-2Rky}}{R^2} (\partial_5^2 f^n - 2Rk \partial_5 f^n) + m_n^2 f^n = 0. \quad (1.46)$$

Again, the solutions are combinations of Bessel functions

$$f^n(y) = e^{Rky} \left[a_n J_1 \left(\frac{m_n}{k} e^{Rky} \right) + b_n Y_1 \left(\frac{m_n}{k} e^{Rky} \right) \right]. \quad (1.47)$$

1.4.5 Scalar fields in warped space

The Lagrangian of a scalar field on a RS background is:

$$\begin{aligned} \mathcal{L} &= \frac{1}{2} \int dy \sqrt{g} \left[g^{MN} \partial_N \phi \partial_M \phi - M_{\text{bulk}}^2 \phi^2 \right] \\ &= -\frac{1}{2} \int dy \sqrt{g} \left[e^{2Rky} \phi \square \phi - \phi \left(\frac{\partial_5^2}{R^2} - 4k \frac{\partial_5}{R} - M_{\text{bulk}}^2 \right) \phi \right] + \underbrace{\frac{1}{2} \left[-\frac{e^{-4Rky}}{R} \phi \partial_5 \phi \right]_0^\pi}_{\mathcal{B}} \end{aligned} \quad (1.48)$$

Using KK decomposition (1.2) and $\square\phi^n = -m_n^2\phi^n$, we find

$$f^n(y) = e^{2Rky} \left[a_n J_{\sqrt{4+(M_{\text{bulk}}/k)^2}} \left(\frac{m_n}{k} e^{Rky} \right) + b_n Y_{\sqrt{4+(M_{\text{bulk}}/k)^2}} \left(\frac{m_n}{k} e^{Rky} \right) \right]. \quad (1.49)$$

The correct bulk mass term will be determined by the respective supersymmetric partner fields.

2 Supersymmetry in 5D warped space

Supersymmetry (SUSY) is probably the best investigated theory of physics beyond the standard model. It postulates a relationship between elementary particles of different quantum nature, bosons and fermions, and nontrivially links spacetime and internal symmetries. Supersymmetry was first discovered around 1970/71. Then in 1973, J. Wess and B. Zumino extended the two-dimensional Supersymmetry discovered in string theory to four dimensional field theories and thus laid the foundation for supersymmetric models of elementary particles. The Wess-Zumino model proposed in 1974 is still popular as toy model to understand properties of supersymmetric field theory. H. Georgi and S. Dimopoulos finally constructed the first realistic supersymmetric version of the standard model in 1981, the minimal supersymmetric standard model (MSSM). Since in this model supersymmetric particles are expected in the mass range of 100 GeV to 1 TeV, there is a good chance that, if Supersymmetry is realized in nature, the LHC will find the first experimental signs of these particles. Supersymmetry provides a solution of the hierarchy problem, which is based on cancellation of divergencies between loops containing standard model particles and the according graphs containing their supersymmetric partners. It also offers stable dark matter candidates as required by cosmology.

The most general Lie algebra of symmetries of the S-Matrix consistent with relativistic quantum field theory is constrained by the powerful no-go theorem of Coleman and Mandula. The Coleman-Mandula theorem is relaxed somehow by the generalization of Lie algebras to graded Lie algebras, including anticommutators $\{, \}$ in addition to the usual commutator $[,]$. A graded Lie algebra schematically takes the form:

$$\{Q, Q'\} = X, \quad [X, X'] = X'', \quad [Q, X] = Q'' \quad (2.1)$$

where Q, Q' and Q'' represent the anticommuting or odd part of the algebra and X, X' and X'' the commuting (even) part.

Haag, Sohnius and Lopuszanski proved that of all graded Lie algebras, only the Supersymmetry algebras generate symmetries of the S-matrix consistent with relativistic quantum field theory [8].

2.1 A brief introduction to 4D SUSY

In this section the basics of superfields in the usual 4 dimensional flat space will be briefly introduced. This should serve to fix the notation before discussing SUSY in warped 5D spacetime. A comprehensive and detailed description of constructing a supersymmetric field theory can be found in [17].

2.1.1 Supersymmetric algebra

In addition to the well-known Poincaré algebra, defined by

$$[P_\mu, P_\nu] = 0 \quad (2.2)$$

$$[M^{\mu\nu}, M^{\rho\sigma}] = i(g^{\mu\rho}M^{\mu\sigma} - g^{\mu\sigma}M^{\nu\rho} - g^{\mu\rho}M^{\nu\sigma} - g^{\nu\sigma}M^{\mu\rho}) \quad (2.3)$$

$$[M^{\mu\nu}, P^\rho] = i(g^{\nu\rho}P^\mu - g^{\mu\rho}P^\nu) \quad (2.4)$$

the most general supersymmetric algebra contains:

$$\begin{aligned}
 [P_\mu, Q_\alpha^L] &= [P_\mu, \bar{Q}_{\dot{\alpha}L}] = 0 \\
 [P_\mu, B_l] &= [P_\mu, X^{\widehat{LM}}] = 0 \\
 \{Q_\alpha^L, \bar{Q}_{\dot{\alpha}M}\} &= -2\sigma_{\alpha\dot{\alpha}}^\mu P_\mu \delta_M^L, \\
 \{Q_\alpha^L, Q_\beta^M\} &= \varepsilon_{\alpha\beta} X^{\widehat{LM}} \\
 \{\bar{Q}_{\dot{\alpha}L}, \bar{Q}_{\dot{\beta}M}\} &= \varepsilon_{\dot{\alpha}\dot{\beta}} X_{\widehat{LM}}^+, \\
 [X^{\widehat{LM}}, \bar{Q}_{\dot{\alpha}K}] &= [X^{\widehat{LM}}, Q_\alpha^K] = 0 \\
 [X^{\widehat{LM}}, X^{\widehat{KN}}] &= [X^{\widehat{LM}}, B_l] = 0 \\
 [B_\mu, B_\nu] &= ic_{\mu\nu}^\rho B_\rho \\
 [Q_\alpha^L, B_\mu] &= S_{\mu M}^L Q_\alpha^M \\
 [\bar{Q}_{\dot{\alpha}L}, B^\mu] &= -S^{*\mu M} \bar{Q}_{\dot{\alpha}M} \\
 X^{\widehat{LM}} &= a^{\mu, \widehat{LM}} B_\mu
 \end{aligned} \tag{2.5}$$

Q_α^L is the SUSY generator. Greek indices α, β denote two-component Weyl spinors and take the values 1, 2. Capital letters L, M correspond to an inner space and run from 1 to \mathcal{N} . SUSY algebras with $\mathcal{N} > 1$ are called extended SUSY algebras.

According to the Coleman-Mandula theorem all even generators are either part of the Poincaré algebra $\mathcal{P} = \text{span}(P_\mu, M_{\mu\nu})$ or belong to a compact Lie algebra \mathcal{A} . \mathcal{A} is the direct sum of a semisimple Lie algebra \mathcal{A}_1 and an abelian Lie algebra \mathcal{A}_2 . Thus, B_μ is a scalar Lorentz operator from $\mathcal{A}_1 \oplus \mathcal{A}_2$. $X^{\widehat{LM}}$ is called central charge. The hat on the indices indicates antisymmetry: $X^{\widehat{LM}} = -X^{\widehat{ML}}$. It can be showed that $X^{\widehat{LM}} \in \mathcal{A}_2$ and that central charges, if present, must be of the form $X^{\widehat{LM}} = a^{\mu, \widehat{LM}} B_\mu$. The a^μ are the ‘‘intertwiners’’ between the representations S_μ and $-S^{*\mu}$. $S_{\mu M}^L$ is a hermitian matrix from $\mathcal{A}_1 \oplus \mathcal{A}_2$.

2.1.2 Superfields

Introducing anticommuting Grassmann parameters ξ , the SUSY algebra (2.5) can be rewritten in terms of commutators only. The $\mathcal{N} = 1$ SUSY algebra without central charges reads:

$$\begin{aligned}
 [\xi Q, \bar{\xi} \bar{Q}] &= -2\xi\sigma^\mu \bar{\xi} P_\mu \\
 [\xi Q, \xi Q] &= [\bar{\xi} \bar{Q}, \bar{\xi} \bar{Q}] = 0 \\
 [P^\mu, \xi Q] &= [P^\mu, \bar{\xi} \bar{Q}] = 0
 \end{aligned} \tag{2.6}$$

The infinitesimal SUSY transformation δ_ξ of a field A is defined as

$$\delta_\xi A = (\xi Q + \bar{\xi} \bar{Q})A. \tag{2.7}$$

From (2.6) it follows directly that the commutator of two SUSY transformations has to close irrespectively of the field

$$\begin{aligned}
 (\delta_\eta \delta_\xi - \delta_\xi \delta_\eta)A &= 2i(\eta\sigma^\mu \bar{\xi} - \xi\sigma^\mu \bar{\eta})\partial_\mu A \\
 \implies [\delta_\eta, \delta_\xi] &= -2(\eta\sigma^\mu \bar{\xi} - \xi\sigma^\mu \bar{\eta})P_\mu A.
 \end{aligned} \tag{2.8}$$

The group element of the SUSY algebra (2.6) is defined as

$$G(x^\mu, \theta, \bar{\theta}) = e^{i(x^\mu P_\mu + \theta Q + \bar{\theta} \bar{Q})}. \tag{2.9}$$

Using the Haussdorff formula it can be showed that

$$G(0, \xi, \bar{\xi})G(x^\mu, \theta, \bar{\theta}) = G(x^\mu + i\theta\sigma^\mu\bar{\xi} - i\xi\sigma^\mu\bar{\theta}, \theta + \xi, \bar{\theta} + \bar{\xi}).$$

The motion in the parameter space induced by multiplication of two group elements $g(\xi, \bar{\xi}) : (x^\mu, \theta, \bar{\theta}) \rightarrow (x^\mu + i\theta\sigma^\mu\bar{\xi} - i\xi\sigma^\mu\bar{\theta}, \theta + \xi, \bar{\theta} + \bar{\xi})$ can be generated by $\xi Q + \bar{\xi}\bar{Q}$. Hence, one finds the explicit differential operators Q and \bar{Q} :

$$\begin{aligned} Q_\alpha &= \frac{\partial}{\partial\theta^\alpha} + i\sigma_{\alpha\dot{\alpha}}^\mu \bar{\theta}^{\dot{\alpha}} \partial_\mu \\ \bar{Q}^{\dot{\alpha}} &= \frac{\partial}{\partial\bar{\theta}^{\dot{\alpha}}} + i\theta^\alpha \sigma_{\alpha\dot{\beta}}^\mu \epsilon^{\dot{\beta}\dot{\alpha}} \partial_\mu \end{aligned} \quad (2.10)$$

Considering right multiplication instead of left multiplication, we find the induced motion to be generated by the differential operators D and \bar{D} , which read:

$$\begin{aligned} D_\alpha &= \frac{\partial}{\partial\theta^\alpha} - i\sigma_{\alpha\dot{\alpha}}^\mu \bar{\theta}^{\dot{\alpha}} \partial_\mu \\ \bar{D}_{\dot{\alpha}} &= +\frac{\partial}{\partial\bar{\theta}^{\dot{\alpha}}} - i\theta^\alpha \sigma_{\alpha\dot{\alpha}}^\mu \partial_\mu \end{aligned}$$

By definition they satisfy the anticommutation relations

$$\begin{aligned} \{D_\alpha, \bar{D}_{\dot{\alpha}}\} &= -2i\sigma_{\alpha\dot{\alpha}}^\mu \partial_\mu, \\ \{D_\alpha, D_\beta\} &= \{\bar{D}_{\dot{\alpha}}, \bar{D}_{\dot{\beta}}\} = 0, \end{aligned} \quad (2.11)$$

and anticommute with Q

$$\{D_\alpha, Q_\beta\} = \{D_\alpha, \bar{Q}_{\dot{\beta}}\} = \{\bar{D}_{\dot{\alpha}}, Q_\beta\} = \{\bar{D}_{\dot{\alpha}}, \bar{Q}_{\dot{\beta}}\} = 0. \quad (2.12)$$

The general superfield F is a function of the superspace denoted by $z = (x, \theta, \bar{\theta})$ and can be written as a fourth order expansion in θ

$$F(x, \theta, \bar{\theta}) = f_1(x) + \theta f_2(x) + \dots + \theta\theta\bar{\theta}\bar{\theta} f_9(x). \quad (2.13)$$

Since Grassmann variables anticommute, all orders higher than $\theta\theta\bar{\theta}\bar{\theta}$ must vanish.

Superfields form linear representations of the Supersymmetry algebra. These representations are in general highly reducible. The problem to find supersymmetric representations is equivalent to find covariant constraints for the superfields, eliminating extra component fields.

Chiral superfields

Chiral superfields are defined by the constraint

$$\bar{D}_{\dot{\alpha}}\Phi = 0. \quad (2.14)$$

In the coordinates $y^\mu = x^\mu + i\theta\sigma^\mu\bar{\theta}$, the chiral multiplet takes a particularly simple form

$$\begin{aligned} \Phi &= \phi(x) + i\theta\sigma^\mu\bar{\theta}\partial_\mu\phi(x) - \frac{1}{4}\theta\theta\bar{\theta}\bar{\theta}\square\phi(x) + \sqrt{2}\theta\Psi(x) - \frac{i}{\sqrt{2}}\theta\theta\partial_\mu\Psi(x)\sigma^\mu\bar{\theta} + \theta\theta F(x) \\ &\stackrel{x\rightarrow y}{=} \phi(y) + \sqrt{2}\theta\Psi(y) + \theta\theta F(y). \end{aligned} \quad (2.15)$$

Vector superfields

The vector superfields are defined by another constraint

$$V = V^\dagger \quad (2.16)$$

Obviously, $V - (\Gamma + \Gamma^\dagger)$ is again a vector superfield for every superfield Γ . If Γ is a chiral field satisfying (2.14), one can explicitly write down the transformations induced by

$$V \rightarrow V - (\Gamma + \Gamma^\dagger) \quad (2.17)$$

on the component fields. One will find that the $\theta\sigma^\mu\bar{\theta}$ coefficient field A_μ transforms like

$$A_\mu \rightarrow A_\mu + i\partial_\mu(\phi - \phi^*) = A_\mu - 2\partial_\mu \text{Im}\phi.$$

The similarity to standard gauge transformation is the motivation to define (2.17) to be the supersymmetric generalization of a gauge transformation. In the Wess-Zumino gauge, all components affected by this gauge transformation, except of A_μ , are zero. Then we are left with

$$V = -\theta\sigma^\mu\bar{\theta}A_\mu + i\theta\theta\bar{\theta}\bar{\lambda} - i\bar{\theta}\bar{\theta}\theta\lambda + \frac{1}{2}\theta\theta\bar{\theta}\bar{\theta}D. \quad (2.18)$$

One can check that λ and D are invariant under (2.17).

2.1.3 SUSY Lagrangian

A supersymmetric Lagrangian of course has to be invariant under SUSY transformations, i.e. SUSY transformation may only give total (spacetime) derivatives. To be renormalizable, the Lagrangian has to be of mass dimension 4.

Chiral part of the Lagrangian

Without proof we state that the most general renormalizable Lagrangian which can be constructed using only chiral superfields is given by:

$$\begin{aligned} \mathcal{L} &= \Phi_i^\dagger\Phi_j \Big|_{\theta\theta\bar{\theta}\bar{\theta}} + \left[\left(\frac{1}{2}m_{ij}\Phi_i\Phi_j + \frac{1}{3}g_{ijk}\Phi_i\Phi_j\Phi_k + \lambda_i\Phi_i \right) \Big|_{\theta\theta} + \text{h.c.} \right] \\ &= -i\partial_\mu\bar{\Psi}_i\bar{\sigma}^\mu\Psi_i - \phi^*\square\phi_i - \frac{1}{2}m_{ik}\Psi_i\Psi_k - \frac{1}{2}m_{ik}^*\bar{\Psi}_i\bar{\Psi}_k \\ &\quad - g_{ijk}\Psi_i\Psi_j\phi_k - g_{ijk}^*\bar{\Psi}_i\bar{\Psi}_j\phi_k^* - \mathcal{V}(\phi_i,\phi_j^*), \end{aligned} \quad (2.19)$$

with m_{ij} and g_{ijk} being symmetric in their indices. When inserting the explicit expression for a chiral superfield (2.14) into the first line of (2.19), one sees that the component F is not a dynamical field and can be eliminated. Therefore, the second line of (2.19) does not contain the auxiliary field F but only the (non-negative) potential $\mathcal{V} = F_k^*F_k = \mathcal{V}(\phi_i,\phi_j^*)$.

Gauge part of the Lagrangian

To construct the gauge part of the Lagrangian, one defines the supersymmetric field strength tensors

$$\begin{aligned} W_\alpha &= -\frac{1}{4}\bar{D}\bar{D}D_\alpha V, \\ \bar{W}_{\dot{\alpha}} &= -\frac{1}{4}DD\bar{D}_{\dot{\alpha}}V, \end{aligned} \quad (2.20)$$

which are just chiral fields and invariant under gauge transformations (2.17). Then

$$\mathcal{L} = \frac{1}{4} (W^\alpha W_\alpha|_{\theta\theta} + \bar{W}_{\dot{\alpha}} \bar{W}^{\dot{\alpha}}|_{\bar{\theta}\bar{\theta}}) = \left(\frac{1}{2} D^2 - \frac{1}{4} F^{\mu\nu} F_{\mu\nu} + i\lambda\sigma^\mu \partial_\mu \bar{\lambda} \right) \quad (2.21)$$

is the supersymmetric gauge invariant generalization of the Lagrangian of a free vector field. $F_{\mu\nu}$ is the familiar field strength tensor. Again, D is an auxiliary field which can be eliminated.

Gauge invariant interactions

Finally, we need to define the gauge interactions between the chiral fields Ψ and the vector fields V . The gauge transformations of chiral fields are

$$\Phi \rightarrow \Phi' = e^\Gamma \Phi \quad \text{and} \quad \Phi^\dagger \rightarrow \Phi'^\dagger = \Phi^\dagger e^{\Gamma^\dagger}, \quad (2.22)$$

where Γ again is a chiral field. Thus, the kinetic part of (2.19) transforms like

$$\Phi^\dagger \Phi \rightarrow \Phi'^\dagger \Phi' = \Phi^\dagger e^{\Gamma^\dagger} e^\Gamma \Phi \quad (2.23)$$

and can be rendered gauge invariant by introducing a term e^V which transforms like

$$e^V \rightarrow e^{V'} = e^{-\Gamma^\dagger} e^V e^{-\Gamma}. \quad (2.24)$$

It is not by chance that we have denoted the exponent in (2.24) with V for vector field. It is easy to see that in the abelian case (2.24) reduces to the gauge transformation of a vector field (2.17), defined in the previous section. The object e^V is sensible when writing both V and Γ as matrices

$$V_{ij} \equiv V^a T_{ij}^a \quad \text{and} \quad \Gamma_{ij} \equiv \Gamma^a T_{ij}^a,$$

where T^a are the generators of the gauge group in question with normalization $\text{Tr}[T^a, T^b] = \frac{1}{2}\delta^{ab}$. At this point, the gauge coupling is still absorbed in the fields. It should be mentioned that e^V is not as complicated as one might think, because due to the anticommuting Grassmann numbers, the exponential series terminates. In Wess-Zumino gauge, the powers of V are given by

$$\begin{aligned} V &= -\theta\sigma^\mu \bar{\theta} v_\mu + i\theta\theta\bar{\theta}\bar{\lambda} - i\bar{\theta}\bar{\theta}\theta\lambda + \frac{1}{2}\theta\theta\bar{\theta}\bar{\theta}D \\ V^2 &= -\frac{1}{2}\theta\theta\bar{\theta}\bar{\theta}A_\mu A^\mu \\ V^n &= 0 \quad \text{for all } n \geq 3 \end{aligned}$$

and the series $e^V = 1 + V + \frac{V^2}{2}$ terminates at the second order. The non-abelian supersymmetric field strength W_α is generalized from (2.20) to

$$W_\alpha = -\frac{1}{4} \bar{D}\bar{D}e^{-V} D_\alpha e^V, \quad (2.25)$$

transforming like

$$W_\alpha \rightarrow W'_\alpha = e^\Gamma W_\alpha e^{-\Gamma}. \quad (2.26)$$

The most general supersymmetric Lagrangian reads:

$$\begin{aligned} \mathcal{L} &= \frac{1}{8g^2} \text{Tr}[W^\alpha W_\alpha|_{\theta\theta} + \bar{W}_{\dot{\alpha}} \bar{W}^{\dot{\alpha}}|_{\bar{\theta}\bar{\theta}}] + \Phi^\dagger e^V \Phi|_{\theta\theta\bar{\theta}\bar{\theta}} \\ &+ \left[\left(\frac{1}{2} m_{ij} \Phi_i \Phi_j + \frac{1}{3} g_{ijk} \Phi_i \Phi_j \Phi_k \right) \Big|_{\theta\theta} + \text{h.c.} \right] \end{aligned} \quad (2.27)$$

2.2 Supersymmetry in extra dimensions

2.2.1 Flat 5D SUSY

In the case of one flat and infinite extra dimension, one simply uses the 5D Dirac matrices fulfilling the Clifford algebra $\{\gamma^M, \gamma^N\} = 2\eta^{MN}$ to straightforwardly generalize the SUSY algebra to

$$\{Q, \bar{Q}\} = -2\gamma^M P_M. \quad (2.28)$$

The commutator of two infinitesimal SUSY transformations then reads

$$[\delta_\eta, \delta_\xi] = -2(\bar{\eta}\gamma^M \xi - \bar{\xi}\gamma^M \eta)P_M. \quad (2.29)$$

When explicitly writing out (2.28), using $Q = (Q_1, \bar{Q}_2)^T$ and $\bar{Q} = (Q_2, \bar{Q}_1)^T$, we obtain:

$$\begin{pmatrix} \{Q_{1,\alpha}, Q_2^\alpha\} & \{Q_{1,\alpha}, \bar{Q}_{1,\dot{\alpha}}\} \\ \{Q_2^\alpha, \bar{Q}_2^{\dot{\alpha}}\} & \{\bar{Q}_2^{\dot{\alpha}}, \bar{Q}_{1,\dot{\alpha}}\} \end{pmatrix} = \begin{pmatrix} -2iP_5 & -2\sigma_{\alpha\dot{\alpha}P_\mu}^\mu \\ -2\bar{\sigma}^{\mu,\dot{\alpha}\alpha}P_\mu & 2iP_5 \end{pmatrix} \quad (2.30)$$

In this explicit expression of (2.28), we see that $\mathcal{N} = 1$ SUSY in 5D is equivalent to a 4D $\mathcal{N} = 2$ SUSY with a central charge iP_5 .

The gauge multiplet

It is well known that one 5D $\mathcal{N} = 1$ SUSY multiplet has the same field content as one 4D gauge and one 4D chiral multiplet¹. In that notion, since A_5 is a real scalar, we require an additional real scalar field Σ to construct the complex scalar within the chiral multiplet. Therefore, we write out the gauge multiplet as:

$$\begin{aligned} V &= -\theta\sigma^\mu\bar{\theta}A_\mu - i\bar{\theta}\bar{\theta}\theta\lambda_1 + \theta\theta\bar{\theta}\bar{\lambda}_1 + \frac{1}{2}\theta\theta\bar{\theta}\bar{\theta}D, \\ \chi &= \frac{1}{\sqrt{2}}(\Sigma + iA_5) + \frac{i}{\sqrt{2}}\theta\sigma^\mu\bar{\theta}\partial_\mu(\Sigma + iA_5) - \frac{1}{4\sqrt{2}}\theta\theta\bar{\theta}\bar{\theta}\square(\Sigma + iA_5) \\ &\quad + \sqrt{2}\theta\lambda_2 - \frac{i}{\sqrt{2}}\theta\theta\partial_\mu\lambda_2\sigma^\mu\bar{\theta} + \theta\theta F \end{aligned} \quad (2.31)$$

Although we separate the A_5 component from the 4D A_μ components, we want to keep the 5D gauge structure of A_M . For the 4D part, transforming like (2.24), we find

$$A_\mu^a \longrightarrow A_\mu^a - 2\partial_\mu\alpha^a + f^{abc}\alpha^b A_\mu^c, \quad (2.32)$$

where $\alpha = \text{Im}\phi$ and ϕ is the scalar component of Γ . By imposing χ to transform like

$$\chi \longrightarrow \chi' = e^\Gamma(\chi - \sqrt{2}\partial_y)\bar{e}^{-\Gamma}, \quad (2.33)$$

we obtain

$$A_\mu^a \longrightarrow A_5^a - 2\partial_5\alpha^a + f^{abc}\alpha^b A_5^c \quad (2.34)$$

which is consistent with (2.32). This consistency is also the reason why A_5 was chosen to be the imaginary part within the scalar field $1/2(\Sigma + iA_5)$ of the gauge sector chiral multiplet χ

¹A vector multiplet contains a vector A and a spinor field λ . In 5D the vector acquires an additional component A_5 . While λ in 4D is a Weyl spinor, in 5D it will be a Dirac spinor with the same degrees of freedom as two Weyl spinors λ_1 and λ_2 . As a 4D chiral multiplet contains a scalar and a (Weyl) spinor, it can absorb the additional degrees of freedom of a 5D vector multiplet compared to a 4D one.

in (2.31) in the first place.

The chiral multiplet has to be implemented in the Lagrangian in a gauge and SUSY invariant way. Additionally it has to provide the fifth component of the gauge field necessary to obtain the complete $F_{MN}F^{MN}$ QED part. The solution is [18]:

$$S_g(V, \chi) = \int d^5x \int d^2\theta \frac{R}{8g^2} \text{Tr}[W^\alpha W_\alpha] + \text{h.c.} \\ + \int d^5x \int d^4\theta \frac{1}{2Rg^2} \text{Tr}[(\sqrt{2}\partial_y + \bar{\chi})e^{-V}(-\sqrt{2}\partial_y + \chi)e^V + \partial_y e^{-V} \partial_y e^V] \quad (2.35)$$

The hypermultiplet

To obtain the chiral multiplet in five dimensions, we need two chiral fermions. Therefore the fields

$$H = h + i\theta\sigma^\mu\bar{\theta}\partial_\mu h - \frac{1}{4}\theta\theta\bar{\theta}\bar{\theta}\square h + \sqrt{2}\theta\Psi - \frac{i}{\sqrt{2}}\theta\theta\partial_\mu\Psi\sigma^\mu\bar{\theta} + \theta\theta F \\ H^c = h^c + i\theta\sigma^\mu\bar{\theta}\partial_\mu h^c - \frac{1}{4}\theta\theta\bar{\theta}\bar{\theta}\square h^c + \sqrt{2}\theta\Psi^c - \frac{i}{\sqrt{2}}\theta\theta\partial_\mu\Psi^c\sigma^\mu\bar{\theta} + \theta\theta F^c, \quad (2.36)$$

are introduced. They transform like

$$H \longrightarrow H' = e^\Gamma H \quad \text{and} \quad H^c \longrightarrow e^{-\Gamma} H^c. \quad (2.37)$$

Using the gauge transformation (2.24) and the expressions in (2.36), it can be showed that

$$S_h(H, H^c, V, \chi) = \int d^5x R \int d^4\theta \left[\bar{H}e^{-V}H + H^c e^V \bar{H}^c \right] \\ + \int d^5x R \int d^2\theta H^c \left[\partial_y/R - \frac{1}{\sqrt{2}R}\chi - M_{5D} \right] H + \text{h.c.} \quad (2.38)$$

is gauge invariant and leads to the correct action of the 5D standard model spinors.

2.2.2 Warped 5D SUSY

In the case of a 5D Minkowski space the metric is invariant under SUSY transformations² and therefore, according to [19], 5D SUSY³ is a global symmetry. This is no longer true for the warped compact extra dimension we are interested in. In order to find the global SUSY transformations in warped space, we have to find the transformations which leave the RS metric g^{MN} unchanged. This is equivalent to demand the SUSY transformations to close into a Killing vector v of the background metric

$$[\delta_\eta, \delta_\xi] = -2(\bar{\eta}\hat{\gamma}^M\xi - \bar{\xi}\hat{\gamma}^M\eta)P_M = v^N P_N, \quad (2.39)$$

where v is defined by the Killing equation

$$v^M \partial_M g_{AB} + g_{AM} \partial_B v^M + g_{BM} \partial_A v^M = 0. \quad (2.40)$$

²Note that usual translation is also part of the general SUSY transformation.

³or equivalently both 4D SUSYs

Here $\hat{\gamma}^M$ are the warped Dirac matrices satisfying $\{\hat{\gamma}^M, \hat{\gamma}^N\} = 2g^{MN}$. We find that (2.39) and (2.40) are satisfied, if the SUSY transformations are generated by the SUSY parameters

$$\xi(x, y) = e^{-Rky/2} \begin{pmatrix} \xi_\alpha^0 \\ 0 \end{pmatrix} \quad \text{and} \quad \eta(x, y) = e^{-Rky/2} \begin{pmatrix} \eta_\alpha^0 \\ 0 \end{pmatrix}, \quad (2.41)$$

where $\xi_\alpha^0, \eta_\alpha^0$ are independent of x^M . Since the admissible SUSY transformations are parameterized by a single Weyl spinor, we find that in warped space only one SUSY survives in 4D.

However, we can still write down the Lagrangian of the supersymmetric theory on a Randall-Sundrum background by just equipping (2.35) and (2.38) with the density factors and according fünfbeins. We obtain for the gauge action

$$S_g(V, \chi) = \int d^5x \int d^2\theta \frac{R}{8g^2} \text{Tr}[W^\alpha W_\alpha] + \text{h.c.} \\ + \int d^5x \int d^4\theta \frac{e^{-2Rky}}{2Rg^2} \text{Tr}[(\sqrt{2}\partial_y + \bar{\chi})e^{-V}(-\sqrt{2}\partial_y + \chi)e^V + \partial_y e^{-V} \partial_y e^V] \quad (2.42)$$

and for the hypermultiplet action

$$S_h(H, H^c, V, \chi) = \int d^5x R \int d^4\theta e^{-2Rky} \left[\bar{H} e^{-V} H + H^c e^V \bar{H}^c \right] \\ + \int d^5x R \int d^2\theta e^{-3Rky} H^c \left[\partial_y/R - \frac{1}{\sqrt{2}R} \chi - \left(\frac{3}{2} - c\right)k \right] H + \text{h.c.} \quad (2.43)$$

Redefinitions

At last, we want to introduce redefinitions which will make life much easier later on. First of all, to make the gauge transformations (2.32) and (2.34) take the usual form

$$A_M^a \longrightarrow A_M^a - \frac{1}{g} \partial_M \alpha^a + f^{abc} \alpha^b A_M^c \quad (2.44)$$

we will scale all fields from the gauge multiplet by a factor $2g$. Furthermore, we want all fermionic fields, including superfields, to take the form of (1.41), all bosonic fields the form of (1.47), and all scalar fields the form of (1.49). Therefore, some of the fields have to be rescaled by powers of $e^{-\frac{1}{2}Rky}$. Finally, to end up with correct units, all component fields of the gauge sector chiral field χ are scaled with an additional factor R . The redefinitions can be summarized as:

$$\begin{aligned} \psi &\longrightarrow e^{-\frac{1}{2}Rky} \psi & \psi^c &\longrightarrow e^{-\frac{1}{2}Rky} \psi^c \\ A_\mu &\longrightarrow 2g A_\mu & \lambda_1 &\longrightarrow 2g e^{-\frac{3}{2}Rky} \lambda_1 \\ A_5 &\longrightarrow 2g R A_5 & \lambda_2 &\longrightarrow -2ig R e^{-\frac{1}{2}Rky} \lambda_2 & \Sigma &\longrightarrow 2g R \Sigma \end{aligned} \quad (2.45)$$

is determined by the gauge couplings. Hence our final gauge structure reads

$$G = SU(3)_C \times SU(2)_L \times SU(2)_R \times U(1)_X, \quad (3.1)$$

where X is the B - L quantum number. The full gauge symmetry will be kept in the bulk. Using the intrinsic hierarchy of the background metric, we break the two $SU(2)$ s and thus electroweak symmetry down to a custodial $SU(2)_D$ at the IR brane:

$$SU(2)_L \times SU(2)_R \longrightarrow SU(2)_D.$$

The custodial symmetry has the generator $T_{3D} = T_{3L} + T_{3R}$. This symmetry protects the ρ parameter, which states that $m_W = \cos \Theta_W m_Z$ at tree level.

On the Planck brane, we break the P_{LR} symmetry between the two $SU(2)$ groups. The breaking pattern is

$$SU(2)_R \times U(1)_X \longrightarrow U(1)_Y,$$

where Y is the Hypercharge. The generator is $Y = T_{3R} + X$. In the end, only a $U(1)_Q$ corresponding to electromagnetism with $Q = T_{3L} + T_{3R} + X$, remains unbroken. This is in agreement with the AdS/CFT correspondence, which requires that a global symmetry of the strongly coupled CFT corresponds to a gauge symmetry in AdS.

3.1.2 Unitarity in higgsless models

Within the SM, the scattering amplitude of longitudinal components of massive vector bosons would spoil the unitarity of the S-matrix, were it not for the presence of the Higgs boson. At first sight, scattering of longitudinal vector bosons with polarization vectors $\epsilon = (p/m, 0, 0, E/m)$ is of the energy behavior $\mathcal{M} = a + bE^2 + cE^4$. It can be showed that the part proportional to E^4 cancels out once the correct couplings are inserted [20]. The component proportional to E^2 cancels when taking into account additional diagrams containing the Higgs boson. The requirement for this cancellation to occur and therefore the requirement for unitarity is a Higgs mass $m_H < 1$ TeV. Obviously, a higgsless model needs a new mechanism to preserve unitarity. In our extra dimensional approach, the Kaluza-Klein resonances are found to be responsible for the cancellation and thus for the consistency of the whole model. Due to Ward identities and 5D BRST invariance¹, cancellation rules among triple and quartic vector boson couplings are fulfilled, hence

$$c \propto \left(g_{nnnn} - \sum_k g_{nnk}^2 \right) = 0, \quad b \propto \left(\frac{4}{3} m_n^2 g_{nnnn} - \sum_k g_{nnk}^2 m_k^2 \right) = 0,$$

where n, m are the KK indices. Similarly to the upper the Higgs mass bound in the SM, the KK resonances $W^{(1)}$ and $Z^{(1)}$ have to be lighter approximately 1.4 TeV.

3.1.3 SUSY breaking on a new IR brane

Supersymmetry must be broken because, beautiful as the idea may be, supersymmetric particles have not been detected up to now and therefore cannot be degenerate in mass with the known SM particles. The straightforward and to a certain extend brute-force method, used in [1] within a model with two branes, is to break SUSY at the Planck brane by giving the SM fields different boundary conditions than their supersymmetric partners. Breaking SUSY at the high energy brane projects the light supersymmetric modes out of the spectrum. The remaining

¹In the previous chapters we have only mentioned gauge symmetry in 5D. As usual, gauge symmetries in perturbative quantum field theory are replaced by the corresponding BRST extension, in order to perform quantization. BRST invariance follows from gauge invariance.

supersymmetric fields are KK excitations with masses of approximately 1.4 TeV, thus widely avoiding trouble with experimental bounds. However, other desirable properties of SUSY like the taming of loop corrections, are lost in this approach. A logical consequence, when extending the extradimensional model outlined in [2] to be supersymmetric, would be to separate SUSY breaking from EWSB. Models living on two “back-to-back” AdS₅ slices with a shared Planck brane have been considered before, within the AdS/CFT interpretation [21], as well as for phenomenological reasons [22]. The new interval leads to new effects in the SM as well as the SUSY sector. The new way of SUSY breaking at the IR brane of the new interval could for example give a comparatively light scalar Σ_0 field.

3.1.4 Two AdS₅ Slices

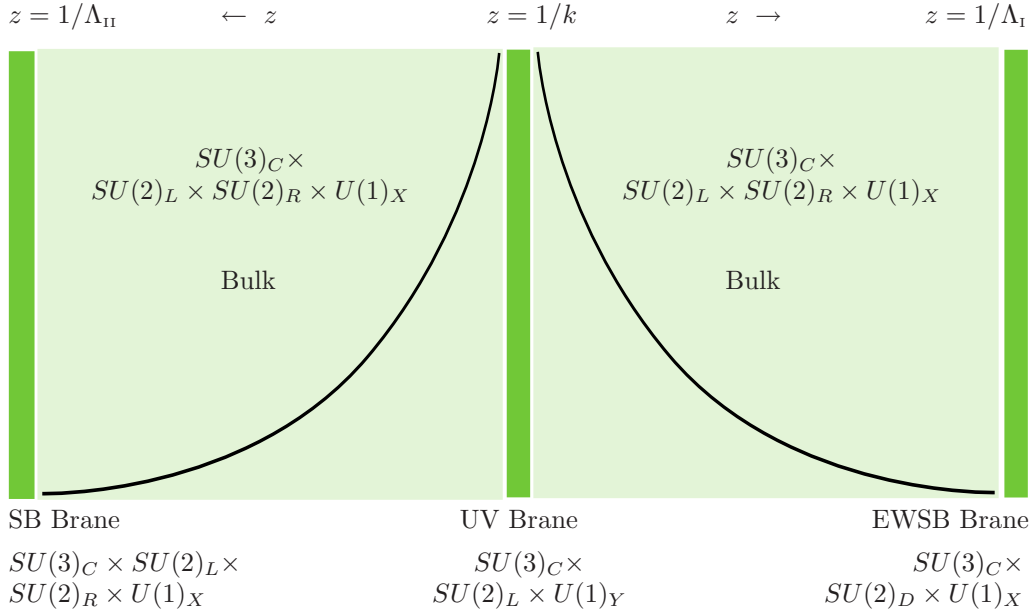


Fig. 3.2: An illustration of the three brane model setup: Two back-to-back slices of AdS₅, sharing one UV brane.

The situation of two “back-to-back” AdS₅ slices, glued together at the Planck brane, is depicted in fig. 3.1.4. Throughout this thesis, the first interval where electroweak symmetry is broken on the IR brane at $z = \Lambda_{\text{I}}$, is called interval I. Similarly, the second interval, where we break Supersymmetry, is referred to as interval II. The high energy brane is called the UV brane and the two IR branes are named after the corresponding symmetry breaking. The IR brane in interval I is the EWSB (elektroweak symmetry breaking) brane and the other IR brane in interval II the SB (Supersymmetry breaking) brane.

The model lives on a Randall-Sundrum background with the metric (1.17). It is often useful when handling two AdS₅ slices, to work in conformal coordinates. These are obtained substituting y by

$$z = \frac{e^{Rky}}{k}, \quad (3.2)$$

where $R = R_{\text{I}}$ in the first (EWSB) interval and $R = R_{\text{II}}$ in the new (SUSY) interval. The

metric in conformal coordinates reads

$$g_{MN} = \frac{1}{(kz)^2} \eta_{MN}. \quad (3.3)$$

When introducing a second warped extradimensional interval, one has to define how fields are connected at the UV brane where the two intervals meet. Take as example fermionic fields. At the IR branes, the requirement for the brane localized contribution \mathcal{B} to the action to vanish

$$\mathcal{B} = \sqrt{g} \bar{\Psi} \hat{\gamma}^M \Psi \Big|_{z=1/\Lambda_{I,II}} = 0 \quad (3.4)$$

is equivalent to

$$f_\eta^{I,II} \Big|_{z=1/\Lambda_{I,II}} = 0 \quad \text{or} \quad f_\chi^{I,II} \Big|_{z=1/\Lambda_{I,II}} = 0. \quad (3.5)$$

The fields from both intervals meet at the Planck brane and the localized part of the action reads:

$$\sqrt{g} \bar{\Psi} \hat{\gamma}^M \Psi \Big|_{z=1/k} = (\eta^I \chi^I + \eta^{II} \chi^{II}) \Big|_{z=1/k} \quad (3.6)$$

The natural generalization of condition (3.5), making (3.6) vanish, is then:

$$\begin{aligned} t f_\eta^I - f_\eta^{II} \Big|_{z=1/k} &= 0 \\ f_\chi^I + t f_\chi^{II} \Big|_{z=1/k} &= 0 \end{aligned} \quad (3.7)$$

We call t the transition coefficient. It parameterizes how the KK wave function coming from one side of the Planck brane is continued at the other side.

The size of the second interval is constrained. The requirement for $W^{(1)}$ and $Z^{(1)}$ to be light enough to insure unitarity leads to an upper bound $\Lambda_{II} \lesssim 4000$ GeV. This bound is relaxed when introducing the kinetic term to split the chargino and the W^\pm mass. The lower bound however is fixed by imposing that the gluinos in our model are above the detection bound of 308 GeV [23]. This requires $\Lambda_{II} \gtrsim 2500$ GeV.

3.1.5 Twisted Boundary Conditions

Although there are a lot of fields, there are not too many combinations of possible boundary conditions. The fields are closely interlinked and when choosing a boundary condition for one field, the conditions for many other fields are automatically determined by that choice. The first and rather trivial principle of assigning boundary conditions is to impose for all fields of an unbroken symmetry group the same boundary conditions. It is a bit more work to determine the relations for the boundary conditions of fields coupled by their equations of motion. We have demonstrated at the end of chap. 1 that all KK wave functions are of the form

$$f_x(z) = (kz)^{(\text{exp})} [a_x J_{(\text{order})}(mz) + b_x Y_{(\text{order})}(mz)], \quad (3.8)$$

where we have suppressed the KK indices. A_μ and A_5 fields are coupled by an e.o.m. which we have derived for the flat case in (1.9). The fermion fields are coupled by (1.37). Corresponding e.o.m. are obtained for the respective superpartner fields, λ_1 , λ_2 and h , h^c . Also in chap. 1, we have derived the solutions for the KK fields. Coupled KK functions f_x and f_y have identical mass eigenstates and –up to a sign choice– identical coefficients $a_x = \pm a_y$ and $b_x = \pm b_y$. We have to make sure the e.o.m. and our choice of boundary conditions for f_x and f_y are in agreement with each other.

The “twisted boundary condition” that follows for a KK function f_x , when assigning f_y a Dirichlet boundary condition, can be determined either directly from the e.o.m connecting f_x

KK field	Structure	Boundary conditions
f_{A_μ} f_{A_5}	$(kz)J_1$ $(kz)^2J_0$	$\ominus : f_{A_\mu} _{z_0=0} = 0 \Rightarrow \oplus : \partial_z(z^{-2}f_{A_5}) _{z_0=0} = 0$ $\ominus : f_{A_5} _{z_0=0} = 0 \Rightarrow \oplus : \partial_z f_{A_\mu} _{z_0=0} = 0$
f_{λ_1} f_{λ_2}	$(kz)J_1$ $(kz)^2J_0$	similar to the case of f_{A_μ} and f_{A_5} above
f_η f_χ	$(kz)^2J_{c+1/2}$ $(kz)^2J_{c-1/2}$	$\ominus : f_\eta _{z_0=0} = 0 \Rightarrow \oplus : \partial_z(z^{-3/2-c}f_\chi) _{z_0=0} = 0$ $\ominus : f_\chi _{z_0=0} = 0 \Rightarrow \oplus : \partial_z(z^{-3/2+c}f_\eta) _{z_0=0} = 0$
f_h f_{h^c}	$(kz)^2J_{c+1/2}$ $(kz)^2J_{c-1/2}$	similar to the case of f_η and f_χ above

Tab. 3.1: Overview over the structure of KK fields before redefinition of the fields and the resulting relations between boundary conditions.

and f_y or from the KK solutions (3.8). For the latter, one uses the identities of the Bessel functions J :

$$\begin{aligned} \partial_z(z^{1/2+c}J_{1/2+c}(mz)) &= m(z^{1/2+c}J_{-1/2+c}(mz)), \\ \partial_z(z^{1/2-c}J_{-1/2+c}(mz)) &= -m(z^{1/2-c}J_{1/2+c}(mz)). \end{aligned} \quad (3.9)$$

Analogous relations hold for Y .

Generally, the twisted boundary condition corresponding to a Dirichlet condition

$$\ominus : f_x|_{z_0=0} = 0,$$

is always a Neumann-like condition

$$\oplus : \partial_z(z^{(\dots)}f_y)|_{z_0=0} = 0$$

and vice versa.

The structure of the KK wave functions and the resulting twisted boundary conditions before and after the field redefinition (2.45) are given in tab. 3.1 and tab. 3.2.

3.2 Setup

3.2.1 The Lagrangian

The Lagrangian, containing all fields of our model and determining their interactions, is the supersymmetric Lagrangian on a warped background worked out in the previous chapter. It is given by (2.42) and (2.43), together with the gauge fixing term (1.43).

KK field	Structure	Boundary conditions
f_{λ_1}	$(kz)^{5/2}J_1$	$\ominus : f_{\lambda_1} _{z_0=0} = 0 \Rightarrow \oplus : \partial_z(z^{-3/2}f_{\lambda_2}) _{z_0=0} = 0$
f_{λ_2}	$(kz)^{5/2}J_0$	$\ominus : f_{\lambda_2} _{z_0=0} = 0 \Rightarrow \oplus : \partial_z(z^{-5/2}f_{\lambda_1}) _{z_0=0} = 0$
f_η	$(kz)^2J_{c+1/2}$	$\ominus : f_\eta _{z_0=0} = 0 \Rightarrow \oplus : \partial_z(z^{-2-c}f_\chi) _{z_0=0} = 0$
f_χ	$(kz)^2J_{c-1/2}$	$\ominus : f_\chi _{z_0=0} = 0 \Rightarrow \oplus : \partial_z(z^{-2+c}f_\eta) _{z_0=0} = 0$

Tab. 3.2: Overview over the structure of KK fields after redefinition of the fields and the resulting relations between boundary conditions.

For clarity, we assemble these expressions and write the complete Lagrangian for the three brane setup in conformal coordinates:

$$\begin{aligned}
\mathcal{L} &= \mathcal{L}_h(H, H^c, V, \chi) + \mathcal{L}_g(V, \chi) + \mathcal{L}_{\text{gf}} \\
&= \int d^4\theta \frac{1}{(kz)^3} \left[\overline{H} e^{-V} H + H^c e^V \overline{H}^c \right] \\
&\quad + \int d^2\theta \frac{1}{(kz)^4} H^c \left[(kz) \partial_z - \frac{1}{\sqrt{2}R_{\text{I,II}}} \chi - \left(\frac{3}{2} - c\right)k \right] H + \text{h.c.} \\
&\quad + \int d^2\theta \frac{1}{8(kz)g^2} \text{Tr}[W^\alpha W_\alpha] + \text{h.c.} \\
&\quad + \int d^4\theta \frac{1}{2kz^3g^2} \text{Tr} \left[(\sqrt{2}z\partial_z + \frac{\overline{\chi}}{R_{\text{I,II}}k}) e^{-V} (-\sqrt{2}z\partial_z + \frac{\chi}{R_{\text{I,II}}k}) e^V + z\partial_z e^{-V} z\partial_z e^V \right] \\
&\quad - \frac{1}{2(kz)\xi} \left(\eta^{\mu\nu} \partial_\mu A_\nu - \xi \frac{1}{(kz)^2} (kz\partial_z - 2k) A_5 \right)^2
\end{aligned} \tag{3.10}$$

The coupling constants corresponding to the gauge groups $SU(3)_C$, $SU(2)_L$, $SU(2)_R$ and $U(1)_X$ are g_{5C} , g_L , g_R and g_{5X} . From here on, we set $g_L = g_R = g_5$. Although it is not mandatory to have equal couplings for $SU(2)_L$ and $SU(2)_R$, the general case of $g_L \neq g_R$ has turned out to be not useful when it comes to phenomenology, and is potentially problematic for perturbative unitarity [24].

3.2.2 Field content

Matter fields are implemented in the model as two doublets for each standard model fermion, transforming under $SU(2)_L$ and $SU(2)_R$, respectively:

$$\begin{aligned}
\Psi_L &= (\eta_L^u, \bar{\chi}_L^u, \eta_L^d, \bar{\chi}_L^d)^T \\
\Psi_R &= (\eta_R^u, \bar{\chi}_R^u, \eta_R^d, \bar{\chi}_R^d)^T
\end{aligned} \tag{3.11}$$

In order to satisfy $Q = T_{3L} + Y$, quarks will be assigned the $U(1)$ quantum numbers $X = 1/6$ and leptons carry $X = -1/2$.

An overview of the final field content of our model, taken from [12], is presented in the appendix in tab. B.1, tab. B.2 and tab. B.3.

3.2.3 Boundary conditions

We conclude this chapter stating the boundary conditions for the fields present in our model. The reasoning for this choice of conditions will follow in chap. 4 and chap. 5, where we discuss the gauge and the matter sector of our model in detail.

Boundary conditions for the gauge multiplet

To present the boundary conditions assigned to the fields from the gauge sector in a compact form, we write them in terms of the gauge multiplet. In order to work with the multiplets, we understand λ_1, λ_2 as the gaugino fields before the redefinitions (2.45), hence they come with the same power of (kz) as the A_μ, A_5 fields. The vector multiplet V is coupled to the chiral multiplet χ by the e.o.m. between A_μ and A_5 as well as between λ_1 and λ_2 . Therefore, when assigning boundary conditions to the vector multiplet V , we have fully defined the gauge multiplet. The chiral multiplet χ will be assigned the corresponding twisted boundary conditions.

- On the EWSB brane

$$\begin{aligned} \begin{bmatrix} 1 & -1 \\ \partial_z & \partial_z \end{bmatrix} \begin{bmatrix} V^{1L} \\ V^{1R} \end{bmatrix} \Big|_{z=1/\Lambda_I} &= 0 \\ \partial_z V^{1X} \Big|_{z=1/\Lambda_I} &= 0 \\ \partial_z V^{1C} \Big|_{z=1/\Lambda_I} &= 0 \end{aligned} \quad (3.12)$$

- On the UV brane

This is the brane where the fields from the two intervals meet. We choose a continuous transition from the interval I to the interval II.

$$V^{1(L,R,X)} \left(\frac{1}{k} \right) = V^{II(L,R,X)} \left(\frac{1}{k} \right) \quad (3.13)$$

This is equivalent to transition coefficients $t = 1$. Furthermore we impose five boundary conditions:

$$\begin{aligned} \begin{bmatrix} g_{5X} \partial_z & g_5 \partial_z \\ -g_5 & g_{5X} \end{bmatrix} \begin{bmatrix} V^{1R_3} + V^{II R_3} \\ V^{1X} + V^{II X} \end{bmatrix} \Big|_{z=1/k} &= 0 \\ \partial_z (V^{1L} + V^{II L}) \Big|_{z=1/k} &= 0 \\ (V^{1R_1, R_2} + V^{II R_1, R_2}) \Big|_{z=1/k} &= 0 \\ \partial_z (V^{1C} + V^{II C}) \Big|_{z=1/k} &= 0 \end{aligned} \quad (3.14)$$

The direction of the coordinate z of the extra dimension is defined as from the UV brane towards the IR branes, c.f. fig. 3.1.4.

- On the SB brane

The choice of SUSY breaking boundary conditions will be discussed in chap. 4. While Supersymmetry within the multiplets is broken, the coupling of boundary conditions by e.o.m. remains untouched.

- Gauge bosons

The $SU(2)_R$ and $U(1)_X$ fields are assigned Neumann (\oplus) boundary conditions:

$$\begin{aligned} \partial_z A_\mu^{II R} \Big|_{z=1/k} &= 0 \\ \partial_z A_\mu^{II X} \Big|_{z=1/k} &= 0 \end{aligned} \quad (3.15)$$

while the \oplus boundary condition of the $SU(2)_L$ fields is modified by a brane kinetic term proportional to κ :

$$\left(\partial_z - \kappa \frac{m^2}{\Lambda_{\text{II}}} k \pi R_2 \right) A_\mu^{\text{II}L} \Big|_{z=1/k} = 0 \quad (3.16)$$

The A_5 fields are assigned the corresponding twisted boundary conditions.

– Gauginos

All λ_1 fields are assigned \oplus boundary conditions

$$\begin{aligned} \partial_z \lambda_1^{\text{II}L} \Big|_{z=1/k} &= 0 \\ \partial_z \lambda_1^{\text{II}R} \Big|_{z=1/k} &= 0 \\ \partial_z \lambda_1^{\text{II}X} \Big|_{z=1/k} &= 0 \end{aligned} \quad (3.17)$$

The above equations refer to the gaugino fields before the field redefinition (2.45). Afterwards, they have to be replaced by $\partial_z \lambda_1 \rightarrow \partial_z (kz)^{-3/2} \lambda_1$. Again, the λ_2 fields receive twisted boundary conditions.

Boundary conditions for fermions and sfermions

Again, we write the boundary conditions in terms of the full multiplet. Using the e.o.m., it is sufficient to specify half of the boundary conditions, the other half being automatically defined as the respective twisted conditions.

The assignment of boundary conditions to the matter fields is analyzed in chap. 5.

- On the EWSB brane

$$\begin{aligned} H_R^1 - \frac{M_D}{\Lambda_{\text{I}}} H_L^1 \Big|_{z=1/\Lambda_{\text{I}}} &= 0 \\ H_L^{1c} + \frac{M_D}{\Lambda_{\text{I}}} H_R^{1c} \Big|_{z=1/\Lambda_{\text{I}}} &= 0 \end{aligned} \quad (3.18)$$

- On the UV brane

– Charged fermions and sfermions:

$$\begin{aligned} H_R^1 + t_R H_R^{\text{II}} \Big|_{z=1/k} &= 0 \\ t_R H_R^{1c} - H_R^{\text{II}c} \Big|_{z=1/k} &= 0 \\ H_L^{1c} + t_L H_L^{\text{II}c} \Big|_{z=1/k} &= 0 \\ t_L H_L^1 - H_L^{\text{II}} \Big|_{z=1/k} &= 0 \end{aligned} \quad (3.19)$$

In contrast to the gauge fields, we do not always impose continuous transition where the two intervals meet. We still choose $t_L = 1$, but use $t_R \neq 1$ to realize the mass splitting between u - and d -type quarks.

– Neutrinos and sneutrinos:

$$\begin{aligned} H_R^1 + t_R H_R^{\text{II}} - \frac{M_M}{k} (H_R^{1c} + \frac{1}{t_R} H_R^{\text{II}c}) \Big|_{z=1/k} &= 0 \\ t_R H_R^{1c} - H_R^{\text{II}c} \Big|_{z=1/k} &= 0 \\ H_L^{1c} + t_L H_L^{\text{II}c} \Big|_{z=1/k} &= 0 \\ t_L H_L^1 - H_L^{\text{II}} \Big|_{z=1/k} &= 0 \end{aligned} \quad (3.20)$$

- On the SB brane

- fermions

$$\begin{aligned}\eta_R^{\text{II}}|_{z=1/\Lambda_{\text{II}}} &= 0 \\ \chi_L^{\text{II}}|_{z=1/\Lambda_{\text{II}}} &= 0\end{aligned}\tag{3.21}$$

- sfermions

$$\begin{aligned}h_L^{\text{II}}|_{z=1/\Lambda_{\text{II}}} &= 0 \\ h_R^{c,\text{II}}|_{z=1/\Lambda_{\text{II}}} &= 0\end{aligned}\tag{3.22}$$

The boundary conditions, which were used in the original two brane setup of [12, 15] with just one AdS₅ slice, are given in App. C.1.

4 Gauge sector

This chapter is dedicated to the gauge sector of our model, containing the fields from the vector multiplet V and from the chiral multiplet χ defined in (2.31). In particular we discuss SUSY breaking. Charginos and neutralinos constitute the lightest and phenomenologically most interesting supersymmetric particles within our model setup, therefore we will analyze their interactions at the end this chapter.

4.1 Boundary conditions

4.1.1 Boundary conditions at the UV and the EWSB brane

The authors of [11] have demonstrated that electroweak symmetry can be broken without violating unitarity in extradimensional higgsless models on a Randall-Sundrum background. For a non-supersymmetric model in a single AdS₅ slice with two branes, they have derived the following boundary conditions for the gauge fields:

$$\begin{bmatrix} 1 & -1 \\ \partial_z & \partial_z \end{bmatrix} \begin{bmatrix} A_\mu^L \\ A_\mu^R \end{bmatrix} \Big|_{z=1/\Lambda_{\text{IR}}} = 0 \quad \partial_z A_\mu^X \Big|_{z=1/\Lambda_{\text{IR}}} = 0 \quad \partial_z A_\mu^C \Big|_{z=1/\Lambda_{\text{IR}}} = 0 \quad (4.1)$$

$$\begin{bmatrix} g_{5X} \partial_z & g_5 \partial_z \\ -g_5 & g_{5X} \end{bmatrix} \begin{bmatrix} A_\mu^{R_3} \\ A_\mu^X \end{bmatrix} \Big|_{z=1/k} = 0 \quad (4.2)$$

$$\partial_z A_\mu^L \Big|_{z=1/k} = 0 \quad A_\mu^{R_1, R_2} \Big|_{z=1/k} = 0 \quad \partial_z A_\mu^C \Big|_{z=1/k} = 0$$

This boundary conditions can be interpreted within the context of orbifold projections, where at the end point $y = 0$ a localized $SU(2)_R$ scalar doublet acquires a VEV and breaks $SU(2)_R \times U(1)_X$ down to $U(1)_Y$ [11]. One can send the VEV to infinity without spoiling the high energy behavior. In that limit, the Higgs field decouples. In the picture of brane localized Higgs fields it is also understandable why gauge couplings g_5 and g_{5X} enter the boundary conditions. To be precise, the ratio

$$g_r := \frac{g_{5X}}{g_5} \quad (4.3)$$

is the relevant magnitude in the boundary conditions (4.2).

For our supersymmetric model, we use the same mechanism and generalize (4.1) and (4.2) to contain complete supersymmetric vector and chiral gauge multiplets. On the UV brane, we additionally have to specify the transition to the second AdS₅ slice. The transitions has to be compatible with vanishing boundary action in analogy¹ to (3.7). We choose continuous transition $A^I|_{y=0} = A^{II}|_{y=0}$. Thereby, we have derived the boundary conditions at the EWSB and UV brane (3.12) and (3.14) which we have stated in the previous chapter.

On the SB brane, where the full bulk symmetry $SU(2)_L \times SU(2)_R \times U(1)_X$ is kept, we have to specify the boundary conditions for each symmetry group. The boundary conditions at the EWSB and UV brane defined so far leave one single massless fields corresponding to $(A_\mu^{L_3} + A_\mu^{R_3}) + g_r A_\mu^X$. In order to keep this massless solution and to later identify it with

¹The boundary action is $\mathcal{B} \propto A_\mu \partial_z A_\mu$, so just replace f_η by f_{A_μ} and f_χ by $\partial_z f_{A_\mu}$.

the physical photon, we are forced to choose Neumann boundary conditions \oplus for all three symmetry groups at the SB brane:

$$\begin{array}{c|c|c} A_\mu^{L_i} & A_\mu^{R_i} & A_\mu^X \\ \hline \oplus & \oplus & \oplus \end{array} \quad (4.4)$$

For gauge bosons, the two intervals act like an enlarged single interval. The mass terms \mathcal{M} of the W^\pm and Z bosons are generated in the EWSB interval, where the KK wave functions are curved in order to fulfill the boundary conditions, compare fig. 4.1 and fig. 4.2. The correct masses are obtained by adjusting the mass scales of the two extradimensional intervals, Λ_1 being the dominating parameter.

4.1.2 SUSY breaking

Sticking to our concept of Supersymmetry breaking, the gauginos receive on the SB brane different boundary conditions than the gauge bosons.

If we constrain ourselves to Neumann (\oplus) and Dirichlet (\ominus) conditions at first, there are 8 possibilities to assign boundary conditions to the gauginos at the SB brane. The scenarios are listed in tab. 4.1. It is understood that the λ_2 automatically receive the respective twisted boundary conditions.

		$\lambda_1^{L_i}$	$\lambda_1^{R_i}$	λ_1^X	charged		neutral	
					$m_{\lambda_1} = 0?$	$m_{\lambda_2} = 0?$	$m_{\lambda_1} = 0?$	$m_{\lambda_2} = 0?$
1	a	\oplus	\oplus	\oplus	no	no	yes	no
	b	\oplus	\oplus	\ominus	no	no	no	no
2	a	\oplus	\ominus	\oplus	no	yes	no	no
	b	\oplus	\ominus	\ominus	no	yes	no	yes
3	a	\ominus	\oplus	\oplus	no	yes	no	no
	b	\ominus	\oplus	\ominus	no	yes	no	yes
4	a	\ominus	\ominus	\oplus	no	yes	no	yes
	b	\ominus	\ominus	\ominus	no	yes	no	yes

Tab. 4.1: Possible assignments of boundary conditions at the SUSY breaking brane to the charginos and neutralinos. Setup 1b is the only one which prohibits all massless solutions.

The only setup in tab. 4.1 without massless chargino or neutralino modes, neither in λ_1 nor in λ_2 , is 1b. However, in this scenario, the chargino boundary conditions are the same as the one for the W^\pm . Therefore, the two fields are degenerate in mass. This is not compatible with the current bound of $m_{\chi^\pm} \geq 95\text{GeV}$ [23].

Obviously, we need to extend our setup of boundary conditions to contain more than just Neumann and Dirichlet conditions.

For the scalar field Σ from the chiral part of the gauge multiplet χ a similar discussion applies. The KK wave function of the Σ is, apart from redefinition factors, the same as the KK functions of the fields within the same SUSY multiplet, A_5 and λ_2 . It is however not connected with fields from the vector multiplet V , and therefore massless modes for Σ_\pm and Σ_0 are absent in scenario 1a and scenario 1b. The neutral Σ_0 is of particular interest due to a curious similarity to the SM Higgs boson. This will be discussed in chap. 9. However, as there is no symmetry protecting the masses of the scalar, significant corrections to the tree level mass are expected.

4.1.3 Brane kinetic terms

We will, as in [1], use a brane localized kinetic term to split the chargino and W^\pm mass. Different to that approach, we will add the localized term on the new IR brane instead of the Planck brane. In chap. 6 we will discuss kinetic terms in the context of the Peskin-Takeuchi parameter S . The corresponding localized action term is:

$$S_{\text{kin}} = -\kappa\pi \int d^5x \frac{1}{(kz)} \delta(z - \Lambda_{\text{II}}^{-1}) \left(\frac{1}{4} \eta^{MO} \eta^{NP} L_{MN} L_{OP} \right) \quad (4.5)$$

where L_{MN} is the field strength tensor of the $SU(2)_L$ vector field. The presence of (4.5) deforms the original Neumann boundary condition to:

$$\partial_z A_\mu^{\text{II}L} \Big|_{z=1/\Lambda_{\text{II}}} \longrightarrow \left(\partial_z - \kappa \frac{m^2}{\Lambda_{\text{II}}} k\pi R_{\text{II}} \right) A_\mu^{\text{II}L} \Big|_{z=1/\Lambda_{\text{II}}} \quad (4.6)$$

Note that for the massless photon the brane kinetic term affects only the normalization. It is also a characteristic for these terms, that κ as introduced in (4.5) has to be positive or else tachyonic solutions appear. This could be tolerable as long as these solutions stay above the cutoff, but it seems safer to just avoid that situation. Later on, we will see that brane kinetic terms with $\kappa > 0$ lower the mass eigenvalue. This is the reason why we assigned the localized term to the boson and not to the gaugino fields in the first place.

4.2 Mass spectrum

Let us now explicitly solve the boundary conditions.

4.2.1 Bosonic Kaluza-Klein wave functions

We start with writing out the KK expansion of the 5D gauge fields in terms of the physical 4D fields

$$A_\mu^{L3}(x, z) = \frac{a_0}{g_5} \gamma_\mu(x) + \sum_k f_{L3}^{(k)}(z) Z_\mu^{(k)}(x), \quad (4.7a)$$

$$A_\mu^{R3}(x, z) = \frac{a_0}{g_5} \gamma_\mu(x) + \sum_k f_{R3}^{(k)}(z) Z_\mu^{(k)}(x), \quad (4.7b)$$

$$A_\mu^X(x, z) = \frac{a_0}{g_{5X}} \gamma_\mu(x) + \sum_k f_X^{(k)}(z) Z_\mu^{(k)}(x), \quad (4.7c)$$

$$A_\mu^{L\pm}(x, z) = \sum_k f_{L\pm}^{(k)}(z) W_\mu^{(k)\pm}(x), \quad (4.7d)$$

$$A_\mu^{R\pm}(x, z) = \sum_k f_{R\pm}^{(k)}(z) W_\mu^{(k)\pm}(x), \quad (4.7e)$$

where we used the fact that the massless photon has a flat KK function $f_\gamma(z) = a_0$. The general form of the bosonic KK wave function as derived in (1.47) is

$$f_i^k(z) = z (c_i^k J_1(m_k z) + d_i^k Y_1(m_k z)). \quad (4.8)$$

Using Taylor expansion for light modes with $m \ll \Lambda_I, \Lambda_{\text{II}}$ this can be approximated by:

$$f_i(z) \approx a_i + m^2 z^2 \left(b_i - \frac{a_i}{2} \log(zk) \right) + m^4 z^4 \left(-\frac{b_i}{8} - \frac{3a_i}{64} + \frac{a_i}{16} \log(zk) \right) + \mathcal{O}(m^6 z^6) \quad (4.9)$$

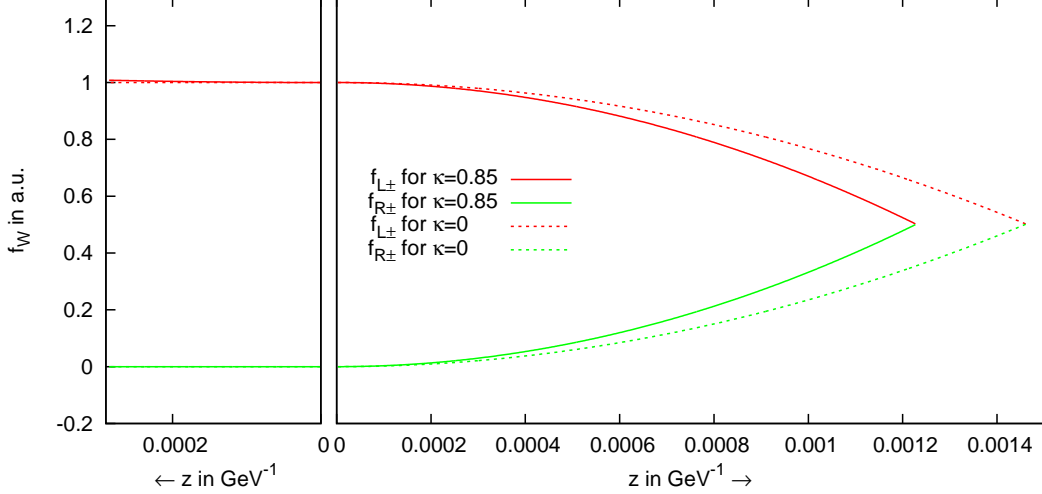


Fig. 4.1: Wavefunction of the W boson in the extra dimension with $\kappa > 0$ (solid line) compared to the case of $\kappa = 0$ (dashed line). As κ increases the wave function normalization, the length of the IR interval has to be decreased in order to reproduce the correct value of M_W .

The coefficients b_i are of order $\mathcal{O}(a_i \log(k/\Lambda))$ and the masses are of the order of $m_W^2, m_Z^2 \approx \Lambda^2 / \log(k/\Lambda)$. With $k = 10^{19}$ GeV and Λ_I, Λ_{II} of the order of $10^2 \dots 10^4$ GeV, we typically have $\log(k/\Lambda_{I,II}) = k\pi R_{I,II} = 30 \dots 40$. We define x , the expansion parameter, and f_R , relating the sizes of the two intervals, as

$$x = \frac{1}{k\pi(R_I + R_{II})} \quad \text{and} \quad f_R = \frac{R_{II}}{R_I + R_{II}}, \quad (4.10)$$

where $x \approx 1/72$ and $f_R \approx \frac{1}{2}$.

By solving the system of coupled boundary conditions we obtain the coefficients a_i, b_i . The approximate coefficients in leading x order are listed in App. B.2. The resulting wave functions are showed in fig. 4.1 and fig. 4.2.

4.2.2 Gauge boson and chargino masses

The solution for the W^\pm mass is given by:

$$m_W^2 = \frac{x}{1 + f_R \kappa} \Lambda_1^2 \frac{1 + \frac{3}{8} \left(\frac{x}{1 + f_R \kappa} \right)}{1 + \frac{1}{2} \left(\frac{f_R \kappa \Lambda_I}{1 + f_R \kappa \Lambda_{II}} \right)^2} + \mathcal{O}(x^2) \quad (4.11)$$

Observe that the mass eigenvalue is lowered by the brane kinetic term proportional to κ . This is due to the increased wave function normalization. To simplify the expression for the Z boson mass, we define

$$C_\kappa = \frac{1 + g_r^2(2 + f_R \kappa)}{(1 + g_r^2)(1 + f_R \kappa)}. \quad (4.12)$$

Then, the Z mass is given by:

$$m_Z^2 = C_\kappa x \Lambda_1^2 \left(1 + \frac{3}{8} x C_\kappa + \mathcal{O}(x^2) \right) \quad (4.13)$$

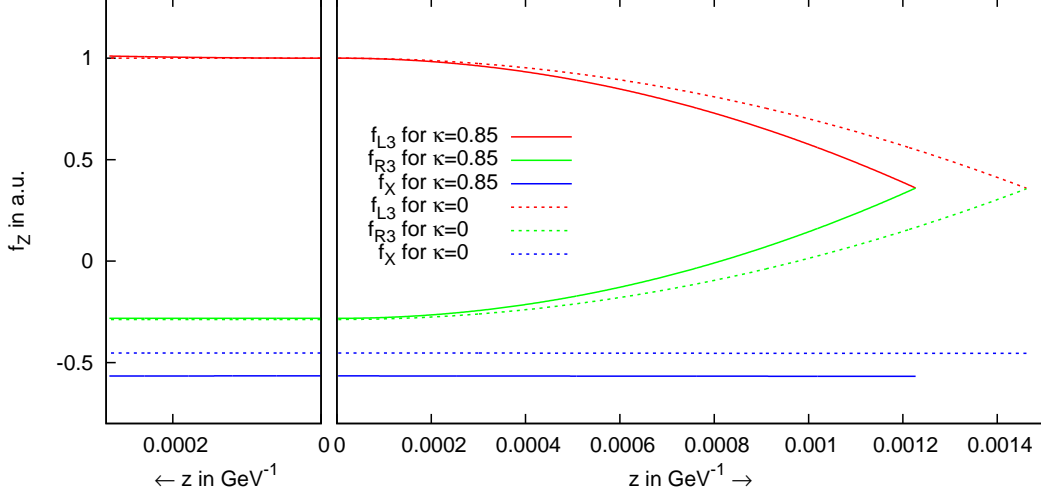


Fig. 4.2: Wavefunction of the Z boson in the extra dimension with $\kappa > 0$ (solid line) compared to the case of $\kappa = 0$ (dashed line). For $\kappa > 0$ the length $\frac{1}{\Lambda_1}$ decreases in order to reproduce the correct W mass. In comparison to the case for $\kappa = 0$, a smaller value for g_r is needed to obtain the correct Z mass, such that $\Phi_x(z)$ is lowered accordingly.

For a given κ , the mass ratio m_Z/m_W is defined by the relative coupling g_r . To leading order in x we exactly reproduce the SM mass relations and couplings. This is a consequence of the custodial symmetry $SU(2)_D$.

The superpartners of the gauge bosons, the chargino and the neutralino, are not affected by the brane kinetic term (4.5). In order to avoid massless solutions, they receive boundary conditions $\oplus \oplus \ominus$ at the SB brane, according to scenario 1b. Since the chargino and W^\pm boundary conditions are identical up to the brane kinetic term, the chargino mass is given by (4.11) for $\kappa \rightarrow 0$ as:

$$m_{\chi^\pm}^2 = x \Lambda_1^2 \left(1 + \frac{3}{8}x + \mathcal{O}(x^2) \right) \quad (4.14)$$

We find that $\kappa \gtrsim 0.8$ is required to make $m_\chi \geq 95\text{GeV}$. The neutralino in scenario 1b is degenerate in mass with the chargino up to order $\mathcal{O}(x^2)$:

$$m_{\chi^0}^2 = x \Lambda_1^2 \left(1 + \frac{3}{8}x + \mathcal{O}(x^2) \right) \quad (4.15)$$

Numerically, the neutralino turns out to be slightly lighter than the chargino, c.f. fig. 4.3.

4.2.3 Neutralino masses

One could ask why we have not introduced a localized mass term to raise the chargino mass instead of lowering the W^\pm mass.

As the symmetries on the SB brane forbid L - R mixing, the only possible mass term would be a Majorana mass term. Such a term couples the KK wave functions of λ_1 and λ_2 , which are of the form:

$$\begin{aligned} f_{\lambda_1}(z) &= (kz)^{5/2} [a_{\lambda_1} J_1(mz) + b_{\lambda_1} Y_1(mz)] \\ f_{\lambda_2}(z) &= (kz)^{5/2} [a_{\lambda_2} J_0(mz) + b_{\lambda_2} Y_1(mz)] \end{aligned} \quad (4.16)$$

The e.o.m. connecting f_{λ_1} and f_{λ_2} requires that $a_{\lambda_1} = \pm a_{\lambda_2}$ and $b_{\lambda_1} = \pm b_{\lambda_2}$. The boundary condition modified by the presence of a brane Majorana mass term contains f_{λ_1} and f_{λ_2} and

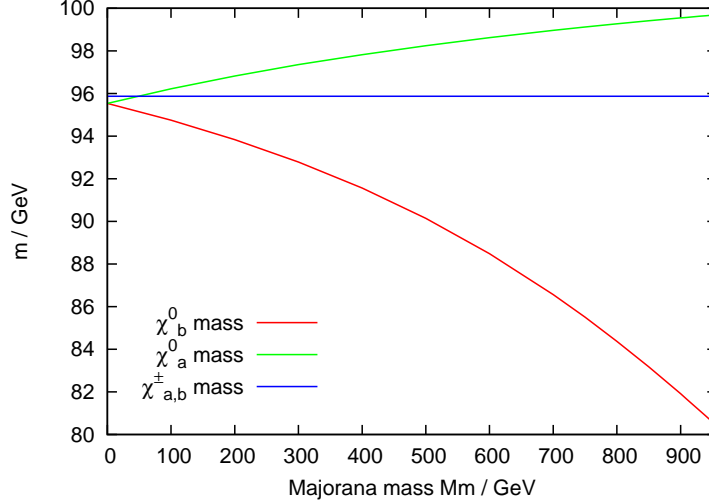


Fig. 4.3: Gaugino mass spectrum as a function of the Majorana mass term.

therefore lifts the degeneracy between the sign choices. Therefore, two solutions will arise, one with a larger and one with a smaller mass eigenvalue compared to the case without the brane localized Majorana mass term. As light charginos are experimentally excluded, Majorana mass terms are not useful for constructing a convincing spectrum for the charged gauginos.

Still, they become interesting in order to control neutralino masses. We assign a Majorana mass term proportional to M_m to the λ^X field, therefore only acting on the neutralinos without affecting the charginos. The localized term reads

$$S_{M_m} = -\frac{1}{2} \int dx^5 \frac{1}{(kz)^4} \cdot \frac{M_m}{z} \left(\lambda_1^X \lambda_1^X + \bar{\lambda}_1^X \bar{\lambda}_1^X \right) \delta(z - \Lambda_{\text{II}}^{-1}) \quad (4.17)$$

and modifies the Dirichlet boundary condition to

$$\lambda_1^X \Big|_{z=1/\Lambda_{\text{II}}} = 0 \quad \rightarrow \quad \lambda_1^X - \frac{M_m}{\Lambda_{\text{II}}} \lambda_2^X \Big|_{z=1/\Lambda_{\text{II}}} = 0.$$

The solutions belonging to the two possible sign choices $a_{\lambda_{2a}} = a_{\lambda_{1a}}$ and $a_{\lambda_{2b}} = -a_{\lambda_{1b}}$ are given by the following implicit expressions:

For the heavy neutralino:

$$m_{\chi_a^0}^2 = x \Lambda_{\text{I}}^2 \frac{1 + m_{\chi_a^0}^2 \frac{1}{x \Lambda_{\text{II}}^2} \left(M_m / m_{\chi_a^0} - \frac{1}{2} \right) (1 + 2g_r^2)}{1 - \frac{3}{8}x + m_{\chi_a^0}^2 \frac{1}{x \Lambda_{\text{II}}^2} \left(M_m / m_{\chi_a^0} - \frac{1}{2} \right) (1 + g_r^2)} \quad (4.18a)$$

And for the light neutralino:

$$m_{\chi_b^0}^2 = x \Lambda_{\text{I}}^2 \frac{1 - m_{\chi_b^0}^2 \frac{1}{x \Lambda_{\text{II}}^2} \left(M_m / m_{\chi_b^0} + \frac{1}{2} \right) (1 + 2g_r^2)}{1 - \frac{3}{8}x - m_{\chi_b^0}^2 \frac{1}{x \Lambda_{\text{II}}^2} \left(M_m / m_{\chi_b^0} + \frac{1}{2} \right) (1 + g_r^2)} \quad (4.18b)$$

The gaugino mass spectrum as a function of the Majorana mass M_m is showed in fig. 4.3. The mass spectrum of the entire gauge sector is presented in fig. 4.4.

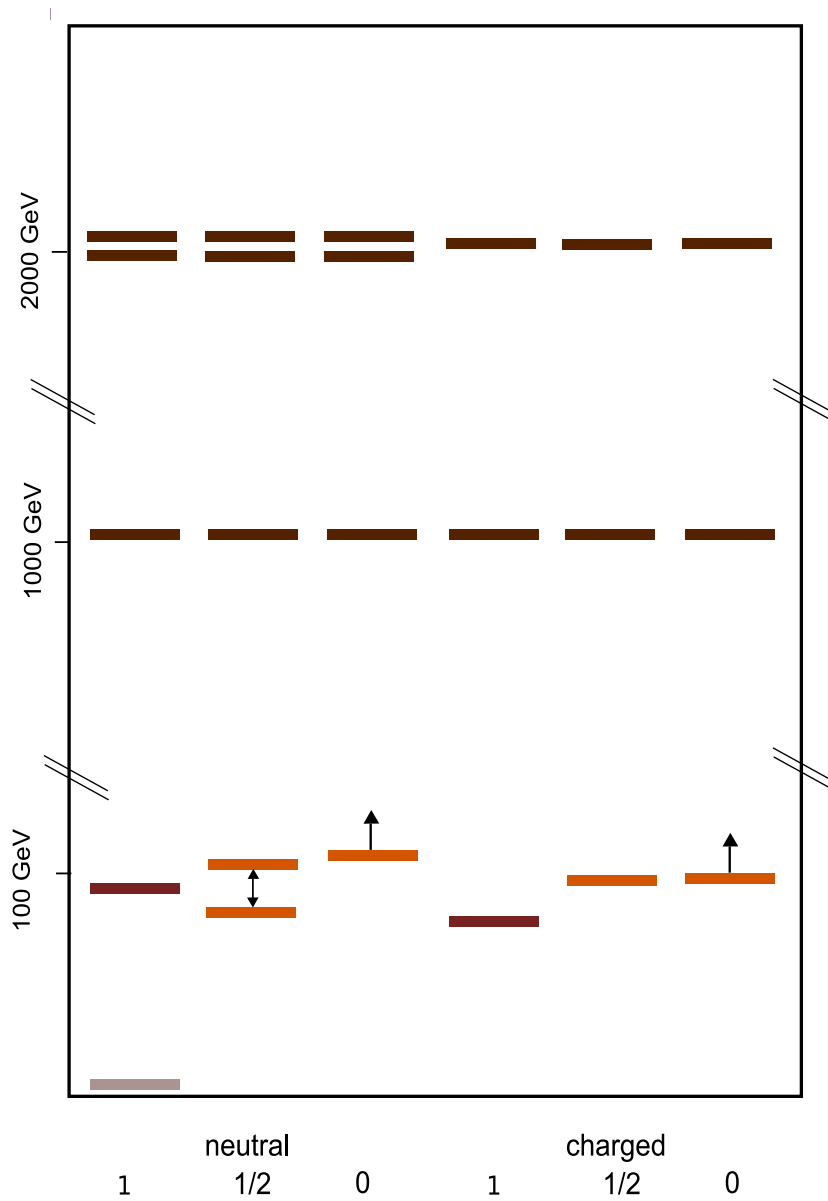


Fig. 4.4: Mass spectrum of the gauge sector. From left to right: γ and Z , neutralinos, Σ_0 , W^\pm , charginos, Σ_\pm . The scalars Σ_0 and Σ_\pm , not protected by a symmetry, are expected to be shifted by loop corrections. The neutralinos are split into a light (χ_b^0) and a heavy neutralino (χ_a^0) by the localized Majorana mass term from (4.17). The gaugino mass spectrum as function of this term is separately showed in fig. 4.3.

4.3 Interactions

Having implemented the gaugino sector, let us take a closer look at the corresponding interactions. We focus on the gaugino interactions which will be needed later.

In agreement to [15], we define the chargino mass eigenstates as:

$$\chi_a^+ = \frac{1}{\sqrt{2}} \begin{pmatrix} \lambda_1^1 - i\lambda_1^2 \\ \bar{\lambda}_2^1 - i\bar{\lambda}_2^2 \end{pmatrix} \quad \chi_b^+ = \frac{1}{\sqrt{2}} \begin{pmatrix} \lambda_2^1 - i\lambda_2^2 \\ \bar{\lambda}_1^1 - i\bar{\lambda}_1^2 \end{pmatrix} \quad (4.19a)$$

Their charge conjugates are defined as:

$$\chi_a^- = \frac{1}{\sqrt{2}} \begin{pmatrix} \lambda_2^1 + i\lambda_2^2 \\ \bar{\lambda}_1^1 + i\bar{\lambda}_1^2 \end{pmatrix} \quad \chi_b^- = \frac{1}{\sqrt{2}} \begin{pmatrix} \lambda_1^1 + i\lambda_1^2 \\ \bar{\lambda}_2^1 + i\bar{\lambda}_2^2 \end{pmatrix} \quad (4.19b)$$

Here, λ_i^1 stands for the 4D KK coefficient function $\lambda_i^1(x)$ of the 5D fields $\lambda_i^{L1}(x, z)$ and $\lambda_i^{R1}(x, z)$. Analogously, λ_i^2 labels the KK coefficients of $\lambda_i^{L2}(x, z)$ and $\lambda_i^{R2}(x, z)$. For the sake of shortness, we have neither written out the dependence on the Minkowski coordinate x^μ nor the KK index. The next KK mode of the chargino appears at ≈ 2 TeV, and we do not need to consider it in the further course of this work.

The neutralino mass eigenstates read:

$$\chi_a^0(x) = \frac{1}{\sqrt{2}} \begin{pmatrix} \lambda_1^0 + \lambda_2^0 \\ \lambda_1^0 + \lambda_2^0 \end{pmatrix} \quad \chi_b^0(x) = \frac{i}{\sqrt{2}} \begin{pmatrix} \lambda_1^0 - \lambda_2^0 \\ \lambda_2^0 - \lambda_1^0 \end{pmatrix} \quad (4.20)$$

Again, λ_i^0 stands for the KK coefficient function to the neutral 5D fields coupled by boundary conditions which are λ_i^{L3} , λ_i^{R3} and λ_i^X .

Observe that the neutralinos are Majorana spinors and that the indices a, b correspond to the sign choice between the f_{λ_1} and f_{λ_2} KK wave functions discussed before.

4.3.1 Gaugino interactions with gauge bosons

Within the gauge part $\mathcal{L}_g(V, \chi)$ of the full Lagrangian (3.10), we identify the pieces describing the gaugino interaction:

$$\begin{aligned} \mathcal{L}_{G,\text{int},\lambda} = & \frac{ig}{(kz)^4} \left[f^{abc} A_\mu^a \lambda_1^b \sigma^\mu \bar{\lambda}_1^c + f^{abc} A_\mu^a \lambda_2^b \sigma^\mu \bar{\lambda}_2^c \right] \\ & - \frac{ig}{(kz)^5} \left[f^{abc} \Sigma^a (\bar{\lambda}_2^b \bar{\lambda}_1^c - \lambda_2^b \lambda_1^c) + i f^{abc} A_5^a (\bar{\lambda}_2^b \bar{\lambda}_1^c + \lambda_2^b \lambda_1^c) \right] \end{aligned} \quad (4.21)$$

Here we have already carried out the redefinitions (2.45). The fields are the complete 5D fields $\phi = \phi(x) f_\phi(z)$.

W^\pm – neutralino – chargino interactions

The charged current interaction Lagrangian from the first line of (4.21) can be rewritten using the Fierz transformation formula

$$\chi \sigma^\mu \bar{\phi} = -\bar{\phi} \bar{\sigma}^\mu \chi,$$

as

$$\begin{aligned}
 \mathcal{L}_{G,\text{int},\lambda} = & -\frac{g_5}{2}(A_\mu^1 - iA_\mu^2)f_{W^\pm} \left[\left((\lambda_2^1 + i\lambda_2^2)f_{\lambda_2^\pm}, (\bar{\lambda}_1^1 + i\bar{\lambda}_1^2)f_{\lambda_1^\pm} \right) \gamma^m \begin{pmatrix} \lambda_1^0 f_{\lambda_1^0} \\ \bar{\lambda}_2^0 f_{\lambda_2^0} \end{pmatrix} \right. \\
 & + \left. \left((\lambda_1^1 + i\lambda_1^2)f_{\lambda_1^\pm}, (\bar{\lambda}_2^1 + i\bar{\lambda}_2^2)f_{\lambda_2^\pm} \right) \gamma^m \begin{pmatrix} \lambda_2^0 f_{\lambda_2^0} \\ \bar{\lambda}_1^0 f_{\lambda_1^0} \end{pmatrix} \right] \\
 & + \text{h.c.},
 \end{aligned} \tag{4.22}$$

where we have explicitly separated 4D coefficient fields and KK fields. Next we have to sum over $SU(2)_L$ and $SU(2)_R$ fields. This is simple, because the 4D fields are identical:

$$A_\mu^{L1,L2}(x,z) + A_\mu^{R1,R2}(x,z) = A_\mu^{1,2}(x)f_{WL^\pm} + A_\mu^{1,2}(x)f_{WR^\pm}$$

. The same holds true the $\lambda(x,z)$ fields. Integrating over the extra dimension, the KK wave functions are absorbed into overlap integrals which we define as:

$$\begin{aligned}
 \langle W^\pm \lambda_i \lambda_j \rangle = & \int_{1/k}^{1/\Lambda_1} dz (kz)^{-4} f_{W^\pm}^I(z) f_{\lambda_i}^I(z) f_{\lambda_j}^I(z) \\
 & + \int_{1/k}^{1/\Lambda_2} dz (kz)^{-4} f_{W^\pm}^{II}(z) f_{\lambda_i}^{II}(z) f_{\lambda_j}^{II}(z)
 \end{aligned} \tag{4.23}$$

With this definition, we can write (4.22) as effective 4D interaction of the bosonic eigenstates $W^\pm = \frac{1}{\sqrt{2}}(A_\mu^1 \mp iA_\mu^2)$ and the chargino and neutralino eigenstates (4.19a) and (4.20) as

$$\mathcal{L}_{G,\text{int},\lambda} = -\frac{1}{\sqrt{2}}W_\mu^+ \left[\overline{\chi}_a^+ \Gamma_a^\mu (\chi_a^0 - i\chi_b^0) + \overline{\chi}_b^+ \Gamma_b^\mu (\chi_a^0 + i\chi_b^0) \right] + \text{h.c.}, \tag{4.24}$$

where the corresponding coupling matrices $\Gamma_{a,b}^\mu$ are:

$$\begin{aligned}
 \Gamma_a^\mu = & g_5 \gamma^\mu \left[P^- (\langle W^{L\pm} \lambda_2^{L\pm} \lambda_2^{L3} \rangle + \langle W^{R\pm} \lambda_2^{R\pm} \lambda_2^{R3} \rangle) \right. \\
 & \left. + P^+ (\langle W^{L\pm} \lambda_1^{L\pm} \lambda_1^{L3} \rangle + \langle W^{R\pm} \lambda_1^{R\pm} \lambda_1^{R3} \rangle) \right] \\
 \Gamma_b^\mu = & \Gamma_a^\mu (P^+ \leftrightarrow P^-).
 \end{aligned}$$

The vertex diagrams are showed in fig. 4.5. The vector coupling is given by

$$g_A = -\frac{1}{2}g_5 (\langle W^{L\pm} \lambda_1^{L\pm} \lambda_1^{L3} \rangle + \langle W^{R\pm} \lambda_1^{R\pm} \lambda_1^{R3} \rangle + \langle W^{L\pm} \lambda_2^{L\pm} \lambda_2^{L3} \rangle + \langle W^{R\pm} \lambda_2^{R\pm} \lambda_2^{R3} \rangle)$$

and the axial-vector coupling by

$$g_A = -\frac{1}{2}g_5 (-\langle W^{L\pm} \lambda_1^{L\pm} \lambda_1^{L3} \rangle - \langle W^{R\pm} \lambda_1^{R\pm} \lambda_1^{R3} \rangle + \langle W^{L\pm} \lambda_2^{L\pm} \lambda_2^{L3} \rangle + \langle W^{R\pm} \lambda_2^{R\pm} \lambda_2^{R3} \rangle).$$

The coupling strength depends on the Majorana mass term M_m modifying the neutralino wave function and indirectly on the neutralino mass.

In fig. 4.6, we show at the left hand side the light neutralino couplings g_A^b and g_B^b in dependence of $m_{\chi_b^0}$. At the right hand side, similarly g_A^a and g_B^a are showed in dependence of $m_{\chi_a^0}$. We observe that the coupling depends only weakly on the mass².

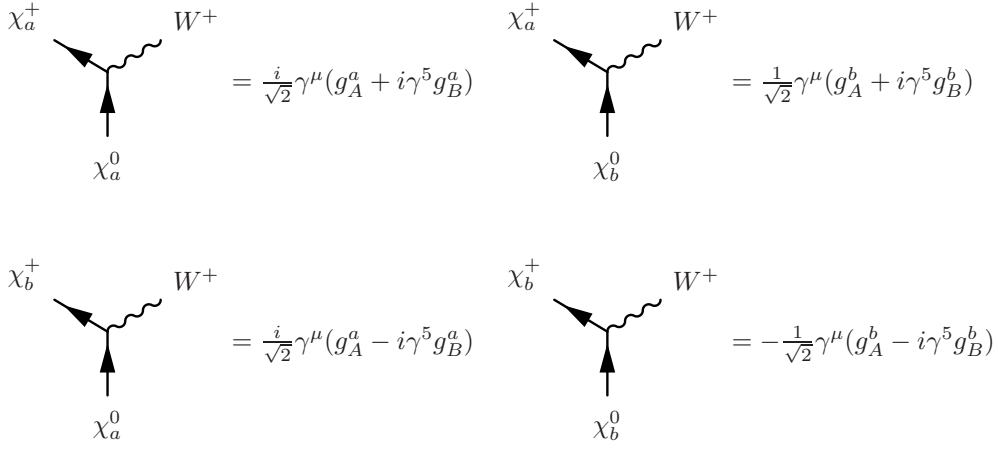
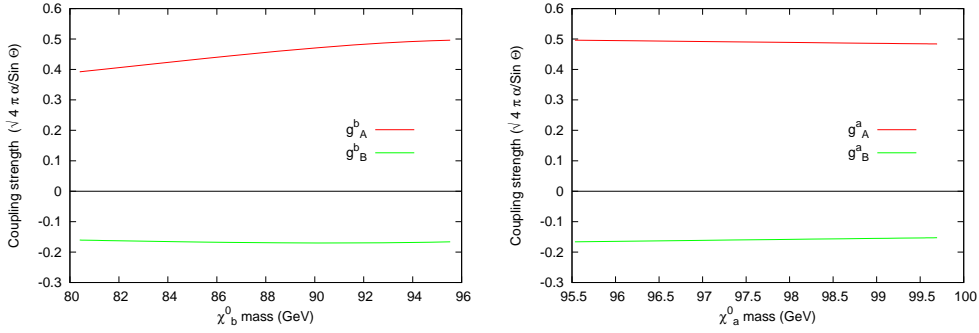


Fig. 4.5: The vertices of the charged current coupling.

Fig. 4.6: Left: Strength of the charged coupling in dependence of light neutralino χ_b^0 mass. Right: Strength of the charged coupling in dependence of heavy neutralino χ_a^0 mass. $g_A^{a,b}$ denotes the vector coupling, $g_B^{a,b}$ the axial-vector coupling.

Z/γ -chargino interactions

The neutral current interaction, obtained in a similar way as the charged current interaction, reads

$$\mathcal{L} = \gamma_\mu(x) \left[\overline{\chi_a^+} \Gamma_{\gamma a}^\mu \chi_a^+ + \overline{\chi_b^+} \Gamma_{\gamma b}^\mu \chi_b^+ \right] + Z_\mu(x) \left[\overline{\chi_a^+} \Gamma_{Z a}^\mu \chi_a^+ + \overline{\chi_b^+} \Gamma_{Z b}^\mu \chi_b^+ \right], \quad (4.25)$$

where the corresponding vertex expressions are

$$\Gamma_{Z a}^\mu = g_5 \gamma^\mu \left[P^+ (\langle Z^{L3} \lambda_1^{L\pm} \lambda_1^{L\pm} \rangle + \langle Z^{R3} \lambda_1^{R\pm} \lambda_1^{R\pm} \rangle) + P^- (\langle Z^{L3} \lambda_2^{L\pm} \lambda_2^{L\pm} \rangle + \langle Z^{R3} \lambda_2^{R\pm} \lambda_2^{R\pm} \rangle) \right] \quad (4.26a)$$

$$\Gamma_{Z b}^\mu = \Gamma_{Z a}^\mu (P^+ \leftrightarrow P^-). \quad (4.26b)$$

The photon vertices are obtained in a similar way. They simplify drastically, taking into account canonical normalization of the charginos and $a_0 = e$, c.f. the matching conditions in (6.25).

²This is an effect of the “soft” SUSY breaking at the second IR brane. In [1], SUSY breaking was done on the UV brane, which suppressed the $\langle W^\pm \lambda_1^\pm \lambda_1^0 \rangle$ overlaps and effectively decreased the coupling strength.

4 Gauge sector

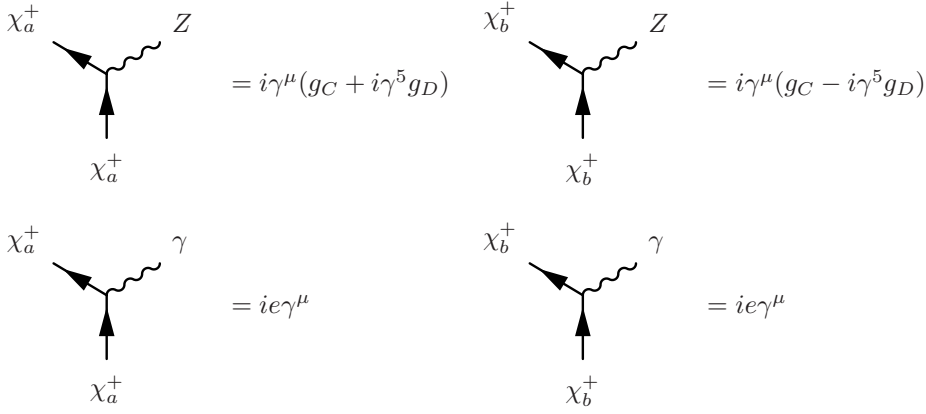


Fig. 4.7: The vertices of the neutral current coupling.

Especially, the coupling is entirely vector-like:

$$\begin{aligned} \Gamma_{\gamma a}^n &= a_0 \gamma^n [P^+ (\lambda_1^{L\pm} \lambda_1^{L\pm}) + \langle \lambda_1^{R\pm} \lambda_1^{R\pm} \rangle \\ &\quad + P^- (\langle \lambda_2^{L\pm} \lambda_2^{L\pm} \rangle + \langle \lambda_2^{R\pm} \lambda_2^{R\pm} \rangle)] , \\ &= e \gamma^n \end{aligned} \quad (4.26c)$$

$$\Gamma_{\gamma b}^n = \Gamma_{\gamma a}^n \quad (4.26d)$$

The vertices are showed in fig. 4.7. The coupling strength obtained from the overlaps intergals in units of $\sqrt{4\pi\alpha} \sin^{-1} \Theta_W$ is

$$g_C = 0.396 \quad \text{and} \quad g_D = -0.188 .$$

Note there is no $Z\chi^0\chi^0$ interaction because of the antisymmetric tensor f^{abc} in (4.21) which forbids the interaction between three neutral gauge fields.

4.3.2 Neutralino interactions with matter

The interactions of gauginos with matter are encoded in the $\mathcal{L}_h(H, H^c, V, \chi)$ part of (3.10). The expansion into the multiplet fields leads to the following terms containing λ_1 and λ_2 :

$$\begin{aligned} \mathcal{L}_{\text{h,int},\lambda} &= \frac{ig}{(kz)^5} \left[\sqrt{2}\lambda_1^l \bar{\psi} T^l h - \sqrt{2}h^\dagger T^l \psi \lambda_1^l - \sqrt{2}h^c T^l \bar{\psi}^c \lambda_1^l + \sqrt{2}\lambda_1^l \psi^c T^l h^{c\dagger} \right. \\ &\quad \left. + \sqrt{2}\lambda_2^l \bar{\psi} T^l h^{c\dagger} + \sqrt{2}h^\dagger T^l \bar{\psi}^c \lambda_2^l - \sqrt{2}h^c T^l \psi \lambda_2^l - \sqrt{2}\lambda_2^l \psi^c T^l h \right] \end{aligned} \quad (4.27)$$

Concentrating only on the neutralino interaction, we obtain as 4D effective Lagrangian:

$$\mathcal{L}_{\text{h,int},\lambda^0} = h_i^j \bar{\Psi}_i^i i \Gamma_{ij} (\chi_a^0 + i \chi_b^0) + h_i^{c\dagger} \bar{\Psi}_i^c i \Gamma_{ij}^c (\chi_a^0 - i \chi_b^0) + \text{h.c.} . \quad (4.28)$$

with the coupling matrices

$$\Gamma_{ij} = g_5 \delta_{ij} \left[\begin{aligned} &T_{3L} [P^- \langle \lambda_1^{L3} \psi_{Li} h_{Lj} \rangle - P^+ \langle \lambda_2^{L3} \psi_{Li}^c h_{Lj} \rangle] \\ &+ T_{3R} [P^- \langle \lambda_1^{R3} \psi_{Ri} h_{Rj} \rangle - P^+ \langle \lambda_2^{R3} \psi_{Ri}^c h_{Rj} \rangle] \\ &+ g_r X [P^- \langle \lambda_1^X \psi_{Li} h_{Lj} \rangle - P^+ \langle \lambda_2^X \psi_{Li}^c h_{Lj} \rangle] \\ &+ g_r X [P^- \langle \lambda_1^X \psi_{Ri} h_{Rj} \rangle - P^+ \langle \lambda_2^X \psi_{Ri}^c h_{Rj} \rangle] \end{aligned} \right]$$

$$\Gamma_{ij}^c = g_5 \delta_{ij} \left[\begin{aligned} & T_{3L} [P^- \langle \lambda_2^{L3} \psi_{Li} h_{Lj}^c \rangle + P^+ \langle \lambda_1^{L3} \psi_{Li}^c h_{Lj}^c \rangle] \\ & + T_{3R} [P^- \langle \lambda_2^{R3} \psi_{Ri} h_{Rj}^c \rangle + P^+ \langle \lambda_1^{R3} \psi_{Ri}^c h_{Rj}^c \rangle] \\ & + g_r X [P^- \langle \lambda_2^X \psi_{Li} h_{Lj}^c \rangle + P^+ \langle \lambda_1^X \psi_{Li}^c h_{Lj}^c \rangle] \\ & + g_r X [P^- \langle \lambda_2^X \psi_{Ri} h_{Rj}^c \rangle + P^+ \langle \lambda_1^X \psi_{Ri}^c h_{Rj}^c \rangle] \end{aligned} \right].$$

This time, the overlap integrals contain the metric factor $(kz)^{-5}$:

$$\begin{aligned} \langle \lambda \psi h \rangle = & \int_{1/k}^{1/\Lambda_I} dz (kz)^{-5} f_\lambda^I(z) f_\psi^I(z) f_h^I(z) \\ & + \int_{1/k}^{1/\Lambda_{II}} dz (kz)^{-5} f_\lambda^{II}(z) f_\psi^{II}(z) f_h^{II}(z) \end{aligned} \quad (4.29)$$

The quantum numbers are $T^{3L,R} = \pm \frac{1}{2}$ and $X = -\frac{1}{2}, \frac{1}{6}$ and the index i runs over the fermion types and generations. The couplings, calculated using the parameter set we will present in the next chapter, are all smaller than $10^{-2} \cdot \sqrt{4\pi\alpha} / \sin \Theta_W$.

5 Fermions and sfermions

In this chapter we want to discuss how fermions and their supersymmetric partner fields are implemented into our model and illustrate the reasons for assigning to them the boundary conditions listed in chap. 3. We conclude this chapter presenting a possible parameter set for the matter sector and discussing the resulting mass spectrum.

5.1 Implementation

We assume that the left handed standard model fermions form $SU(2)_L$ doublets and the right handed SM fermions, including a right handed neutrino, form $SU(2)_R$ doublets [25]. As discussed in subsection 1.4.3, 5D bulk spinors are of Dirac type and contain two 4D Weyl spinors. By boundary conditions, one has to insure that within every 5D fermion only one single massless 4D Weyl fermion exists. The zero modes will be identified with the SM fermions. The overall bulk symmetry is

$$SU(3)_C \times SU(2)_L \times SU(2)_R \times U(1)_X.$$

The leptons are in the representation

$$L_L \sim (\mathbf{1}, \mathbf{2}, \mathbf{1}, -1) \quad L_R \sim (\mathbf{1}, \mathbf{1}, \mathbf{2}, -1) \quad (5.1)$$

and the quarks are in

$$Q_L \sim (\mathbf{3}, \mathbf{2}, \mathbf{1}, 1/3) \quad Q_R \sim (\mathbf{3}, \mathbf{1}, \mathbf{2}, 1/3). \quad (5.2)$$

Writing each Dirac spinor in terms of a pair of two-component spinors $(\eta, \bar{\chi})^T$, the doublets constituting a fermion generation are

$$\begin{aligned} \Psi_L &= (\eta_L^u, \bar{\chi}_L^u, \eta_L^d, \bar{\chi}_L^d)^T, \\ \Psi_R &= (\eta_R^u, \bar{\chi}_R^u, \eta_R^d, \bar{\chi}_R^d)^T. \end{aligned} \quad (5.3)$$

The superscript u stands either for a neutrino or a quark of electric charge $2/3$ (u -type) with $T_{3D} = T_{3L} + T_{3R} = 1/2$. Similarly, d denotes either a charged lepton or a quark with charge $-1/3$ (d -type) and $T_{3D} = -1/2$.

In the supersymmetric extension of the model, the lefthanded η spinors are embedded into the H part of the hypermultiplet (2.36) and the righthanded χ spinors into the H^c part. This means that for each SM fermion doublet one set of (H_L, H_L^c, H_R, H_R^c) is added to our model.

5.2 Matter

We start with describing how the standard model matter content is reproduced.

5.2.1 Massless fermions

Consider the following boundary conditions:

	SB brane	UV brane	EWSB brane	
η_L	\oplus	\Leftrightarrow	\oplus	(5.4)
χ_R	\oplus	\Leftrightarrow	\oplus	
η_R	\ominus	\Leftrightarrow	\ominus	
χ_L	\ominus	\Leftrightarrow	\ominus	

The “ \Leftrightarrow ” symbolizes a transition condition of the form (3.7). The corresponding KK towers of η_L and χ_R will each contain a zero mode, while for η_R and χ_L there will be no massless solutions.

Of course we do not really want massless fermions, but considering the relevant mass scale of KK excitations of approximately 1 TeV, they are a good start. The analytic expressions of the massless KK wavefunctions can easily be obtained by solving the differential equations (1.40) for the massless case. The KK wave functions are given in tab. 5.1. To satisfy the boundary

	$z \in [\frac{1}{k}, \frac{1}{\Lambda_I}]$	$z \in [\frac{1}{k}, \frac{1}{\Lambda_{II}}]$
$f_{0\eta_L}(z) =$	$A_{0\eta_L}(kz)^{2-c_{LI}}$	$t_L A_{0\eta_L}(kz)^{2-c_{LII}}$
$f_{0\eta_R}(z) =$	$t_R A_{0\eta_R}(kz)^{2-c_{RI}}$	$-A_{0\eta_R}(kz)^{2-c_{RII}}$
$f_{0\chi_L}(z) =$	$t_L A_{0\chi_L}(kz)^{2+c_{LI}}$	$-A_{0\chi_L}(kz)^{2+c_{LII}}$
$f_{0\chi_R}(z) =$	$A_{0\chi_R}(kz)^{2+c_{RI}}$	$t_R A_{0\chi_R}(kz)^{2+c_{RII}}$

Tab. 5.1: KK functions of massless fermions.

conditions given in sec. 3.2.3, $A_{0\eta_R} = A_{0\chi_L} = 0$ is required. The remaining normalizations $A_{0\eta_L}$ and $A_{0\chi_R}$ are found by the normalization condition:

$$\int_{1/k}^{1/\Lambda_I} \frac{dz}{(kz)^4} (f_0^I)^2 + \int_{1/k}^{1/\Lambda_{II}} \frac{dz}{(kz)^4} (f_0^{II})^2 = 1$$

The metric factor $(kz)^{-4}$ results from the density factor $\sqrt{g} = (kz)^{-5}$ and from the inverse fünfbein e_a^M coming along with the Dirac matrix in the spinor field kinetic term in (1.33). The normalizations read:

$$\begin{aligned} A_{0\eta_L} &= \sqrt{k} \left(\frac{1 - (\frac{\Lambda_I}{k})^{2c_{LI}-1}}{2c_{LI} - 1} + t_L^2 \frac{1 - (\frac{\Lambda_{II}}{k})^{2c_{LII}-1}}{2c_{LII} - 1} \right)^{-1/2} \\ A_{0\chi_R} &= \sqrt{k} \left(\frac{1 - (\frac{\Lambda_I}{k})^{-2c_{RI}-1}}{-2c_{LI} - 1} + t_R^2 \frac{1 - (\frac{\Lambda_{II}}{k})^{-2c_{RII}-1}}{-2c_{RII} - 1} \right)^{-1/2} \end{aligned} \quad (5.5)$$

Since Λ/k is a very small number of $\mathcal{O}(10^{-16})$, we find a kind of seesaw behavior depending on

whether the exponents are positive or negative. It is useful to define:

$$\alpha_{L\text{I,II}} := c_{L\text{I,II}} - \frac{1}{2} \quad (5.6a)$$

$$\alpha_{R\text{I,II}} := -c_{R\text{I,II}} - \frac{1}{2} \quad (5.6b)$$

$$\text{and } A_{0L,R} := \left(\frac{1 - \left(\frac{\Lambda_{\text{I}}}{k}\right)^{2\alpha_{L\text{I},R\text{I}}}}{\alpha_{L\text{I},R\text{I}}} + t_{L,R}^2 \frac{1 - \left(\frac{\Lambda_{\text{II}}}{k}\right)^{2\alpha_{L\text{II},R\text{II}}}}{\alpha_{L\text{II},R\text{II}}} \right)^{-1/2} \quad (5.6c)$$

Then

$$A_{0\chi_R} = \sqrt{2k}A_{0R} \quad \text{and} \quad A_{0\eta_L} = \sqrt{2k}A_{0L}.$$

In proper distance coordinates, the normalized KK wavefunctions $\sqrt{R}e^{-3/2 Rk\pi} f_{\eta\chi 0}$ are Planck localized if $\alpha_L, \alpha_R > 0$ and IR localized if $\alpha_L, \alpha_R < 0$, c.f. tab. 5.1.

5.2.2 Massive fermions via Dirac mass terms

At the EWSB brane, the remaining unbroken symmetry is $SU(2)_D$ and the theory is non-chiral. Therefore, we can add a localized Dirac mass term

$$S_{M_D} = - \int dx^5 \frac{1}{(kz)^4} \delta(z - z_0) \frac{M_D}{\Lambda_{\text{I}}} \left(H_R H_L^c + \overline{H}_L^c \overline{H}_R + H_L H_R^c + \overline{H}_R^c \overline{H}_L \right), \quad (5.7)$$

where $z_0 = \Lambda_{\text{I}}^{-1}$ is the position of the EWSB brane. The localized term (5.7) leads to a δ -shaped modification of the original e.o.m. of the fermions given in (1.37). The deformed e.o.m. for η_L in the interval I is

$$-i \sigma^\mu \partial_\mu \overline{\eta}_L^{\text{I}} + \partial_z \chi_L^{\text{I}} - \frac{(2+c)}{z} \chi_L^{\text{I}} - \frac{M_D}{\Lambda_{\text{I}}} \chi_R^{\text{I}} \delta(z - z_0 + \varepsilon) = 0, \quad (5.8)$$

where we have shifted the localized term by an infinitesimal amount ε away from the brane. By integrating (5.8) one finds that χ_L^{I} undergoes a jump:

$$[\chi_L^{\text{I}}]_{z_0-\varepsilon} = -\frac{M_D}{\Lambda_{\text{I}}} \chi_R^{\text{I}}|_{z_0-\varepsilon}$$

If χ_L^{I} previously has satisfied a Dirichlet boundary condition $\chi_L^{\text{I}}|_{z_0} = 0$, we now obtain in the limit of $\varepsilon \rightarrow 0$ the modified condition

$$\chi_L^{\text{I}}|_{z_0} = -\frac{M_D}{\Lambda_{\text{I}}} \chi_R^{\text{I}}|_{z_0}. \quad (5.9)$$

Analogously, the Dirichlet boundary condition of the η_R field in the presence of the Dirac mass term (5.7) is modified to

$$\eta_R^{\text{I}}|_{z_0} = \frac{M_D}{\Lambda_{\text{I}}} \eta_L^{\text{I}}|_{z_0}. \quad (5.10)$$

These are just the boundary conditions we have specified in (3.18). Note that they still eliminate the boundary term

$$\mathcal{B} = \frac{1}{(kz)^4} (\eta_L^{\text{I}} \chi_L^{\text{I}} + \eta_R^{\text{I}} \chi_R^{\text{I}})|_{z=z_0} = \frac{1}{(kz)^4} \left(\eta_L^{\text{I}} \chi_L^{\text{I}} \left[1 + \frac{M_D}{\Lambda_{\text{I}}} \left(-\frac{\Lambda_{\text{I}}}{M_D} \right) \right] \right) = 0.$$

Solving the modified system of boundary conditions for the fermions, using $m_f \ll \Lambda_{\text{I}}, \Lambda_{\text{II}}$, finally gives the approximate expression

$$m_f \approx 2M_D \left(\frac{\Lambda_{\text{I}}}{k} \right)^{\alpha_{L\text{I}}} \left(\frac{\Lambda_{\text{I}}}{k} \right)^{\alpha_{R\text{I}}} A_{0L} \cdot A_{0R} \quad (5.11)$$

for the fermion mass. Even for the top quark with $m_t = 171$ GeV (5.11) is still a good approximation. By numerically solving the boundary conditions and plugging the obtained mass solution back into the fermionic KK wavefunctions, one can check that the light fermions predominantly¹ live in the formerly massless KK wave functions $f_{\eta L}$ and $f_{\chi R}$. This justifies the appearance of the massless normalization terms A_{0L} and A_{0R} in (5.11).

Observe that the fermion mass m_f depends mainly on the localization within the I interval. The localization parameters of the II interval α_{LII} and α_{RII} enter only via the normalization terms A_{0L} and A_{0R} . In particular, the mass will be suppressed if the fermion is Planck localized ($\alpha_{LI}, \alpha_{RI} > 0$). The fermion becomes heavy if is located near the EWSB brane ($\alpha_{LI}, \alpha_{RI} < 0$). Since the mass is the effect of the EWSB localized Dirac mass term, this is the behavior one would expect.

5.2.3 Mass splitting

So far, neutrinos and charged leptons, as well as u - and d -type quarks, are degenerate due to unbroken global $SU(2)_R$ symmetry. To obtain a realistic spectrum, we have to break $SU(2)_R$ by boundary conditions. According to our symmetry breaking pattern, this is done at the Planck brane. The simplest possibility is to change the transition parameter t_R , defining the connection between $f_{\eta R}, f_{\chi R}^I$ and $f_{\eta R}, f_{\chi R}^{II}$. The “ \Leftrightarrow ” condition at the Planck brane (3.19) reads:

$$\begin{aligned} f_{\chi R}^{II} &= t_R f_{\chi R}^I \\ f_{\eta R}^{II} &= -\frac{1}{t_R} f_{\eta R}^I \end{aligned} \quad (5.12)$$

By choosing a larger value of t_R for the lighter part of the $SU(2)_R$ doublet, the proportion of $f_{\chi R}^{II}/f_{\chi R}^I$ is increased, effectively weakening the influence of the Dirac term at the EWSB brane. This is how we will generate the mass splitting in the quark sector. We choose the other transition parameter $t_L = 1$ for all leptons and quarks.

In the two brane model, the splitting is achieved by an additional UV localized 4D spinor, coupling only to the u -type part [25]. Solving the e.o.m., this looks like an additional kinetic term for the u -quarks, effectively decreasing the mass. The resulting boundary conditions can be found in the appendix in C.1. The mechanism of mass splitting is similar to the three brane case in the sense that the mass shift is obtained by changing the normalization of the lighter quarks.

5.2.4 Neutrinos

At first sight, one could try to implement the neutrino similarly. The mass splitting has to be various orders of magnitude, because the neutrino is much lighter than the charged leptons, and would require an enormously large t_R value. However, the neutrino is not just light, it is also different from the charged fermions because there are no (observed) righthanded neutrinos. Therefore, let us consider the case of adding a localized Majorana mass term at the Planck brane, reading

$$S_{M_M} = \frac{1}{2} \int dx^5 \frac{1}{(kz)^4} \delta(z - z_0) \frac{M_M}{k} \left(H_R^c H_R^c + \overline{H}_R^c \overline{H}_R^c \right), \quad (5.13)$$

where $z_0 = 1/k$. The analysis of the e.o.m. leads to the deformed boundary condition

$$\eta_R^I + t_R \eta_R^{II} - \frac{M_M}{k} \left(\chi_R^I + \frac{1}{t_R} \chi_R^{II} \right) \Big|_{z=1/k} = 0, \quad (5.14)$$

¹For example in case of the electron 99.99996% of the normalization is generated by the formerly massless KK wave functions.

which is the same we stated in (3.20). We discussed in sec. 4.2.3 of the previous chapter, that a localized Majorana term lifts the degeneracy of the mass eigenstates corresponding to the two possible sign choices of the coefficients $(a_\eta, b_\eta) = \pm(a_\chi, b_\chi)$. Since the Majorana mass term is assigned on the UV brane, it has a very strong effect and leads to a seesaw mechanism, giving rise to one very light solution and another heavy one which is pushed out of the spectrum. For further details on Majorana masses and the seesaw mechanism see [26]. The light solution is given by

$$m_\nu \approx \frac{M_D^2}{M_M} A_{0L}^2 \left(\frac{\Lambda_I}{k} \right)^{2(\alpha_{LI} + \alpha_{RI})} = \frac{1}{4} \frac{m_f^2}{M_M A_{0R}^2}. \quad (5.15)$$

The required very small neutrino mass can be achieved by a Majorana mass term of the order $M_M \approx 10^{11}$ GeV. Despite the large number, this is rather small compared to the relevant scale at the Planck brane of $k = 10^{19}$ GeV.

The Majorana mass term M_M couples f_{χ_R} and f_{η_R} . Due to the choice of the boundary conditions on the EWSB and the SB brane, f_{η_R} is zero in the massless case, or very close to zero for $M_D \neq 0$. Therefore, f_{χ_R} will be strongly suppressed. Due to the IR boundary conditions, also f_{χ_L} is suppressed. So ultimately, we find the right handed modes to vanish. Thus, we have achieved the right handed neutrino to be sterile as required by (the absence of) experimental observation.

5.3 Smatter

Due to unbroken Supersymmetry, the entire multiplet is assigned the same boundary conditions on the EWSB and Planck brane and the same localization parameters α_{LI} , α_{LII} , α_{RI} and α_{RII} . SUSY is broken on the remaining IR brane in the second interval.

5.3.1 Charged sfermions

We choose to break Supersymmetry by simply giving the sfermion fields boundary conditions opposite to the ones we have defined for fermions in (5.4) at the SB brane:

	SB brane	UV brane	EWSB brane
h_L	\ominus	\Leftrightarrow	$\oplus(M_D)$
h_R^c	\ominus	$\Leftrightarrow (t_R, M_M)$	$\oplus(M_D)$
h_R	\oplus	$\Leftrightarrow (t_R, M_M)$	$\ominus(M_D)$
h_L^c	\oplus	\Leftrightarrow	$\ominus(M_D)$

(5.16)

We have indicated the modifications to the “massless” boundary conditions on the EWSB and the UV brane in brackets.

Note that at the Planck brane, it is not mandatory to assign the h^c field twisted boundary conditions compared to those assigned to h . However, it is useful, because that choice leaves the mass eigenstates to h and h^c degenerated. The conditions (5.16) forbid massless solutions, regardless of whether a Dirac mass term M_D is present or not. The sfermion mass is generated predominantly within the SB interval. Neglecting the Dirac mass term M_D leaves us with boundary conditions symmetric under the simultaneous exchange of

$$f_{\eta_L} \longleftrightarrow f_{\chi_R} \quad \text{and} \quad f_{\chi_L} \longleftrightarrow f_{\eta_R}.$$

Therefore, we find two approximately independent solutions for the mass of the charged sfermion, one predominantly consisting of Ψ_L fields (carrying $SU(2)_L$ quantum numbers) and the other

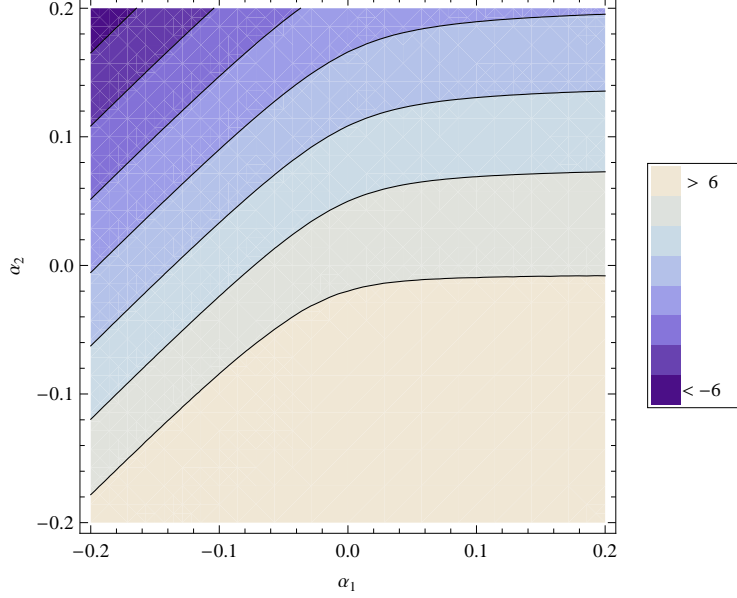


Fig. 5.1: Contour plot of $\text{Log}_{10}(m_{\tilde{f}}/\text{GeV})$ for $t = 1$ in dependence of α_I (horizontal) and α_{II} (vertical). There are two charged sfermions with masses approximately described by $m_{\tilde{f},L}(\alpha_{LI}, \alpha_{LII}, t_L)$ and $m_{\tilde{f},R}(\alpha_{RI}, \alpha_{RII}, t_R)$.

predominantly consisting of Ψ_R fields. These are described by two similar expressions:

$$\begin{aligned}
 m_{\tilde{f},L} &\approx 2\Lambda_{II} \left(\frac{\Lambda_{II}}{k}\right)^{\alpha_{LII}} \left(\frac{1 + \alpha_{LII}}{A_{0L}^{-2} - t_L^2 \left(\frac{\Lambda_{II}}{k}\right)^{2\alpha_{LII}}}\right)^{1/2} t_L \\
 m_{\tilde{f},R} &\approx 2\Lambda_{II} \left(\frac{\Lambda_{II}}{k}\right)^{\alpha_{RII}} \left(\frac{1 + \alpha_{RII}}{A_{0R}^{-2} - t_R^2 \left(\frac{\Lambda_{II}}{k}\right)^{2\alpha_{RII}}}\right)^{1/2} t_R
 \end{aligned} \tag{5.17}$$

The assignment to either (L) or (R) can be validated determining the relative contributions of the respective Ψ_L or Ψ_R modes to the field normalization \mathcal{Z} , which are typically about more than 99.95%. Depending on the choice of parameters, the solutions can be light. However, they can also be in the range of typical KK excitations with more than 1 TeV. The approximate expressions hold for small L - R mixing at the EWSB brane. In the case the third quark generation, where a large mixing is required in order to obtain a heavy top quark, the above expressions get large corrections and the classification into (L) and (R) modes becomes diffuse. The qualitative behavior of the sfermion mass is demonstrated in fig. 5.1, where we show a contour plot of $\text{Log}_{10}(m_{\tilde{f}}/\text{GeV})$ for $t = 1$ in dependence of α_I and α_{II} .

Comparison of (5.17) with (5.11) shows that sfermion and fermion masses qualitatively have an opposite characteristic. Light sfermions and heavy fermions are obtained for $\alpha_I < 0$, $\alpha_{II} > 0$, while we get heavy sfermions and light fermions for $\alpha_I > 0$, $\alpha_{II} < 0$.

5.3.2 Sneutrinos

The neutrino superpartners are also affected by the Majorana mass term on the UV brane. They are found to obey the implicit approximate expression

$$m_{\tilde{\nu}} \approx 2\Lambda_{\text{II}} \left(\frac{\Lambda_{\text{II}}}{k} \right)^{\alpha_{\text{RH}}} \left(\frac{1 + \alpha_{\text{RH}}}{A_{0R}^{-2} - t_R^2 \left(\frac{\Lambda_{\text{II}}}{k} \right)^{2\alpha_{\text{RH}}} + 4 \frac{M_M}{m_{\tilde{n}}}} \right)^{1/2} t_R. \quad (5.18)$$

In order to keep them sufficiently heavy to avoid detection bounds, we choose $t_R > 1$ for the second and third lepton generation. Generally, the large mass splitting within the $SU(2)$ SM doublet causes also a large splitting in the corresponding sfermionic sector. As this splitting is achieved by different boundary conditions on the Planck brane to the Ψ_R doublet the modes, the corresponding sfermion (R) modes in the doublet are widely separated, c.f. tab. 5.2. The same reasoning applies for the different masses of the stop and sbottom (R) modes, which is a consequence of the large mass splitting between top and bottom quark.

5.4 Discussion of the spectrum

In tab. 5.2 and fig. 5.2, we show the tree level mass spectrum of the matter sector of our model. The parameter set leading to this spectrum is given in tab. 5.3 and tab. 5.4.

The parameter set in tab. 5.3 and tab. 5.4 is intended to serve as example. In the absence of definite physical restrictions on all the parameters, it did neither seem worth the effort nor possible to investigate the effectively eight (leptons) or seven (quarks) dimensional parameter space in a systematical way. However we want to discuss the guidelines we followed for choosing our parameter set and the fingerprints of this choices. The resulting mass spectrum is showed in fig. 5.2.

The principal requirement of course was to correctly reproduce the masses of leptons and quarks as given in [23]. Furtheron, we insured that the electrons are localized such that the S parameter does not deviate. The issue of electroweak precision observables will be discussed in chap. 6. The mass splitting via Majorana mass terms M_M between leptons and neutrinos was chosen only as strong as necessary to stay below the upper mass bounds for neutrinos. As the electron is already very light, not more than a Majorana mass of the order of $M_M = 10^4$ GeV is needed for a realistic ν_e mass. This is miniscule compared to the relevant scale at the Planck brane which is determined by $k = 10^{19}$ GeV. Therefore, the seesaw effect discussed in sec. 5.2.4 is not very strong and the heavy solution appears at 896 GeV. For μ and τ , the mass difference between charged leptons and neutrinos and therefore the necessary Majorana mass is larger. Hence the heavy seesaw solution is projected out of the spectrum. It has to be noted, that if we had made all the neutrinos lighter all heavy seesaw solutions would have been above the cutoff.

Further on, we choose the parameters in a way that all sfermion masses are above 200 GeV and avoiding current detection bounds. Similarly to other supersymmetric models, light SM particles tend to have heavy supersymmetric partners and vice versa. In general, the KK spectrum above 1 TeV is rather degenerate and only weakly affected from SUSY breaking. Note that according to (5.17), we find sfermions which are predominantly localized either in the Ψ_L or in the Ψ_R doublet. Our criterion for ‘‘predominantly’’ is a that more than 99.5% of the normalization is generated either by $f_{\eta L}$, $f_{\chi L}$ alone for a (L) mode or by $f_{\eta R}$, $f_{\chi R}$ for a (R) mode. For most indicated modes, this preference for (L) or (R) is even stronger, with contributions to the normalization from the dominant doublet which are about six to eight orders of magnitude larger than from the other doublet. As the couplings are defined by overlap integrals, we would find an (R) mode to couple in a different way than an (L) mode. An

4D field	first mode(s) m/GeV	KK excitations m/GeV
e^-	$5.11 \cdot 10^{-4}$	1170 2784
\tilde{e}	521 (R) 801 (L)	1170 2784
ν_e	$2.91 \cdot 10^{-10}$ 896	1170 2784
$\tilde{\nu}_e$	238 (R) 801 (L)	1170 2784
μ^-	0.105	1213 2554
$\tilde{\mu}^-$	397 (L) 2707 (R)	1214 2554
ν_μ	$1.91 \cdot 10^{-9}$	1213 2554
$\tilde{\nu}_\mu$	228 (R) 397 (L)	1213 2554
τ^-	1.77	1186 2571
$\tilde{\tau}^-$	218 (L) 1563 (R)	1185 2571
ν_τ	$1.89 \cdot 10^{-9}$	1186 2571
$\tilde{\nu}_\tau$	214 (R) 218 (L)	1186 2571
u	$2.31 \cdot 10^{-3}$	1226 2709
\tilde{u}	512 (L) 556 (R)	1226 2709
d	$5.33 \cdot 10^{-3}$	1226 2709
\tilde{d}	512 (L+R)	1226 2709
c	1.27	1258 2561
\tilde{c}	442 (L+R)	1259 2561
s	0.108	1257 2560
\tilde{s}	443 (L) 565 (R)	1257 2560
t	173	1300 2718
\tilde{t}	217 (75% R) 1613 (86% L)	1141 2760
b	4.20	1021 2471
\tilde{b}	884 (83%L) 2268 (R)	1534 2516

Tab. 5.2: Mass spectrum of the matter sector. We include all KK modes below 3000 GeV. Sfermions which live predominantly in Ψ_L or Ψ_R we have indicated with (L), (R). As the mass splitting between elektron and elektron neutrino is comparatively small, the heavy seesaw solution is not projected out of the spectrum as it is for the other two generations. Further one observes how the large L - R necessary for a sufficiently heavy top distorts the sfermion solutions.

example is the coupling to W bosons, which would be suppressed for (R) sfermions because the $f_{WR\pm}$ KK wave function is zero over almost the entire extra dimension, c. f. fig. 4.1. The (L) or (R) modes acquire their masses mainly within the second interval. The resulting mass depends on the choice of the parameters, c.f. fig. 5.1, and can be quite light (like the $\tilde{\nu}_\tau$ with 214 GeV) or as heavy as for example the (R) mode of the $\tilde{\mu}$ with 2707 GeV. First KK excitation modes typically appear in the mass range of 1100 GeV to 1300 GeV.

For \tilde{d} and \tilde{c} , the L-set of parameters α_{L_I} , $\alpha_{L_{II}}$ and t_L is identical to the R-set, consisting of α_{R_I} , $\alpha_{R_{II}}$ and t_R . Therefore, the expressions (5.17) give $m_{\tilde{f},L} = m_{\tilde{f},R}$ and we find a single mode which is equally distributed over Ψ_L and Ψ_R . Observe further that due to unbroken $SU(2)_L$, the (L) modes within one sfermion doublet are degenerate. In contrast, the (R) modes are quite strongly affected by the splitting, which is realized via a different choice of t_R or by using the

	$\alpha_{L\text{I}}$	$\alpha_{L\text{II}}$	$\alpha_{R\text{I}}$	$\alpha_{R\text{II}}$	t_L	t_R	M_M/GeV	M_D/Λ_{I}
$\begin{pmatrix} e^-/\tilde{e} \\ \nu_e/\tilde{\nu}_e \end{pmatrix}$	0.15	0.00	0.15	0.02	1	$\begin{pmatrix} 1 \\ 1 \end{pmatrix}$	$\begin{pmatrix} 0 \\ 1.0 \cdot 10^4 \end{pmatrix}$	1.24
$\begin{pmatrix} \mu^-/\tilde{\mu}^- \\ \nu_\mu/\tilde{\nu}_\mu \end{pmatrix}$	0.02	0.02	0.02	-0.14	1	$\begin{pmatrix} 1 \\ 15 \end{pmatrix}$	$\begin{pmatrix} 0 \\ 2.2 \cdot 10^{11} \end{pmatrix}$	0.97
$\begin{pmatrix} \tau^-/\tilde{\tau}^- \\ \nu_\tau/\tilde{\nu}_\tau \end{pmatrix}$	0.02	0.04	0.02	-0.05	1	$\begin{pmatrix} 1 \\ 400 \end{pmatrix}$	$\begin{pmatrix} 0 \\ 3.3 \cdot 10^{11} \end{pmatrix}$	1.015

Tab. 5.3: Model parameters for the fermions and their superpartners.

	$\alpha_{L\text{I}}$	$\alpha_{L\text{II}}$	$\alpha_{R\text{I}}$	$\alpha_{R\text{II}}$	t_L	t_R	M_D/Λ_{I}
$\begin{pmatrix} u/\tilde{u} \\ d/\tilde{d} \end{pmatrix}$	0.12	0.02	0.12	0.02	1	$\begin{pmatrix} 2.5 \\ 1 \end{pmatrix}$	1.1
$\begin{pmatrix} c/\tilde{c} \\ s/\tilde{s} \end{pmatrix}$	0.04	0.02	0.04	0.02	1	$\begin{pmatrix} 1 \\ 15 \end{pmatrix}$	0.93
$\begin{pmatrix} t/\tilde{t} \\ b/\tilde{b} \end{pmatrix}$	-0.10	-0.10	-0.20	-0.10	1	$\begin{pmatrix} 1 \\ 1505 \end{pmatrix}$	1.14

Tab. 5.4: Model parameters for the quarks and their superpartners.

localized Majorana mass term M_M . For the third quark generation, the L - R mixing induced at the EWSB brane in order to achieve heavy enough top quarks is strong and the assumption of independent L and R boundary conditions in (5.17) does not hold any longer. The top $m_{\tilde{f},L}$ is predicted at 251 GeV but the solution is found at 217 GeV. Therefore, stop and sbottom do not show preferences for Ψ_L or Ψ_R stronger than about 75% and do not qualify as (L) and (R) solutions according to our definition. The distortion is still visible in the first KK excitations. Another consequence of strong L - R mixing regarding the quark sector is the severe problem of the $Zb\bar{b}$ coupling. This will be discussed separately in chap. 7.

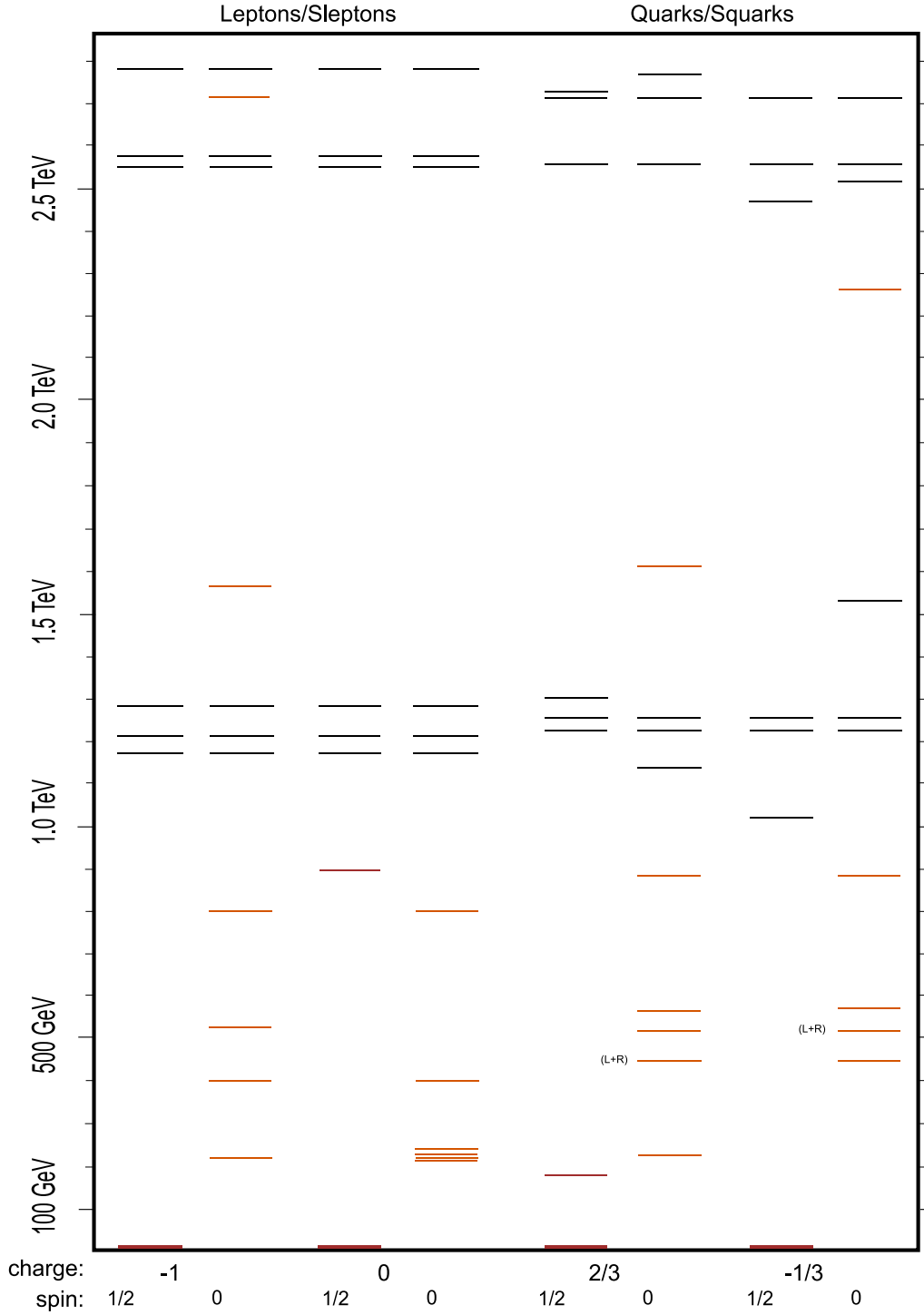


Fig. 5.2: Mass spectrum of the matter sector for the parameter sets tab. 5.3 and tab. 5.4. The first modes, for which the above derived approximate expressions hold, are indicated in red (fermions) and orange (sfermions). The degenerate modes are denoted (L+R). As a consequence of the mass splitting in the SM sector, some (R) modes become very heavy. The KK excitations in black are, apart from the distorted third quark sector, almost degenerate.

6 Electroweak precision observables

A very convenient method to probe BSM models are the famous electroweak precision observables S and T , introduced by Peskin and Takeuchi [27] in 1991. Having built the supersymmetric extradimensional model and discussed the mass spectra, we can test the viability of our model and constrain its parameter space by means of these parameters.

6.1 The Peskin-Takeuchi parameters S and T

The procedure of renormalization in perturbation theory leads to different kinds of corrections. Direct vertex corrections are absorbed in the couplings. There are so-called “oblique” corrections which arise due to vacuum polarization diagrams and affect the gauge boson propagators. More corrections exist, for example those corresponding to box or pentagon diagrams. However, the first two types are the dominant ones for the relevant $e^+e^- \rightarrow Z \rightarrow f\bar{f}$ processes at LEP, which have been measured at the Z -pole with astonishing precision.

It turns out that the oblique corrections to most weak interaction observables can be described in terms of only two parameters defined from vacuum polarization amplitudes.

Generally speaking, the S parameter is a measure for the number of degrees of freedom of the particles participating in the electroweak sector. The value of this parameter is inferred from measurements of the magnitude of parity violation in atomic physics and from weak interaction asymmetries A_{LR} and A_{FB} at the Z -Peak. While the S parameter is isospin-symmetric, the T parameter quantifies the strength of weak isospin breaking through radiative corrections. There is also a third parameter U . It parameterizes a dimension-eight operator, while S and T correspond to dimension-six operators and usually contributions to U from new physics models are very small. As in most publications, we restrict ourselves to S and T . They are defined [27] as:

$$S \equiv 16\pi(\Pi'_{33} - \Pi'_{3Q}) \quad (6.1)$$

$$T \equiv \frac{4\pi}{\sin^2 \Theta_W \cos^2 \Theta_W m_Z^2} (\Pi_{11}(0) - \Pi_{33}(0)) \quad (6.2)$$

where the Π are the vacuum polarization amplitudes we will discuss in the next section. The authors of [27] showed that most contributions from vacuum polarization can be parameterized in terms of S and T .

Their values are usually extracted from measurement data assuming of a standard model Higgs of a certain mass. So it is not a priori clear how they should be compared with values calculated in a model without a Higgs. According to the picture of our higgsless model corresponding to the limit of a Higgs field with $\text{VEV} \rightarrow \infty$, one usually takes as reference a fit that assumes a large Higgs mass value, namely with m_H above the cutoff.

S and T can be found in [23] and turn out to be strongly correlated (87%). For a Higgs mass of $m_H = 117$ GeV, S should be within $-0.20 \leq S \leq 0.10$ and T within $-0.10 \leq T \leq 0.15$. For a heavy Higgs of $m_H = 1000$ GeV, which would be the closest to an “Higgs above the cutoff”, the boundaries are shifted to $-0.35 \leq S \leq 0.00$ and $0.10 \leq T \leq 0.40$. While the T parameter is protected by custodial symmetry, the main problem for extradimensional models usually have been large positive values of S .

The vacuum polarization amplitude Π_{XY} is defined as the one-particle irreducible self energy, which at leading order written with Feynman graphs is:

$$g^2\Pi_{XY} = X \text{---} \text{---} \text{---} Y = X \text{---} \text{---} \text{---} Y + X \text{---} \text{---} \text{---} Y \quad (6.8)$$

Considering gauge bosons from the electroweak sector, the indices (XY) are placeholders for (11), (22), (33), (3Q) and (QQ). To split the momentum independent from the momentum dependent part, one defines

$$\Pi_{XY}(q^2) = : \Pi_{XY}(0) + q^2\Pi'_{XY}(q^2). \quad (6.9)$$

For small momenta, this is just a Taylor expansion with $\Pi'_{XY}(q^2) = \frac{d}{dp^2}\Pi_{XY}|_{p^2=0}$. The physical propagator at $\mathcal{O}(g^2)$ is given by the Dyson series:

$$\begin{aligned} G &= \text{---} + \text{---} \text{---} \text{---} + \text{---} \text{---} \text{---} \text{---} + \dots \\ &= G^0 + G^0 g \Pi g G^0 + G^0 g \Pi g G^0 g \Pi g G^0 + \dots \end{aligned} \quad (6.10)$$

Since Π , as defined above, is finite and in particular $g^2\Pi$ is small at relevant energies of $s \sim m_Z^2$, the series converges and (6.10) reduces to

$$G = G^0 \sum_{n=0}^{\infty} (g^2\Pi G^0)^n = G^0 \frac{1}{1 - g^2\Pi G^0} = \frac{1}{(G^0)^{-1} - g^2\Pi}. \quad (6.11)$$

The propagator at leading order $\mathcal{O}(g^0)$ is just

$$G^{0,\mu\nu} = \frac{ig^{\mu\nu}}{q^2 - m_R^2} + \text{terms in } q^\mu q^\nu,$$

and finally we obtain

$$G^{\mu\nu} = \frac{ig^{\mu\nu}}{q^2(1 - g^2\Pi') - (m_R^2 + g^2\Pi(0))} + \text{terms in } q^\mu q^\nu. \quad (6.12)$$

The pole is shifted by an amount $\Delta m^2 = g^2\Pi(0)$. The residuum of the pole is equivalent to the wave function renormalization¹ $Z = 1 - g^2\Pi$. Let us apply this to the physical mass eigenstates γ , W^\pm and Z . The vacuum polarization corrections to their propagators are depicted in fig. 6.1. Due to unbroken $U(1)_{\text{em}}$ it is guaranteed that $\Pi_{11} = \Pi_{22}$. Also, $\Pi_{3Q}(0) = \Pi_{QQ}(0) = 0$ due to the QED Ward identity. The relations between the renormalized magnitudes and the vacuum amplitudes read [27]:

$$Z_Z = 1 - \frac{g^2}{\cos^2 \Theta_W} (\Pi_{33} - 2 \sin^2 \Theta_W \Pi'_{3Q} + \sin^4 \Theta_W \Pi'_{QQ}) \quad (6.13a)$$

$$Z_W = 1 - g^2 \Pi'_{11} \quad (6.13b)$$

$$m_Z^2 = m_{0Z}^2 + \frac{g^2}{\cos^2 \Theta_W} (\Pi_{33} - 2 \sin^2 \Theta_W \Pi_{3Q} + \sin^4 \Theta_W \Pi_{QQ}) \quad (6.13c)$$

$$m_W^2 = m_{0W}^2 + g^2 \Pi_{11} \quad (6.13d)$$

¹This Z is *not* the same as the Z_R from (6.4), which in particular is not finite.

$$\begin{aligned}
 \gamma \text{ wavy } \gamma + \gamma \text{ wavy with blob } \gamma + \dots &= G_{\gamma\gamma}^0 + G_{\gamma\gamma}^0 g^2 \sin^2 \Theta_W \Pi_{QQ} G_{\gamma\gamma}^0 + \dots \\
 Z \text{ wavy with blob } \gamma + \dots &= G_{ZZ}^0 g^2 \frac{\sin \Theta_W}{\cos \Theta_W} (\Pi_{3Q} - \sin^2 \Theta_W \Pi_{QQ}) G_{\gamma\gamma}^0 + \dots \\
 Z \text{ wavy } Z + Z \text{ wavy with blob } Z + \dots &= G_{ZZ}^0 + G_{ZZ}^0 g^2 \frac{\sin^2 \Theta_W}{\cos^2 \Theta_W} \left(\Pi_{33} \right. \\
 &\quad \left. - 2 \sin^2 \Theta_W \Pi_{3Q} + \sin^4 \Theta_W \Pi_{QQ} \right) G_{ZZ}^0 + \dots \\
 W \text{ wavy } W + W \text{ wavy with blob } W + \dots &= G_{WW}^0 + G_{WW}^0 g^2 \Pi_{11} G_{WW}^0 + \dots
 \end{aligned}$$

Fig. 6.1: Definition of the vacuum amplitudes, c.f. [27].

6.3 Tree level calculation of S and T parameter

Let us now come to the explicit calculation of the precision observables within our model. As we have discussed in chap. 1, wave function normalization terms \mathcal{Z} and mass terms \mathcal{M} arise automatically when integrating out the extra dimension. These are defined by the geometry, i.e. by the KK solutions in the extra dimensional interval with boundary conditions. In general \mathcal{Z} will be different from one, in contrast to the SM, where $Z \neq 1$ arises only at loop level. Thus, the effective tree level Lagrangian² obtained from a 5D theory can also be written as $\mathcal{L}_{5D} = \mathcal{L}_{0,4D} + \mathcal{L}_{CT}$ and we can at leading order identify \mathcal{Z} and \mathcal{M} with the renormalized magnitudes Z and m from (6.13) in the 4D SM picture. Note that, as there is no Higgs VEV, the entire boson mass stems from $\Pi(0)$, as happens in technicolor models as well.

As a consequence of the unbroken $U(1)_{em}$, it is always possible to canonically normalize the photon wave function, hence $\Pi'_{QQ} = 0$. At tree level $\Pi'_{3Q} = 0$ holds as well because there is no Z - γ mixing. With these simplifications, we obtain from (6.13) the relations:

$$\mathcal{Z}_Z = 1 - \frac{g^2}{\cos^2 \Theta_W} \Pi'_{33} \quad (6.14a)$$

$$\mathcal{M}_Z = \frac{g^2}{\cos^2 \Theta_W} \Pi_{33}(0) \quad (6.14b)$$

$$\mathcal{M}_W = g^2 \Pi_{11}(0) \quad (6.14c)$$

Inverting these relations and plugging them into the definitions of S and T we finally obtain:

$$S = 16\pi \frac{\cos^2 \Theta_W}{g^2} (1 - \mathcal{Z}_Z) \quad (6.15)$$

$$T = \frac{4\pi}{g^2 \sin^2 \Theta_W \cos^2 \Theta_W m_Z^2} (\mathcal{M}_W - \mathcal{M}_Z \cos^2 \Theta_W) \quad (6.16)$$

We can immediately read off from (6.15) that the S parameter will be positive for $\mathcal{Z}_Z < 1$ and negative for $\mathcal{Z}_Z > 1$.

For the calculation of \mathcal{Z}_Z , \mathcal{M}_Z and \mathcal{M}_W we require the KK wave functions of the gauge bosons which have been discussed in chap. 4. The KK expansion of the physical bosons is given

²Of course, also in the 5D theory there are loop contributions at higher orders. In the 5D picture, these contributions lead to additional brane localized operators, modifying the KK functions. We constrain ourselves to the leading (tree level) contributions to S and T .

by (4.7). As mentioned before, the photon wave function is flat and can always be canonically normalized

$$a_0^2 \cdot \frac{1}{g_5^2} \left(\pi(R_1 + R_{11}) \frac{2g_r^2 + 1}{g_r^2} + \pi R_{11} \kappa \right) = 1. \quad (6.17)$$

The KK wave functions of the massive bosons can be approximated by (4.9)

$$\begin{aligned} f_i^0(z) &= z (c_i^0 J_1(mz) + d_i^0 Y_1(mz)) \\ &\approx a_i + m^2 z^2 \left(b_i - \frac{a_i}{2} \log(zk) \right) + m^4 z^4 \left(-\frac{b_i}{8} - \frac{3a_i}{64} + \frac{a_i}{16} \log(zk) \right) + \mathcal{O}(m^6 z^6). \end{aligned}$$

To calculate the overlap integrals, we need the coefficients a_i , b_i which are obtained by solving the respective boundary conditions. The approximate analytical expressions are listed in App. B.2. The resulting KK wave functions of the W and the Z boson are showed in fig. 4.1 and fig. 4.2.

The explicit expressions for the normalizations \mathcal{Z} in terms of the KK wave functions are

$$\begin{aligned} \mathcal{Z}_W &= \int_{1/k}^{1/\Lambda_1} dz \left(\frac{1}{kz} \right) ([f_{L1}^I]^2 + [f_{R1}^I]^2) \\ &\quad + \int_{1/k}^{1/\Lambda_{11}} dz \left(\frac{1}{kz} \right) ([f_{L2}^{II}]^2 + [f_{R2}^{II}]^2 + \kappa k \pi R_{11} [f_{L2}^{II}(0)]^2) \end{aligned} \quad (6.18)$$

and

$$\begin{aligned} \mathcal{Z}_Z &= \int_{1/k}^{1/\Lambda_1} dz \left(\frac{1}{kz} \right) ([f_{L3}^I]^2 + [f_{R3}^I]^2 + [f_X^I]^2) \\ &\quad + \int_{1/k}^{1/\Lambda_{11}} dz \left(\frac{1}{kz} \right) ([f_{L3}^{II}]^2 + [f_{R3}^{II}]^2 + [f_X^{II}]^2 + \kappa k \pi R_{11} [f_{L3}^{II}(0)]^2). \end{aligned} \quad (6.19)$$

The integrals \mathcal{M} over the ∂_z -derivatives of the mode functions, acting like mass terms in the 4D Lagrangian, are

$$\begin{aligned} \mathcal{M}_W &= \int_{1/k}^{1/\Lambda_1} dz \left(\frac{1}{kz} \right) ([\partial_z f_{L1}^I]^2 + [\partial_z f_{R1}^I]^2) \\ &\quad + \int_{1/k}^{1/\Lambda_{11}} dz \left(\frac{1}{kz} \right) ([\partial_z f_{L2}^{II}]^2 + [\partial_z f_{R2}^{II}]^2) \end{aligned} \quad (6.20)$$

and

$$\begin{aligned} \mathcal{M}_Z &= \int_{1/k}^{1/\Lambda_1} dz \left(\frac{1}{kz} \right) ([\partial_z f_{L3}^I]^2 + [\partial_z f_{R3}^I]^2 + [\partial_z f_X^I]^2) \\ &\quad + \int_{1/k}^{1/\Lambda_{11}} dz \left(\frac{1}{kz} \right) ([\partial_z f_{L3}^{II}]^2 + [\partial_z f_{R3}^{II}]^2 + [\partial_z f_X^{II}]^2). \end{aligned} \quad (6.21)$$

Observe that the brane kinetic term κ increases the wave function normalizations \mathcal{Z} . The 5D model parameters a_0 , a_Z , a_W , g_r and g_5 can now be fixed by requiring that the 4D couplings are correctly reproduced.

For the calculation, we assume gauge bosons to couple to massless fermions. Apart from the third quark generation which will be discussed separately in chap. 7, the mass is sufficiently small that fermions can be described by the massless KK functions $f_{0\eta L}$ and $f_{0\chi R}$. Since the

electroweak parameters have been measured in $e^+ e^-$ collisions, the assumption of massless test fermions is valid. The analytical expression for the lefthanded KK wave function is (c.f. tab. 5.1):

$$f_{\eta_{0L}}(z) = \begin{cases} \sqrt{2k} A_{L0} (kz)^{3/2-\alpha_{L\text{I}}} & z \in [\frac{1}{k}, \frac{1}{\Lambda_{\text{I}}}] \\ \sqrt{2k} t_L A_{L0} (kz)^{3/2-\alpha_{L\text{II}}} & z \in [\frac{1}{k}, \frac{1}{\Lambda_{\text{II}}}] \end{cases} \quad (6.22)$$

The normalization A_{L0} is given by (5.5). Using (4.7), the interaction term of two lefthanded fermions with a gauge boson reads

$$\mathcal{L}_{f\bar{f}A} = \eta_L^2(x) \left[a_0 Q \gamma_\mu + g_5 \langle \eta_{0L} \eta_{0L} A_{L\pm} \rangle T_{L\mp} W_\mu^\pm + g_5 \langle \eta_{0L} \eta_{0L} A_{L3} \rangle \left(T_{3L} + g_r \frac{\langle \eta_{0L} \eta_{0L} A_X \rangle}{\langle \eta_{0L} \eta_{0L} A_{L3} \rangle} Y \right) Z_\mu(x) \right], \quad (6.23)$$

where the overlap integrals are defined as

$$\langle \eta_{0L} \eta_{0L} A_i \rangle = \int_{1/k}^{1/\Lambda_{\text{I}}} dz (kz)^{-4} (f_{\eta_{0L}}^{\text{I}})^2 f_{A_i}^{\text{I}}(z) + \int_{1/k}^{1/\Lambda_{\text{II}}} dz (kz)^{-4} (f_{\eta_{0L}}^{\text{II}})^2 f_{A_i}^{\text{II}}(z). \quad (6.24)$$

The matching conditions are (c.f. [29]):

$$a_0^2 = g^2 \sin^2 \Theta_W \quad (6.25a)$$

$$g_5 \langle \eta_{0L} \eta_{0L} A_{L\pm} \rangle = g \quad (6.25b)$$

$$g_5 \langle \eta_{0L} \eta_{0L} A_{L3} \rangle = g \cos \Theta_W \quad (6.25c)$$

$$-g_r \frac{\langle \eta_{0L} \eta_{0L} A_X \rangle}{\langle \eta_{0L} \eta_{0L} A_{L3} \rangle} = \tan^2 \Theta_W \quad (6.25d)$$

The fact that the 5D parameters, fixed by the couplings, lead to the correct m_W/m_Z ratio is due to the custodial symmetry in our model.

6.4 Results

6.4.1 The S parameter without a brane kinetic term

In the absence of a brane kinetic term ($\kappa = 0$), the wave function normalization of the Z boson is given by

$$\mathcal{Z}_Z = a_Z^2 \frac{C_0}{kx} \left(1 - \frac{3}{8} x C_0 \right) + \mathcal{O}(x), \quad (6.26)$$

where $C_0 = (1 + 2g_r^2)/(1 + g_r^2)$, c.f. 4.12. In the simplest case of UV localized fermions (large α_L), the overlap integrals (6.24) reduce to

$$\langle \eta_{0L} \eta_{0L} A_i \rangle \rightarrow f_{A_i}|_{z=1/k}.$$

This situation was discussed for the 2 brane setup in [24]. The S parameter turned out to be $S \approx 1.15$, which is alarmingly large. The qualitative reason for this is the following: A Planck localized $SU(2)_L$ fermion ‘‘sees’’ an f_{L3} value larger than the average over the whole extra dimension. In order to get the correct T_{3L} coupling, the Z wave function normalization has to be lowered. This effectively results in a very large S parameter.

When the second interval is introduced, the average value of f_{L3} increases and thus the S parameter is reduced. For Planck localized test fermions we find:

$$a_0^2 = \frac{g_5^2 g_r^2}{\pi(R_I + R_{II})(2g_r^2 + 1)} \quad (6.27a)$$

$$\langle \eta_{0L} \eta_{0L} A_{L3} \rangle = a_Z + \mathcal{O}(x) \quad (6.27b)$$

$$\langle \eta_{0L} \eta_{0L} A_X \rangle = -\frac{g_r}{1 + g_r^2} a_Z + \mathcal{O}(x) \quad (6.27c)$$

Using the matching conditions (6.25), the 5D parameters are found to be constrained by:

$$\frac{g_5^2 g_r^2}{\pi(R_I + R_{II})(2g_r^2 + 1)} = g^2 \sin^2 \Theta_W \quad (6.28a)$$

$$g_5 a_Z = g \cos \Theta_W \quad (6.28b)$$

$$\frac{g_r^2}{1 + g_r^2} = \tan^2 \Theta_W \quad (6.28c)$$

Using these equations, we obtain $\mathcal{Z}_Z = (1 - \frac{3}{8} \frac{x}{\cos^2 \Theta_W}) + \mathcal{O}(x^2)$ and finally with (6.15):

$$S = \frac{6\pi x}{g^2} \approx 0.6.$$

This is still way too large.

To obtain a realistic value of S , the fermions need to be delocalized towards the IR brane, in order to decrease their overlap with f_{L3} . Therefore, we have to choose $\alpha_{L_I} \sim 0$. As the f_{L3} and the f_X wave functions are approximately flat in the second (SB) interval, the localization parameter $\alpha_{L_{II}}$ does not have much effect at all, c.f. fig. 6.4. The photon coupling is not affected by fermion localization and (6.27a) remains unchanged. For the overlap integrals we find:

$$\langle \eta_{0L} \eta_{0L} A_X \rangle = -a_Z \frac{g_r}{1 + g_r^2} + \mathcal{O}(x) \quad (6.29)$$

$$\langle \eta_{0L} \eta_{0L} A_{L3} \rangle = a_Z \cdot \left(1 - C_0 A_{0L}^2 \frac{\left(\frac{\Lambda_I}{k}\right)^{2\alpha_{L_I}}}{2(1 - \alpha_{L_I})} \right) + \mathcal{O}(x) \quad (6.30)$$

We determine the three 5D parameters g_r , g_5 and a_Z , now depending on the fermion localization, from (6.27a), (6.29) and (6.30). By plugging them into (6.26), we obtain $\mathcal{Z}_Z(\alpha_{L_I})$. Finally inserting this expression into (6.15) gives the result:

$$S = \frac{16\pi}{g^2} \left(\frac{3}{8} x - \frac{A_{0L}^2}{2(1 - \alpha_{L_I})} \left(\frac{\Lambda_I}{k}\right)^{2\alpha_{L_I}} \right) + \mathcal{O}(x^2) \quad (6.31)$$

To obtain a realistic S parameter, the fermion localization is required to be $\alpha_{L_I} \approx -0.007$ in the case of three branes or respectively $\alpha_L \approx -0.013$ in the two brane setup. This means the fermions have to be almost completely delocalized within the extra dimension.

6.4.2 The S parameter with a brane kinetic term

The normalization of the photon in the case of $\kappa \neq 0$ is

$$a_0^2 = g_5^2 \left(\pi(R_I + R_{II}) \frac{2g_r^2 + 1}{g_r^2} + \pi R_{II} \kappa \right)^{-1}, \quad (6.32)$$

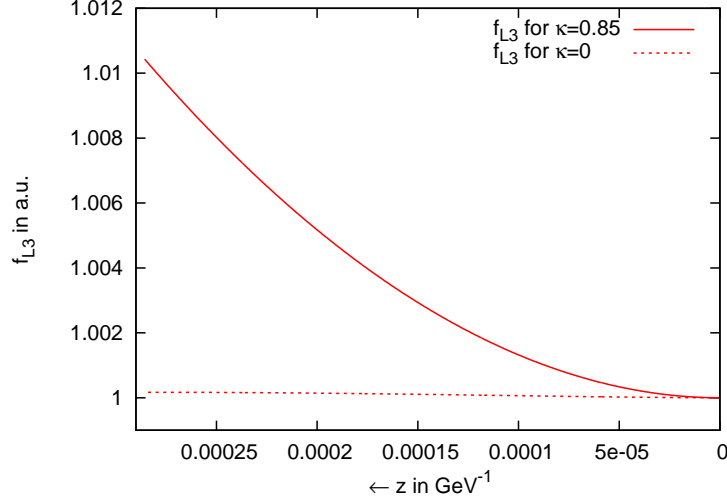


Fig. 6.2: Zoom on the $f_{L3}^{\text{II}}(z)$ wave function of the Z boson in the SB interval: The kinetic term $\kappa > 0$ (solid line) induces an upward bending, which is not present for $\kappa = 0$ (dashed line). The $f_{L\pm}^{\text{II}}(z)$ which corresponds to the W boson looks similar in the SB interval.

And the overlaps change to:

$$\langle \eta_{0L} \eta_{0L} A_X \rangle = -a_Z \cdot \frac{g_r}{1 + g_r^2} (1 + f_R \kappa) + \mathcal{O}(x) \quad (6.33)$$

$$\begin{aligned} \langle \eta_{0L} \eta_{0L} A_{L3} \rangle = a_Z \cdot & \left(1 - C_\kappa A_{0L}^2 \frac{\left(\frac{\Lambda_I}{k}\right)^{2\alpha_{LI}}}{2(1 - \alpha_{LI})} (1 + f_R \kappa) \right. \\ & \left. + C_\kappa \left(\frac{\Lambda_I}{\Lambda_{\text{II}}}\right)^2 t_L^2 A_{0L}^2 \frac{\left(\frac{\Lambda_{\text{II}}}{k}\right)^{2\alpha_{L\text{II}}}}{2(1 - \alpha_{L\text{II}})} f_R \kappa + \mathcal{O}(x) \right) \end{aligned} \quad (6.34)$$

Observe that $\langle \eta_{0L} \eta_{0L} A_X \rangle$ is, compared to (6.29), multiplied by a factor $(1 + f_R \kappa)$. The wave function normalization is

$$\begin{aligned} \mathcal{Z}_Z = a_Z^2 \frac{C_\kappa}{kx} (1 + f_R \kappa)^2 \\ \left(1 - \frac{3}{8} x C_\kappa + \left(\frac{f_R \kappa}{1 + f_R \kappa} \frac{\Lambda_I}{\Lambda_{\text{II}}} \right)^2 \left[1 + x \left(\frac{1}{f_R \kappa} + \frac{3}{8} C_\kappa \right) \right] \right) + \mathcal{O}(x). \end{aligned} \quad (6.35)$$

The negative contribution proportional to $\frac{3}{8} x C_\kappa$ is similar to the one in (6.26). In addition, we find a positive contribution proportional to

$$\left(\frac{f_R \kappa}{1 + f_R \kappa} \frac{\Lambda_I}{\Lambda_{\text{II}}} \right)^2.$$

This contribution is an effect of the brane kinetic term, which induces an upward bending in f_{L3}^{II} (c.f. fig. 6.2). Depending on κ and the ratio $\Lambda_I/\Lambda_{\text{II}}$ we thus are able to fix S without having to delocalize the test fermion. Again, S is obtained from (6.1), (6.14), (6.25) and from (6.32) to (6.35).

In fig. 6.3, the S parameter is showed in dependence of the localization of the massless test fermion within the EWSB interval for different values of $\kappa = 0$. As long as the test fermion

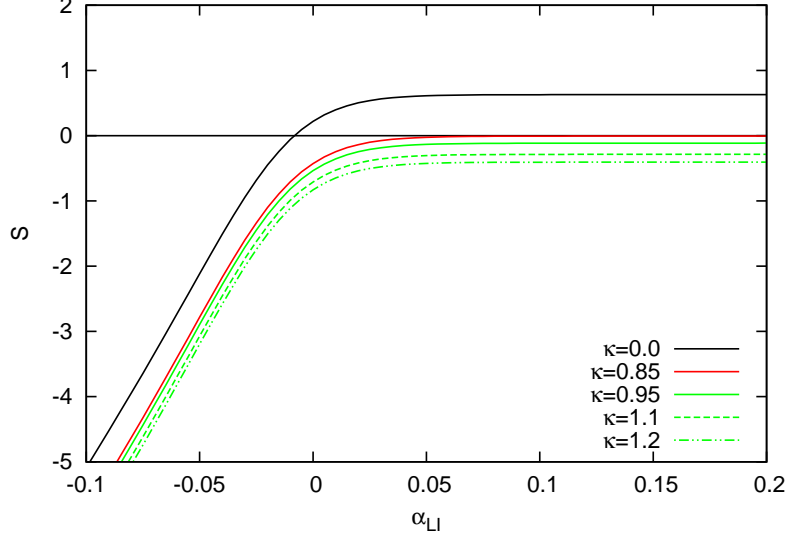


Fig. 6.3: The S parameter for $\kappa = 0$ (black), $\kappa = 0.85$ (red) and $\kappa = 0.95, 1.1, 1.2$ (green) corresponding to chargino masses of $m_{\chi} = 80.4, 95.9, 97.5, 100.0$ and 101.6 GeV. We have fixed $\alpha_{LII} = 0.15$

within the EWSB interval is not too strongly localized towards the IR brane, its overlap with the Z boson is approximately constant and so is S . However, S decreases drastically once α_{L1} becomes small. Note how the kinetic term lowers the S parameter. This enables us to choose κ in a way that S is in the realistic range (equal to zero or slightly negative), not only for one fixed value of α_{L1} but for the entire plateau.

6.4.3 The T parameter

The procedure to calculate the T parameter at tree level is analogous to the calculation of the S parameter. Again, we use the matching conditions (6.25) to fix the 5D parameters a_0, a_Z, g_r and g_5 . The parameters are then plugged into the expressions for \mathcal{M}_Z and \mathcal{M}_W from which then T is obtained by using (6.14).

The T parameter turns out to be protected to a certain extent by the custodial symmetry. As long as the massless test fermion is not too strongly delocalized towards the IR brane³, $T \approx 0$. In fig. 6.5, we show the T parameter in dependence of the localization of the massless test fermion within the EWSB interval for $\kappa = 0$ (dashed) and $\kappa = 0.85$ (solid line).

The qualitative explanation of fig. 6.5 is as follows: If the test fermion is strongly delocalized towards the EWSB brane by choosing α_{L1} large and negative, $\langle \eta_{0L} \eta_{0L} A_{L3} \rangle$ decreases while $\langle \eta_{0L} \eta_{0L} A_X \rangle$ remains unchanged. The ratio of these overlap integrals is used to fix g_r , which in turn sets the m_Z^2/m_W^2 ratio. For large negative α_{L1} , g_r becomes small and thus the Z boson becomes too light. Both ρ and T parameter are spoiled simultaneously.

A brane kinetic term induces a bending of f_{L3}^{II} near the SB brane, which increases both \mathcal{M}_Z and \mathcal{M}_W . That enhancement is bigger for \mathcal{M}_W than for \mathcal{M}_Z , leading to a larger value of T . Still, this particular effect is very tiny⁴. For $\kappa \neq 0$, the overlap $\langle \eta_{0L} \eta_{0L} \Phi_{L3} \rangle$ receives a small positive contribution $\propto \left(\frac{f_R \kappa}{1+f_R \kappa} \right)^2 \left(\frac{\Lambda_I}{\Lambda_{\text{II}}} \right)^2$, c.f. (6.34). This is the reason why the T parameter

³Too strong delocalization is already forbidden because it leads to a large negative S , compare fig. 6.3

⁴Note the zoom in fig. 6.2. The curvature of f_{L3}^{II} is nearly invisible in fig. 4.2.

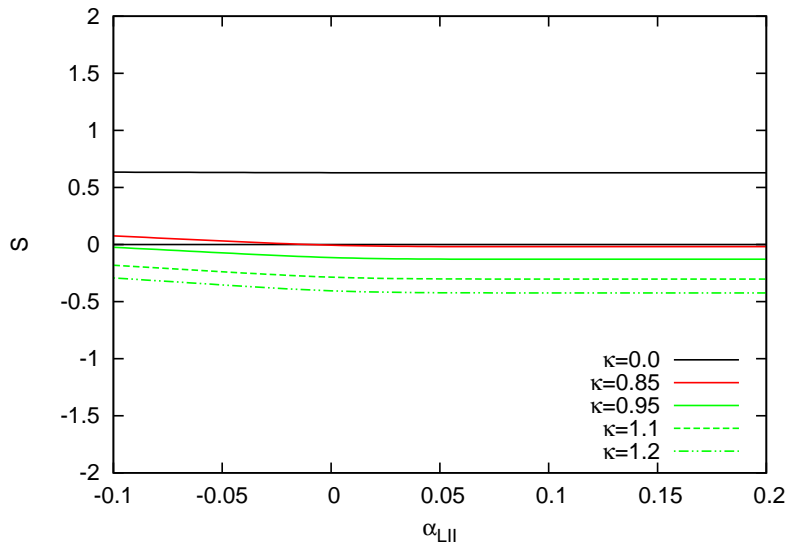


Fig. 6.4: For $\alpha_{LI} = 0.15$, the S parameter for $\kappa = 0$ (black), $\kappa = 0.85$ (red) and $\kappa = 0.95, 1.1, 1.2$ (green). The S parameter depends only weakly on α_{LII} .

increases slower if the test fermion is delocalized towards the EWSB brane as it does without a brane kinetic term.

Taking as reference value bounds for T from [23] for $m_H = 1000$ GeV, we find that T is too small. Although the brane kinetic terms shift it a bit towards the optimal region of $0.10 \leq T \leq 0.4$, it is too well protected by custodial symmetry. A significant deviation from $T = 0$ for α_{LI} may only arise at next-to-leading order in perturbation theory, where vacuum polarization diagrams containing top and bottom quarks violate custodial symmetry.

6.5 Discussion

Within our extra dimensional model we have determined the parameter space, where the electroweak precision observables are in a realistic range. For example, for $\kappa = 0.85$, $\Lambda_I = 815$ GeV, $\Lambda_{II} = 3500$ GeV, an electron with $\alpha_{LI} = 0.15$ and $\alpha_{LII} = 0$ would have $S = -0.0057$ and $T = 0.0003$. To obtain the correct electron mass, the remaining parameters could be chosen to be $\alpha_{RI} = 0.15$, $\alpha_{RII} = 0.02$ together with a Dirac mass of $M_D = 1011$ GeV.

Fermion localization

Note that the combination of the second interval and brane kinetic term allows a realistic value of S at $\alpha_{LI} > 0.1$. This is a good feature since in that case the small masses for light fermions then appear quite naturally.

For a single extradimensional interval without brane kinetic term, we would need $\alpha_{LI} \approx -0.013$ [24]. Even with an extreme choice of the other localization parameters α_i , we would require a Dirac mass term of the order of $M_D \sim 10^{-5} \Lambda_I$ to make the electron sufficiently light. One would consider M_D as “natural” for $M_D \sim \Lambda_I$.

In the two brane model, a brane kinetic term on the Planck brane would lead to an even smaller value of α_{LI} . The additional interval $[\frac{1}{k}, \frac{1}{\Lambda_{II}}]$ in the extra dimension alone does not solve the problem either. It just slightly increases the value of α_{LI} required to make S vanish. This is

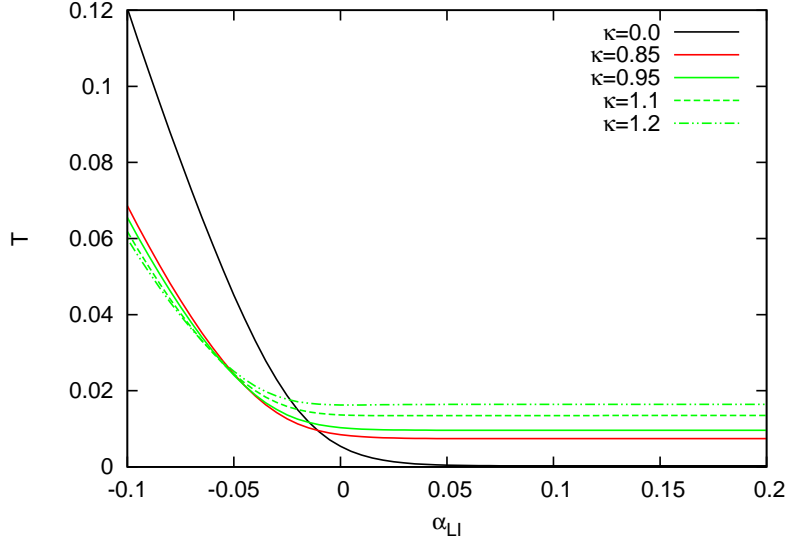


Fig. 6.5: For $\alpha_{LII} = 0$, the T parameter for or $\kappa = 0$ (black), $\kappa = 0.85$ (red) and $\kappa = 0.95, 1.1, 1.2$ (green).

due to the fact that with two intervals, the order of typical corrections is $x = \frac{1}{k\pi(R_I + R_{II})}$ instead of $x = \frac{1}{k\pi R}$. However, that effect is too small to solve the problem of a realistic parameter set for light fermions.

Although introduced for other reasons, we find that the combination of the brane kinetic term and the new IR brane where to put this term allows to implement light fermions without having to choose unnaturally small Dirac mass terms.

Restrictions on the brane kinetic term

We find that the precision observables give a restriction on the value of κ .

For small κ the S parameter will be too large for Planck localized fermions. We will then find one single value of α_{L1} , where the fermion is sufficiently localized towards the IR brane to give a realistic S . Via the brane kinetic term, we can decrease the S parameter such that the entire plateau in $S(\alpha_{L1})$ comes to lie within experimentally allowed range. For $\Lambda_I = 815$ GeV and $\Lambda_{II} = 3500$ GeV this is the case at $\kappa = 0.85$. Then, the fermion localization is not restricted to one specific value of α_{L1} .

For large values of κ , S will be too small for all localizations. This gives an upper bound on κ , which depends on the size of the second interval. The lower limit for κ is given by the minimal chargino mass necessary for avoiding detection bounds.

The brane kinetic term is a good example for the general interdependence of the parameters in our setup. This interdependence can be seen both as an advantage or disadvantage. On one hand it is quite cumbersome to change a parameter without rendering the model to be in disagreement with experimental bounds. On the other hand, the parameter space can be strongly restricted.

7 The $Zb_l\bar{b}_l$ problem

A characteristic problem of higgsless models of electroweak symmetry breaking arises for the third quark generation. The question is how to obtain a sufficiently large top quark mass without distorting the gauge coupling of the lefthanded bottom quark or the W and Z masses themselves [22]. In the literature, this is referred to as the $Zb_l\bar{b}_l$ problem.

7.1 Origin of the $Zb_l\bar{b}_l$ problem

We have discussed in chap. 5 how chiral fermions are constructed from two bulk fermions,

$$\Psi_L = \begin{pmatrix} t_L \\ b_L \end{pmatrix} \sim (\mathbf{2}, \mathbf{1})_{1/6} \quad \text{and} \quad \Psi_R = \begin{pmatrix} t_R \\ b_R \end{pmatrix} \sim (\mathbf{1}, \mathbf{2})_{1/6}, \quad (7.1)$$

where the fields t_L , t_R , b_L and b_R are Dirac spinors of the form $(\eta, \bar{\chi})^T$. The coupling of the left handed fermions η to the Z boson is given in terms of overlap integrals by

$$g_{Zf\bar{f}} = g_5 \left(T_{3L} \langle \eta_L \eta_L A_{L3} \rangle + T_{3R} \langle \eta_R \eta_R A_{R3} \rangle + g_r X \langle (\eta_L \eta_L + \eta_R \eta_R) A_X \rangle \right). \quad (7.2)$$

For light fermions this can be approximated by

$$g_{Zf_l\bar{f}_l} \approx g_5 T_{3L} \langle \eta_{0L} \eta_{0L} A_{L3} \rangle + g_r X \langle \eta_{0L} \eta_{0L} A_X \rangle, \quad (7.3)$$

where f_{0L} , f_{0R} are the massless KK modes. The relative corrections result from L - R mixing, which can be quantified in terms of

$$\mathcal{C}_\eta := \frac{\langle \eta_R \eta_R \rangle}{\langle \eta_L \eta_L \rangle + \langle \eta_R \eta_R \rangle}. \quad (7.4)$$

For the electron we find $\mathcal{C}_\eta < 10^{-4}\%$. Thus the η_R contributions are completely negligible. For the tauon, which is the heaviest fermion next to top and bottom quarks, the corrections are with $\mathcal{C}_\eta < 0.4\%$ still moderate. However, the top is so heavy that significant corrections arise in the third quark generation. Therefore, when matching the 5D parameters to reproduce the correct couplings for light fermions, namely electrons, the couplings for the third quark generation cannot simultaneously be reproduced.

The top quark is made heavy either by localizing its KK wave function near the EWSB brane¹ or via a large Dirac mass term M_D . Both is problematic for the coupling strength. The W and Z wave functions are distorted by electroweak symmetry breaking at the EWSB brane and therefore the couplings of any field nearby are modified. In particular, the lefthanded coupling to the Z (7.3) is too small since f_{L3} decreases near the EWSB brane, c.f. fig. 4.2. Additional negative contributions come from the Dirac mass term M_D inducing L - R mixing.

Furthermore, one needs to split the bottom quark mass from the top mass by about two orders of magnitude. The symmetries of our setup require the parameters α_{LI} , α_{LII} , α_{RI} , α_{RII} , M_D and t_L to be identical within the $(t_L, b_L)^T$ doublet. Only t_R is allowed to vary, due to broken $SU(2)_R$ at the Planck brane. By choosing a large value of t_R , the normalization

$$\mathcal{Z} = \langle \eta_L \eta_L \rangle + \langle \eta_R \eta_R \rangle = \langle \chi_L \chi_L \rangle + \langle \chi_R \chi_R \rangle \quad (7.5)$$

¹This translates into choosing small values for α_{LI} , α_{RI} .

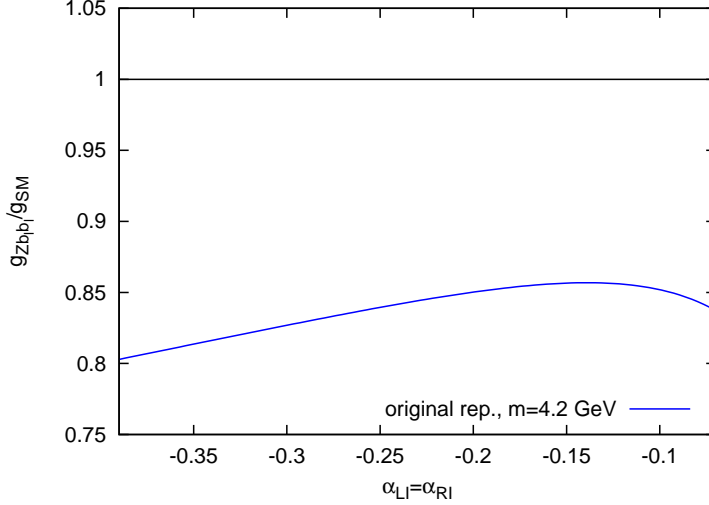


Fig. 7.1: The $Zb_l\bar{b}_l$ coupling is way too small. We have fixed $\alpha_{LII} = \alpha_{RII} = 0$ and scan through $\alpha_{LI} = \alpha_{RI}$, automatically adopting M_D and T_R to correctly reproduce top and bottom masses.

is increased. Qualitatively, the bottom mass suppression can be understood as “diluting” \mathcal{M} by enhancing \mathcal{Z} . In the original two brane setup of [2], the analogous effect is realized using a brane kinetic term ρ , which effectively increases the normalization

$$\mathcal{Z} = \langle \eta_L \eta_L \rangle + \langle \eta_R \eta_R \rangle = \langle \chi_L \chi_L \rangle + \langle \chi_R \chi_R \rangle + \rho^2 \langle \chi_R \chi_R \rangle|_{y=0}.$$

Since the mass splitting is done by increasing the relative weight of $SU(2)_R$ parts, \mathcal{C}_η is increased further. In our example setup presented in chap. 5, we find $\mathcal{C}_\eta = 1.9\%$ for the top quark but $\mathcal{C}_\eta = 8.5\%$ for the bottom. Consequently, the value of $g_{Zb_l\bar{b}_l}$ is almost 20% too small², c.f. fig. 7.1. From experiments, we know that the deviation has to be smaller than 0.25%. Note that in contrast to $Zb_l\bar{b}_l$, the $Zb_R\bar{b}_R$ coupling is not problematic: The righthanded coupling of massless fermions

$$g_{Zf_r\bar{f}_r} \approx g_5 T_{3R} \langle \chi_{0R} \chi_{0R} A_{R3} \rangle + g_r X \langle \chi_{0R} \chi_{0R} A_X \rangle \quad (7.6)$$

acquires corrections proportional to

$$\mathcal{C}_\chi := \frac{\langle \chi_L \chi_L \rangle}{\langle \chi_L \chi_L \rangle + \langle \chi_R \chi_R \rangle}. \quad (7.7)$$

When enhancing the $SU(2)_R$ contributions in order to do mass splitting, \mathcal{C}_χ will be suppressed. While for the top quark we find $\mathcal{C}_\chi = 18.9\%$, for the bottom the corrections $\mathcal{C}_\chi = 0.01\%$ are negligible.

Note that the $Zb_l\bar{b}_l$ problem goes back to the mechanism of creating fermion masses and EWSB in the interval I, thus it cannot be cured by the extension of our model to contain the new interval II.³

²In the setup of [30], the deviations are $\approx 40\%$, because the UV scale was set to 10^8 GeV only.

³One could of course implement a lefthanded bottom living predominantly in $SU(2)_L$ acquiring its mass, similar to a $SU(2)_L$ sfermion, within the second interval. But then the mass would be independent of t_R and one would have no instrument to split the top and bottom masses.

7.2 An alternative representation of custodial symmetry

A possible solution to the $Zb_l\bar{b}_l$ problem was proposed in [22]. The authors introduced an additional Randall-Sundrum throat and made the light fermions and the third generation couple separately to EWSB on two different IR branes. Note that apart from the existence of two AdS slices this has nothing in common with our extension of the higgsless model: We do not break electroweak symmetry at $z = \Lambda_{\text{I}}$. However, in the approach of [22], the top is necessarily strongly coupled to a Higgs and/or resonances localized on the new IR brane, which renders the top sector non-perturbative.

Later, in [30], the same authors adopted the idea of [31] to solve the $Zb_l\bar{b}_l$ problem based on an enlarged representation for the third generation. The idea is as follows: The BSM sector is built upon $SU(2)_c \times U(1)_X$ and two $SU(2)$ groups, which are broken with the pattern $SU(2)_L \times SU(2)_R \rightarrow SU(2)_D \times P_{LR}$. P_{LR} is the discrete parity interchanging symmetry $L \leftrightarrow R$. The crucial point is that if the fermion is a (+1) eigenstate of P_{LR} , the coupling is protected. Therefore, the bulk fields

$$\Psi_L = \begin{pmatrix} t_L & X_L \\ b_L & T_L \end{pmatrix} \sim (\mathbf{2}, \mathbf{2})_{2/3} \quad \Psi_R = \begin{pmatrix} X_R \\ T_R \\ b_R \end{pmatrix} \sim (\mathbf{1}, \mathbf{3})_{2/3} \quad t_R \sim (\mathbf{1}, \mathbf{1})_{2/3} \quad (7.8)$$

are implemented [30]. The assignment of quantum numbers to the bulk fields is displayed in tab. 7.1. Note that $X = 2/3$ instead of $1/6$ in order to reproduce the correct charges. The lefthanded b quark is embedded in a bi-doublet of $SU(2)_L \times SU(2)_R$ and carries $T_{3L} = T_{3R}$. Therefore, it is a P_{LR} eigenstate, coupling to $L+R$ instead of only to L . The coupling strength is stabilized by custodial symmetry. Note that due to $SU(2)_R \times U(1)_X \rightarrow U(1)_Y$ at the Planck brane, P_{LR} is an approximate symmetry only. We come back to this later. In the representation

bulk fields	T_{3L}	T_{3R}	X	Q
X_L	1/2	1/2		5/3
T_L	-1/2	1/2	2/3	2/3
t_L	1/2	-1/2		2/3
b_L	-1/2	-1/2		-1/3
X_R	0	1		5/3
T_R	0	0	2/3	2/3
b_R	0	-1		-1/3
t_R	0	0	2/3	2/3

Tab. 7.1: Quantum numbers of the fermionic bulk fields in the enlarged representation. The corresponding localization parameters α are given in brackets.

(7.8), two different Dirac mass terms M_1 and M_3 can be assigned to the singlet $\frac{1}{\sqrt{2}}(t_L - T_L)$ and to the triplet $(X_L, \frac{1}{\sqrt{2}}(t_L + T_L), b_L)$ at the EWSB brane:

$$\mathcal{L}_{\text{Dirac}} = e^{-4k\pi R_1} \frac{M_3}{\Lambda_{\text{I}}} \left[\frac{1}{\sqrt{2}} T_R (t_L + T_L) + b_L b_R + X_R X_L \right] + e^{-4k\pi R_1} \frac{M_1}{\Lambda_{\text{I}}} \frac{1}{\sqrt{2}} t_R (t_L - T_L) + h.c. \quad (7.9)$$

In this way, the SM bottom mass can be reproduced by a moderate M_3 , while the top mass is generated mainly via the mass term M_1 . The complete set of boundary conditions to the bulk

fields can be found in the appendix in tab. C.1. In particular, the additional fields are assigned boundary conditions of Neumann type (\ominus) at the UV brane. Therefore, no zero modes of these fields survive and the first KK modes are heavy. In fig. 7.2 to the left, the effect of the custodial

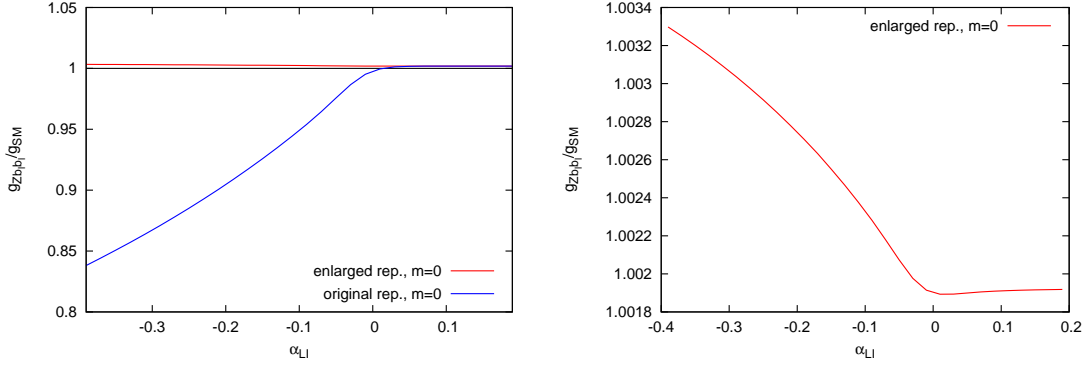


Fig. 7.2: The deviation of the $Zb_l\bar{b}_l$ coupling from the SM value, where $\alpha_{LII} = \alpha_{RII} = 0$ and $\alpha_{LI} = \alpha_{RI}$. Left: For a massless d -type quark in the original (blue) and the alternative (red) realization of custodial symmetry. Right: $Zb_l\bar{b}_l$ coupling of the massless quark in the enlarged representation. The value is in agreement with experimental bounds. However, it can be observed that it is not exactly constant, because P_{LR} is an approximate symmetry.

symmetry is shown. In the original representation the coupling of massless fermions suffers from severe corrections as soon as the fermion has significant overlap with f_{L3} near the EWSB brane. The coupling is protected in the enlarged representation by custodial symmetry. Note that the massless quark coupling in the enlarged representation is correct and therefore one could uniformly embed all quarks into the representations (7.8). This is an improvement to [30], where the Z coupling of the light quarks in the enlarged representation differed by 4-5%, which is experimentally excluded. This is just another nice effect of the brane kinetic term κ , deforming the f_{L3} KK wave function in a way that a massless test fermion does not have to be delocalized in order to reproduce a realistic value of S . Observe further in fig. 7.2 to the right that the coupling in the enlarged representation depends very slightly on the localization. This is because P_{LR} is an approximate symmetry only, as mentioned above.

Let us consider massive b quarks. Deviations to the Z coupling arise as soon as the Dirac term M_3 is switched on, because b_L mixes with the b_R from the $SU(2)_R$ triplet, coupling with $T_{3R} = -1$. The resulting coupling strength is plotted for two different fixed values of $\alpha_{LII} = \alpha_{LI} = 0$ as a function of $\alpha_{RII} = \alpha_{RI} = 0$ in fig. 7.3. For custodial symmetry to protect all the b fields, one would need to complete Ψ_R to $(\mathbf{3}, \mathbf{1})_{2/3} \oplus (\mathbf{1}, \mathbf{3})_{2/3}$. Then nothing would change with respect to $M_3 = 0$. In our case, this means that $g_{Zb_l\bar{b}_l}$ would be correct for all localizations, while in the original setup [30] an overall deviation of around 4-5% persists.

However, we see from fig. 7.3 that we do not require to further increase the field content by again enlarging the representation. For example with the parameter set:

$$\begin{array}{llll} \alpha_{LI} = \alpha_{LII} = -0.2 & \alpha_{RI} = \alpha_{RII} = 0.03 & \alpha_{RI}^* = 0 & \alpha_{RII}^* = -0.25 \\ M_1/\Lambda_1 = 0.164 & \text{and} & M_3/\Lambda_1 = 0.840 & \end{array}$$

we obtain the correct quark masses and the additional Q field in the EWSB interval is heavy $m_Q^I = 1702 \text{ GeV}$. The additional fields in the SB interval appear only at $m_Q^II = m_T^II = 7309 \text{ GeV}$.

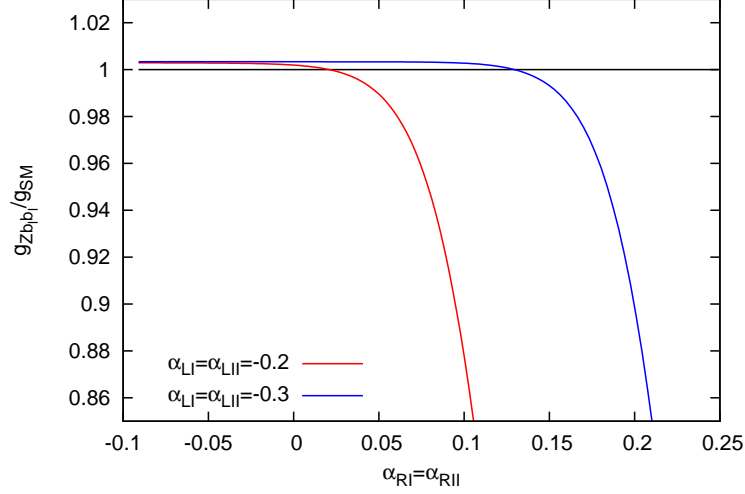


Fig. 7.3: For fixed values of $\alpha_{LI} = \alpha_{LII} = -0.2$ (red) and $\alpha_{LI} = \alpha_{LII} = -0.3$ (blue), the ratio of $g_{Zb_l\bar{b}_l}$ to g_{SM} for massive bottom quarks in the alternative representation. M_3 is adjusted to obtain $m_b = 4.2$ GeV.

The deviations of the resulting couplings from the standard model are:

$$\begin{aligned} g_{Zb_l\bar{b}_l}/g_{SM} &= 1.001 \\ g_{Zb_r\bar{b}_r}/g_{SM} &= 0.984 \end{aligned}$$

While the Z couplings of the bottom are protected by custodial symmetry, the couplings of the top are not. $Zt\bar{t}$ and $Wt\bar{b}$ turn out to have sizable deviations from the SM predictions, in our example:

$$\begin{aligned} g_{Zt_l\bar{t}_l}/g_{SM} &= 0.814 \\ g_{Zt_r\bar{t}_r}/g_{SM} &= 1.275 \\ g_{Wt_l\bar{b}_l}/g_{SM} &= 0.927 \\ g_{Wt_r\bar{b}_r}/g_{SM} &= 0.002 \end{aligned}$$

The recent bounds from single top production at Tevatron for the coupling of t, b are $|V_{tb}| > 0.71\%$ from CDF [32] and $|V_{tb}| > 0.78\%$ from DO [33], both at 95% confidence level. Our value for the lefthanded coupling $g_{Wt_l\bar{b}_l}/g_{SM} = 0.927$ would be in agreement with these bounds.

8 Dark matter

The standard model, although extremely successful in describing the presently available data, lacks explanation both for the mechanism of electroweak symmetry breaking and for the presence of dark matter in the universe. While EWSB can be done in the standard model – unsatisfactorily or not – via the Higgs mechanism, there is no explanation for dark matter. All particles known so far are excluded as dark matter candidates. Although unexplained, the existence of dark matter is experimentally well confirmed, for example by measurements of galactic rotation curves, galaxy clusters or the anisotropy in the cosmic microwave background.

The issue of dark matter is among the most important motivations for BSM physics as such. Studying the relic density in a model in question is among the first things under investigation. If or if not the parameter space allows a result compatible with experimental data is crucial for the attractiveness of the model. The current experimental value for the density of cold dark matter in the universe based on the WMAP five year data is $\Omega h^2 = 0.1099 \pm 0.0062$ [34].

Even if no dark matter particle has ever been observed directly, there are very strong clues regarding its properties. Structure formation simulations favor non-relativistic cold dark matter¹. Thus, promising candidates for dark matter are neutral, stable and weakly interacting massive particles (WIMPs). The sought-after particle has to be stable at cosmological scales. This means, if that particle is coupled to the SM sector, there must be a symmetry that prohibits decays into light SM particles. In supersymmetric theories, the symmetry in question is usually R-parity. So in supersymmetry, as long as R-parity is conserved, the lightest supersymmetric particle (LSP) is protected against decay. The LSP in most scenarios is the neutralino, a neutral spin 1/2 particles originating from the electroweak sector of the Lagrangian. The neutralino can be seen as a superposition of the fermionic superpartners of the gauge bosons². The LSP is a typical WIMP. In models with universal extra dimensions, the protecting symmetry could also be KK-parity³. However in higgsless models of EWSB, the symmetry breaking terms on the branes, the existence of branes themselves and the warp factors break translational invariance and thus KK-parity.

8.1 Calculation of the relic density

In our calculation of the relic density we follow [35, 36]. The idea to solve the relic abundance of a WIMP dark matter candidate is the following: In the early universe a particle is in thermal equilibrium with the rest of the spectrum as long as the temperature T exceeds its mass. Due to expansion the universe cools down, and not enough energy is available to produce particles with $m \gg T$. Protected by the symmetry, the WIMP cannot decay directly. So its number can be decreased only by annihilation processes. The probability of scattering decreases as the universe expands. At a certain point, the WIMPs hardly find each other to annihilate and their number density per comoving volume remains constant. One says the particle “freezes out”.

¹Would dark matter consist of light and fast particles, i.e. hot dark matter, the universe would have formed in a top-down process. This means that large structures (galaxy clusters) would have preceded the small structures (stars). It is generally accepted that the story went the other way around and structure formation happened in a hierarchical (bottom-up) way. Thus, hot dark matter can make –if any– only small contributions to the total the dark matter content.

²In models with a Higgs field, also Higgs superpartners contribute to the neutralino.

³For example, the lightest Kaluza-Klein particle (LKP) in UED models has been investigated regarding its suitability as dark matter candidate in [35].

The evolution of the number density of the particle is described by the Boltzmann equation

$$\frac{dn}{dt} + 3Hn = -\langle\sigma v\rangle (n^2 - n_{\text{eq}}^2), \quad (8.1)$$

where H is the Hubble parameter, n_{eq} the number density at thermal equilibrium and $\langle\sigma v\rangle$ the thermally averaged cross section multiplied by the relative velocity.

8.1.1 Annihilation

To solve the Boltzmann equation for a particle species \mathcal{Z}_0 , one needs to calculate the complete annihilation cross section $\sigma = \sum_i \sigma(\mathcal{Z}_0 \mathcal{Z}_0 \rightarrow \text{All})$. Then $\langle\sigma v\rangle$ is obtained by a non-relativistic expansion. The center-of-mass energy in the total cross section is replaced by $s = 4m_0^2 + m_0^2 v^2$, where m_0 is the mass of the dark matter candidate⁴. This leads to $\sigma v \approx a + bv^2 + \mathcal{O}(v^4)$. The expansion contains only orders of v^2 , because the cross section is defined as scattering probability divided by the flux. So, $\langle\sigma v\rangle$ is directly proportional to the scattering probability, and has to be Lorentz invariant. In the non-relativistic limit $\langle v^2 \rangle = 6T/m$ holds, where v is the relative velocity (or two times the CMS velocity of an individual particle). Defining $x := m/T$, the expansion reads

$$\langle\sigma v\rangle \approx a + 6\frac{T}{m}b = a + 6b/x. \quad (8.2)$$

Solving the Boltzmann equation analytically using appropriate approximations [35, 37] leads to the expression

$$\Omega h^2 = \frac{1.04 \cdot 10^9 \text{ GeV}^{-1}}{M_{\text{pl}}} \frac{x_f}{\sqrt{g_*}} \frac{1}{a + 3b/x_f}, \quad (8.3)$$

where $x_f = m/T_f$ is the ratio of the mass to the freeze out temperature T_f , h stands for the normalized expansion rate ($H_0 = 100h \text{ km s}^{-1} \text{ Mpc}^{-1}$), and g_* is the number of effective degrees of freedom in the thermal bath at freeze out.

We see from (8.3) that the relic density is roughly proportional to the inverse cross section and to x_f . The dependence on the cross section is easy to understand, because the more effective the annihilation, the less relic particles are left. The dependence on x_f , denoting the inverse freeze out temperature in units of the mass of the relic particle, can also be understood qualitatively: The lower the freeze out temperature, the longer the relic particle has been produced thermally and the less time it has had to annihilate before the the universe reached its present temperature of $2.7K$. Therefore, the number of relic particles present in the universe is proportional to the freeze out temperature T_f or inversely proportional to x_f .

By integrating the Boltzmann equation [35], the parameter $x_f = m/T_f$ is found to obey the implicit equation

$$x_f = \log \left(\frac{5}{4} \sqrt{\frac{45}{8}} \frac{g}{2\pi^3} \frac{m_0 M_{\text{pl}} (a + 6b/x_f)}{\sqrt{g_*} x_f} \right), \quad (8.4)$$

which is solved iteratively. Note that g_* has to be chosen in consistence with the result of (8.4), as it is a function of the freeze out temperature. Describing the degrees of freedom in the thermal bath, it is given by the sum of d.o.f. of all particles with $m < T_f$. Due to the Fermi-Dirac statistics, fermionic degrees of freedom will be weighted with a relative factor of

$$\int_0^\infty d\epsilon \frac{\epsilon^3}{(e^{\epsilon\beta} + 1)} / \int_0^\infty d\epsilon \frac{\epsilon^3}{(e^{\epsilon\beta} - 1)} = 7/8. \quad (8.5)$$

⁴When it comes to coannihilation processes with two particles of unequal mass this expansion reads $s = (m_i + m_j)^2 + m_i m_j v^2$.

8.1.2 Coannihilation

In the case of the relic particles not only interacting among themselves but also with particles of higher mass, one speaks of coannihilation. If the spectrum contains particles with masses not much heavier than the relic particle, these are thermally accessible as well and coannihilation processes will also affect the relic abundance. Let us assume the relic particle is denoted \mathcal{Z}_0 and has the mass $m_0 = m$. To include the effects of other particles \mathcal{Z}_i with mass m_i , one needs to calculate the total cross sections of $\sigma(\mathcal{Z}_i\mathcal{Z}_j \rightarrow \text{All})$. After all heavier modes have decayed into the relic particle, its the number density is $n = \sum_{i=0}^N n_i$. An effective cross section

$$\sigma_{\text{eff}}(x) = \sum_{i,j=0}^N \sigma_{ij} \frac{g_i g_j}{g_{\text{eff}}^2} (1 + \Delta_i)^{3/2} (1 + \Delta_j)^{3/2} e^{-x(\Delta_i + \Delta_j)}, \quad (8.6)$$

with

$$g_{\text{eff}}(x) = \sum_{i=0}^N g_i (1 + \Delta_i)^{3/2} e^{-x\Delta_i} \quad \text{and} \quad \Delta_i = \frac{m_i - m}{m} \quad (8.7)$$

is used, where g_i is the number of d.o.f. of \mathcal{Z}_i . The Boltzmann equation then is rewritten as

$$\frac{dn}{dt} + 3Hn = -\langle \sigma_{\text{eff}} v \rangle (n^2 - n_{\text{eq}}^2). \quad (8.8)$$

The freeze out temperature x_f is determined using (8.4) with the replacements $a \rightarrow a_{\text{eff}}(x)$, $b \rightarrow b_{\text{eff}}(x)$. The relic abundance finally reads:

$$\Omega h^2 = \frac{1.04 \cdot 10^9 \text{ GeV}^{-1}}{M_{\text{pl}}} \frac{x_f}{\sqrt{g_*}} \frac{1}{I_a + 3I_b/x_f} \quad (8.9a)$$

where I_a and I_b are defined as:

$$I_a = x_f \int_{x_f}^{\infty} x^{-2} a_{\text{eff}}(x) dx \quad (8.9b)$$

$$I_b = 2x_f^2 \int_{x_f}^{\infty} x^{-3} b_{\text{eff}}(x) dx \quad (8.9c)$$

Contrary to the first intuition, coannihilation processes do not necessarily decrease the relic density. Additional decay channels are available, but also the relative freeze out x_f increases.

8.2 Neutralino dark matter in our model

In our model, the lightest new physics particle and therefore the dark matter candidate is the neutralino. Still, it has to be emphasized that the neutralino is not the only and not necessarily the best dark matter candidate. Firstly, the masses of the matter superpartners are to a certain extent arbitrary and could be different from the example given in tab. 5.3 and tab. 5.4 for another parameter set. We show in the following section, that sfermion masses are unimportant for the neutralino relic density because the corresponding processes are suppressed by the coupling strength. Still, in a setup where a sneutrino acts as dark matter particle the widely unconstrained smatter spectrum should lead a certain freedom to obtain a realistic relic density. Secondly, one should keep gravitinos in mind. We have not included supergravity so far, but there are indications [38] that an answer to the dark matter problem could be found in that sector, too.

Nevertheless, we concentrate in the following on the neutralino relic density. Its setup in our extradimensional model has been carefully discussed in chap. 4 and we concluded that it can be described sensibly in terms of one parameter, namely the Majorana mass term in (4.17) set to the λ^X field.

8.2.1 Annihilation

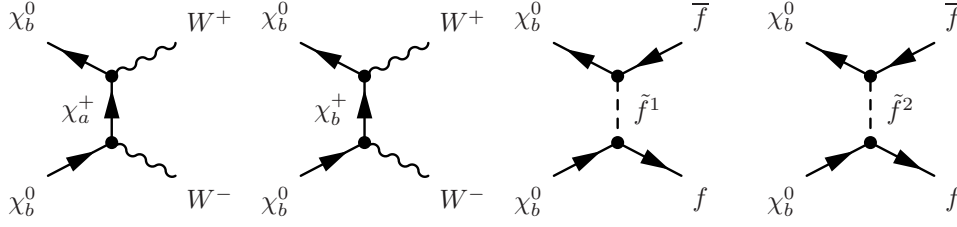


Fig. 8.1: The graphs contributing to annihilation of the light neutralino at tree level.

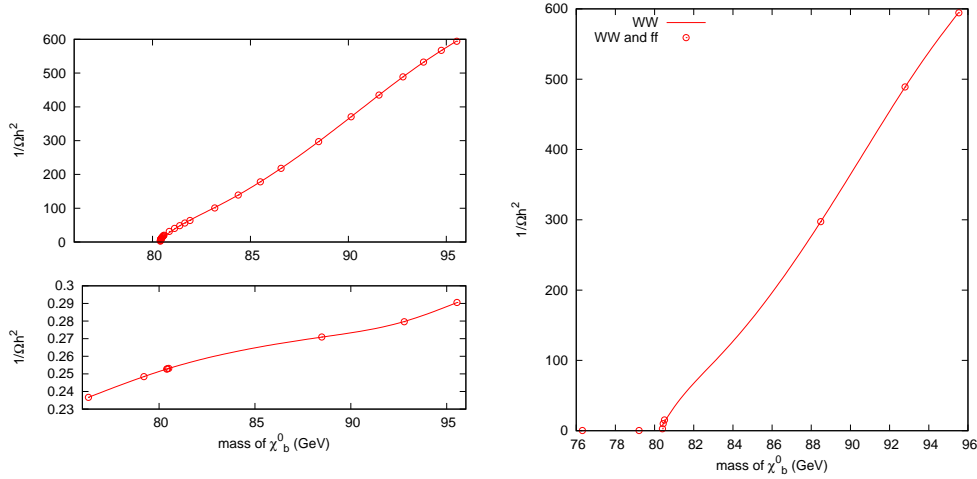


Fig. 8.2: Left: Annihilation into W^\pm (above) and fermion pairs (below). Right: Both annihilation channels combined.

The annihilation channels for the light neutralino are annihilation into W^\pm pairs via chargino exchange and into fermions via sfermion exchange. We find that the latter is suppressed and does almost not contribute. The annihilation processes are drawn in fig. 8.1.

The neutralino mass depends on the value of the Majorana mass set to the λ^X fields at the SB brane. This mass term also lifts the degeneracy between the two Majorana neutralino χ_a^0 and χ_b^0 .

Annihilation into W^\pm pairs

The coupling of the neutralino to W^\pm and chargino is given by overlap integrals. As can be seen in fig. 4.6, the strength of the coupling decreases slightly with the Majorana mass parameter. We calculated the annihilation cross section and did a phase space integration, using that the polar angle can always be expressed in terms of the Mandelstam variable t . The total cross section, depending only on the CMS energy s , was expanded in the limit of small relative velocities. Thus we obtained the coefficients a and b . The freeze out temperature was calculated iteratively using (8.4) and was found to lie in the range of $3.4 \text{ GeV} \leq T_f \leq 3.8 \text{ GeV}$.

Thus, we have:

$$\begin{aligned}
& \text{bosonic d.o.f. (weight 1):} && \left\{ \begin{array}{l} 2 \quad \text{photon} \\ 2 \times 8 \quad \text{gluon} \end{array} \right. \\
& \text{fermionic d.o.f. (weight 7/8):} && \left\{ \begin{array}{l} 3 \times 2 \quad \text{neutrino} \\ 3 \times 4 \quad \text{charged leptons} \\ 4 \times 4 \times 3 \quad \text{quarks without t and b} \end{array} \right. \\
& \implies g_* = 75 \frac{3}{4}
\end{aligned}$$

Although we said $m < T_f$ to be the criterion for whether a particle contributes to g_* or not, one should understand this as orientation rather than to take the formula literally. The bottom quark mass is not that far away from the freeze out temperature. So we did each of our calculations twice: with $g_* = 75 \frac{3}{4}$ and, including the bottom d.o.f., with $g_* = 86 \frac{1}{2}$. We find the result to be quite independent of this choice.

This was done for a range of Majorana mass parameters, giving light neutralinos masses between 80.397 GeV (W mass) and 95.874 GeV (the chargino mass in our setup). The result is plotted in fig. 8.2 to the left. We find that the cross section is too large to give a relic density compatible with experimental data in most of the investigated neutralino mass range. A realistic relic density is only found when the cross section is suppressed kinematically. That means, the neutralinos in our model are an explanation for dark matter only if their mass is close to the mass the W bosons into which they decay.

Annihilation into fermion pairs

The second annihilation channel is found to give negligible contributions. It is not obvious from the start why this observation, which was already made in [1], remains true in our case. This is because the exchanged sfermions are much lighter than in the two brane model. There, the sfermions have masses $m_{\tilde{f}} \geq 1200$ GeV [15], while in our setup $m_{\text{sf}} \geq 200$ GeV. However, the suppression due to small neutralino-fermion-sfermion couplings is so strong that also with lighter sfermions the contributions from the last two graphs in fig. 8.1 are negligible compared to the contributions from the first two graphs.

We find that the largest contribution comes from the decay into bottom quarks. This fits into the general picture of the third quark generation being special [22]. But even if all leptons and quarks gave contributions as if they were bottom replica, the annihilation cross section into fermion pairs would still be really small and would not change the resulting relic density. On the other hand, we know from the difficulties when establishing an example of a reasonable parameter set in chap. 5, how closely these are related. So even if our choice of parameters ($\alpha_{L\text{I}}, \alpha_{L\text{II}}, \alpha_{R\text{I}}, \alpha_{R\text{II}}, t_L$ and t_R) is not unique, we do not expect drastic deviations, because that would most certainly spoil the mass spectra completely. With that reasoning we feel save to state that our result is general.

The inverse relic density of the annihilation channels into W and fermion pairs combined is showed in fig. 8.2. Fermionic contributions being so small and the matter couplings being rather laborious to calculate for the sheer number of overlap integrals, we have done the calculation of the relic density for this process only for 8 different values of the Majorana mass parameter. We also calculated two example values in the range of $m_{\chi_b^0} < m_W$, where the dominating annihilation channel is closed. While a realistic value for the inverse relic density would be $1/\Omega h^2 = 9 \dots 11$, we found $1/\Omega h^2 < 0.3$ for annihilation into fermions alone.

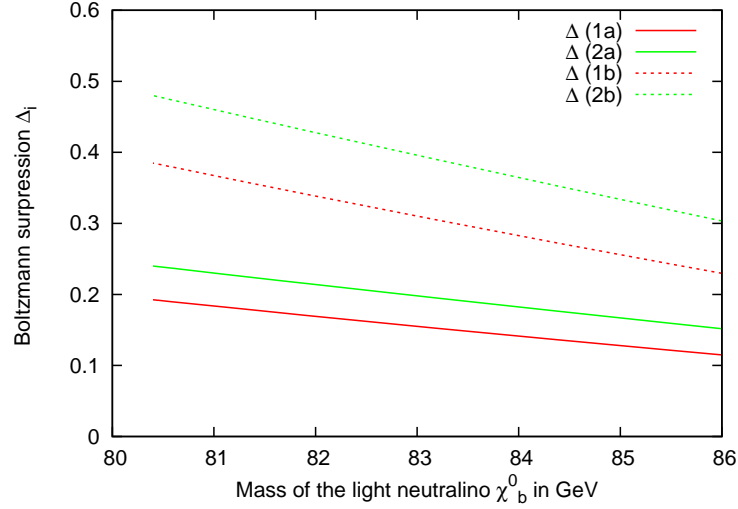


Fig. 8.3: Boltzmann suppression exponents Δ for the coannihilation processes (1a): $\chi_b^0, \chi_{a,b}^+ \rightarrow \text{All}$, (2a): $\chi_b^0, \chi_a^0 \rightarrow \text{All}$, (1b): $\chi_{a,b}^+, \chi_{a,b}^+ \rightarrow \text{All}$ and (2b): $\chi_a^0, \chi_a^0 \rightarrow \text{All}$

8.2.2 Coannihilation

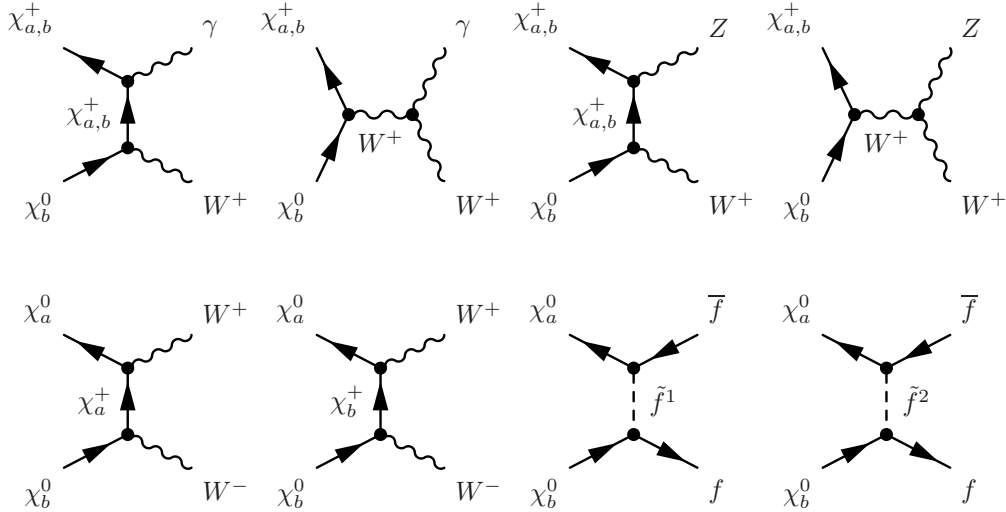


Fig. 8.4: Tree level graphs of coannihilation processes with smallest (first line) and next to smallest (second line) Boltzmann suppression.

Let us discuss the contributions from coannihilation. As mentioned in sec. 8.1.2, these contributions are Boltzmann suppressed. The suppression is given by $\exp(-x\Delta_i)$, where $x = m/T \approx 20$ at freeze out and $\Delta_i = (m_i - m)/m$. m is the mass of the dark matter candidate and m_i the mass of the next heavier particles. In our case, the next heavier particles are the charginos $\chi_{a,b}^\pm$ and the heavy neutralinos χ_a^0 . We have depicted the Boltzmann suppression for coannihilation processes with these particles in fig 8.3. The coannihilation channels with the smallest Boltzmann suppression are showed in fig. 8.4. The contributions of the first coannihilation process

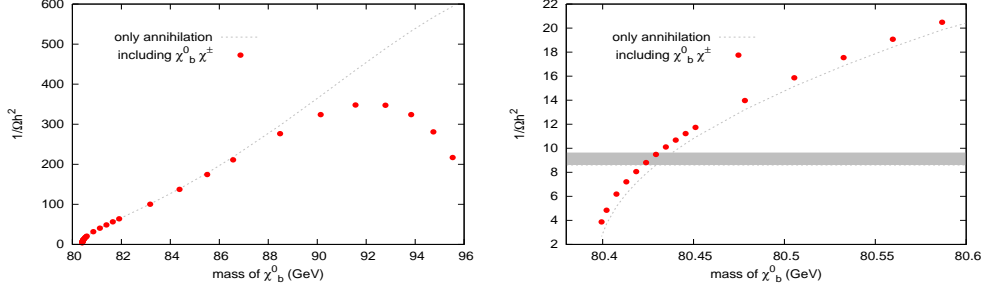


Fig. 8.5: Relic density including the coannihilation processes $\chi_b^0, \chi_{a,b}^\pm \rightarrow W^\pm, \gamma$ and $\chi_b^0, \chi_{a,b}^\pm \rightarrow W^\pm, Z$.

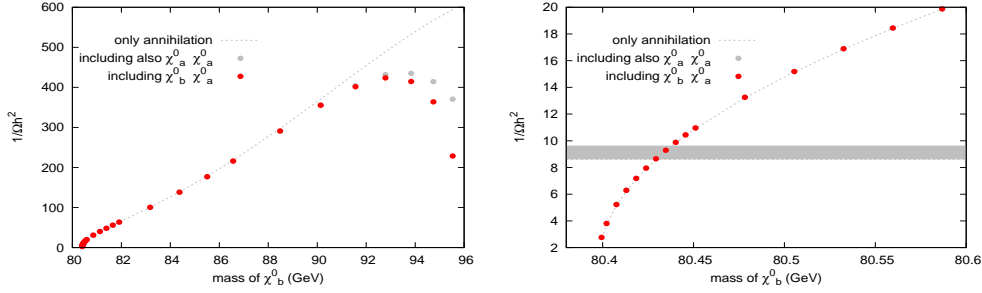


Fig. 8.6: Relic density including the coannihilation processes $\chi_a^0, \chi_b^0 \rightarrow W^+ W^-$. The result for when also the $\chi_a^0, \chi_a^0 \rightarrow W^+ W^-$ channels is included is represented by grey dots.

are showed in fig. 8.5. The contribution decreases when the mass difference between neutralino and chargino increases. In the interesting region around $m_{\chi_b^0} \gtrsim m_W$, despite the mass difference is larger than 15 GeV, we still have a correction of about 8%.

The contribution of heavy neutralino coannihilation only (without chargino coannihilation) is showed in fig. 8.6. We see this process does not appreciably contribute in the interesting mass region. This is even more the case for the doubly Boltzmann suppressed channel of to heavy neutralinos decaying into a W pair. It is not important but interesting to see in the left picture of fig. 8.6 that taking into account coannihilation can both increase and decrease the relic density as we have stated before. While coannihilation of one light and one heavy neutralino increases the relic density in the region of small mass splittings, coannihilation of two heavy neutralinos gives a contribution in the opposite direction. Both contributions become negligibly small in the region of $m_{\chi_b^0} \gtrsim m_W$.

As we found out that the processes depicted in the second line of fig. 8.4 do not change the relic density in the interesting part of the neutralino mass region, we can safely assume that higher order processes will be negligible, too.

Finally, in fig. 8.7, we show the complete result, including annihilation and chargino and heavy neutralino coannihilation. The value of the relic density is very sensitive to the mass of the light neutralino. A realistic relic density requires a neutralino slightly heavier than the W boson. The light neutralino is a realistic dark matter candidate only if its mass is $m_{\chi_b^0} = 80.426 \pm 0.004$ GeV, which translates in our setup into a localized Majorana mass parameter of $M_m = 955.7 \pm 0.3$ GeV.

In the case of taking into account the bottom quark d.o.f. as well, which is slightly heavier but than the freeze out temperature, the qualitative conclusion that the neutralino mass is heavily

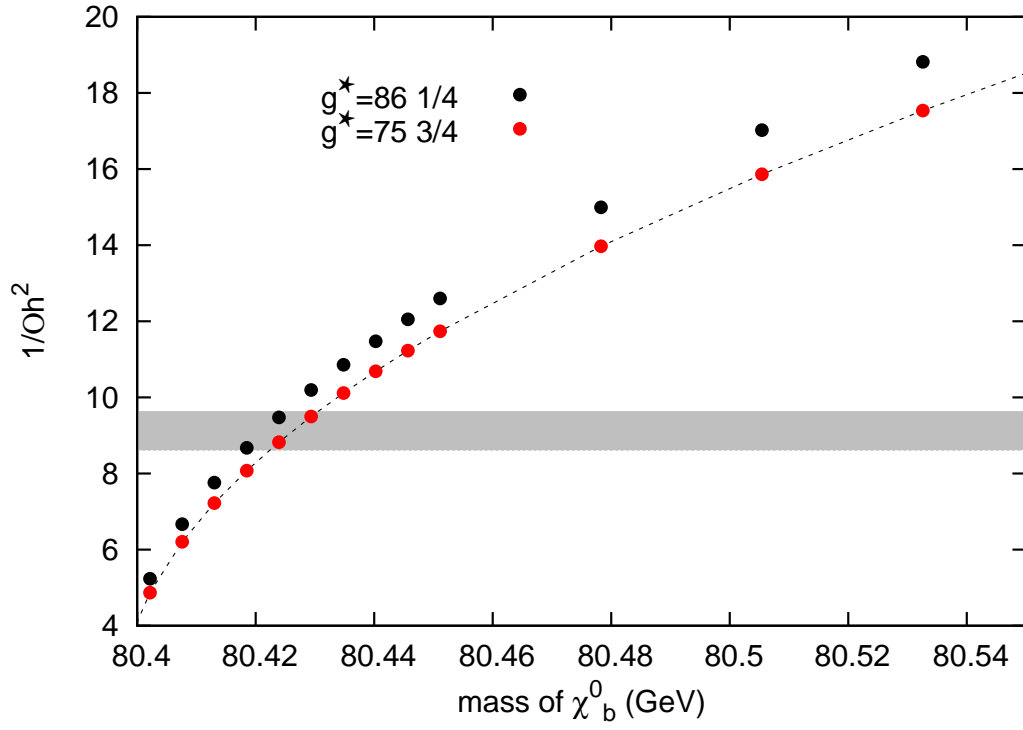


Fig. 8.7: Inverse relic density of the neutralino. The result for including the bottom d.o.f. is showed as well.

constrained remains unchanged.

9 Outlook: Collider signatures of a neutral scalar field

We want to conclude this work discussing a particularly interesting possible signal of our model at colliders.

As mentioned above in chap. 4, a neutral scalar particle Σ_0 from the gauge multiplet is present in our model. The boundary conditions on the EWSB and UV brane are the multiplet boundary conditions (3.12) and (3.14). At the SB brane, in order to avoid zero modes, we can assign either

$$\frac{\Sigma_{L_i}^{\text{H}}}{\ominus} \Big| \frac{\Sigma_{R_i}^{\text{H}}}{\ominus} \Big| \frac{\Sigma_X^{\text{H}}}{\oplus} \quad \text{or} \quad \frac{\Sigma_{L_i}^{\text{H}}}{\ominus} \Big| \frac{\Sigma_{R_i}^{\text{H}}}{\ominus} \Big| \frac{\Sigma_X^{\text{H}}}{\ominus}$$

The first choice would make Σ_0 degenerate with the neutralinos, c. f. tab. 4.1. The second choice leads to a lightest mode with a tree level mass of

$$m_{\Sigma_0}^2 = C_0 x \Lambda_1^2 \left(1 + \frac{3}{8} C_0 x\right)$$

which for $\kappa = 0.85$ corresponds to

$$m_{\Sigma_0} = 105 \text{ GeV}.$$

As there is no Higgs VEV, the Σ_0 does not couple to gauge bosons. Therefore, there is neither the vector boson fusion nor the Higgsstrahlung channel present for Σ_0 production and the LEP detection bounds for the Higgs mass do not apply. Mass corrections arise from the loop graphs

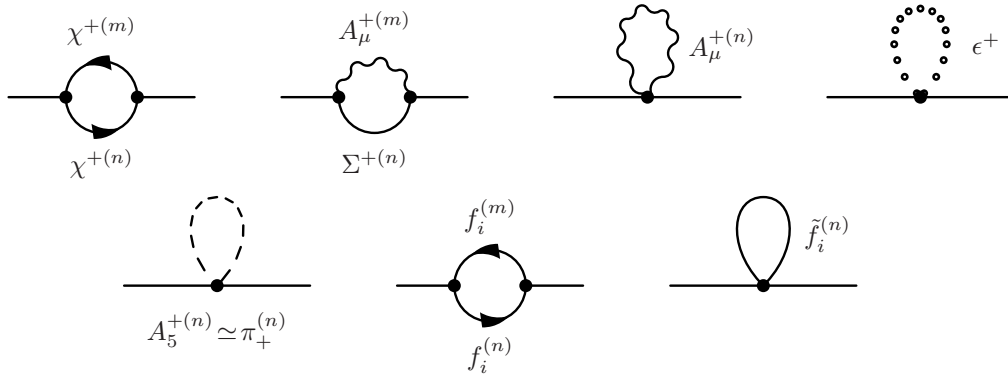


Fig. 9.1: Contributions to the self energy of the scalar Σ . Quadratic divergencies are extracted by going to $d \rightarrow 2$. Therefore contributions of the epsilon scalars, which provide the missing two vector degrees of freedom, are needed. Summation over the Kaluza-Klein indices m and n is implied.

shown in fig. 9.1, which in case of Σ_0 contain fermions, sfermions, vector bosons, a scalar A_5 and additional scalars ϵ , acting as substitutes for the missing vector degrees of freedom. In the

absence of SUSY these corrections are quadratic in Λ_c , while for unbroken SUSY they cancel with the additional superfield graphs. The procedure of renormalization in 5D SUSY is by no means trivial and beyond the scope of this work. However, we can expect corrections in the order of the mass difference of the SM fields and their supersymmetric partners. In our scheme of SUSY breaking, which is comparatively soft, the lightest supersymmetric partnerfields are of masses around 200 GeV, instead of approximately 1.5 TeV as in the setup [1] where SUSY breaking is done at the Planck brane. The spectrum of light supersymmetric modes is highly non-degenerate, c.f. 5.2, and it is difficult to estimate the size of the mass corrections. However, unlike in [1], in our setup there is the possibility, perhaps requiring an adjustment of our example sfermion spectrum, that the Σ_0 mass corrections are moderate. A Σ_0 of about 100-300 GeV would be the same mass range where the SM Higgs boson is searched.

The coupling to the fermions is determined by the interaction from the chiral part of the vector multiplet:

$$\mathcal{L}_{\Sigma f \bar{f}} = g \frac{1}{(kz)^5} (\Sigma + iA_5)^l \chi T^l \eta + h.c. \quad (9.1)$$

and the resulting Yukawa couplings are

$$y_{\text{eff}}^0 = g_5 \left(T_{3L} \langle \Sigma_0^{L3} \eta_L \chi_L \rangle + T_{3R} \langle \Sigma_0^{R3} \eta_R \chi_R \rangle + g_r X (\langle \Sigma_0^X \eta_L \chi_L \rangle + \langle \Sigma_X \eta_R \chi_R \rangle) \right) \quad (9.2)$$

It is curious that because Σ_0 couples to the combination $\eta \cdot \chi$, the coupling y_{eff}^0 depends indirectly on the mass of the fermions. For massless fermions with $f_{0\eta R} = f_{0\chi L} = 0$ the Yukawa coupling y_{eff}^0 vanishes. The couplings are listed in tab. 9.1, where we denote the top and a bottom quark in the enlarged representation with t^* and b^* . Observe that the y_{eff}^0 is roughly

Particle	y_{eff}^0	m/y_{eff}^0
u	$9.58 \cdot 10^{-6}$	241 GeV
d	$2.21 \cdot 10^{-5}$	241 GeV
c	$5.24 \cdot 10^{-3}$	242 GeV
s	$4.45 \cdot 10^{-4}$	243 GeV
t^*	0.61	281 GeV
b^*	$1.67 \cdot 10^{-2}$	251 GeV
t	0.53	326 GeV
(b)	$1.58 \cdot 10^{-2}$	265 GeV

Tab. 9.1: Yukawa couplings of the neutral Σ_0 with the quarks in our model. The bottom of in the original representation b is given in brackets, as it is in conflict with experiment due to the $Zb_l \bar{b}_l$ problem.

proportional to the mass similar to the SM Higgs Yukawa couplings y_H . The coupling strength is somewhat smaller than in the standard model where $m/y_H \sim 174.5$ GeV. Therefore, the Σ_0 could be produced similar to the SM Higgs via gluon fusion:



where the process to the right is disfavored because of the large top mass. The cross section would be the same as in the SM but suppressed by a factor $(y_\Sigma/y_H)^2$.

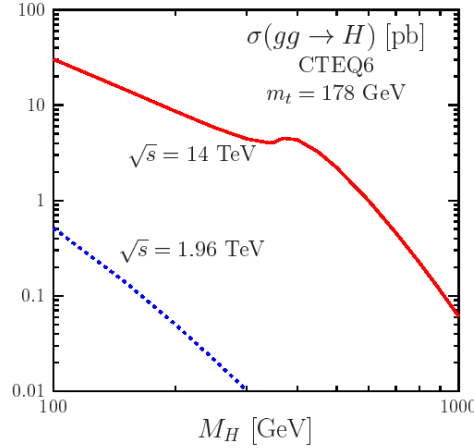


Fig. 9.2: Higgs production via gluon fusion at leading order as function of the Higgs mass M_H [39]. The authors fixed the renormalization and the factorization scale to $\mu_R = \mu_F = M_H$ and used as input: $m_t = 178$ GeV, $m_b = 4.88$ GeV, set of PDFs: CTEQ.

For the t^* the suppression factor is $1/2.6$. The top-gluon coupling does not depend on the choice of the representation and is identical to the SM coupling. The production of Σ_0 therefore can be estimated by simply scaling the SM cross section with the suppression factor. The Higgs production cross section via gluon fusion from [39] is shown in fig. 9.2. Neglecting vertex corrections, we expect for an integrated luminosity of 100 fb^{-1} about 115 events for $m_\Sigma \approx 100$ GeV and still approximately 30 events if mass corrections shift the neutral scalar to $m_\Sigma \approx 200$ GeV. The gluon fusion process suffers from high QCD corrections and uncertainties due to the gluon structure functions. Comparing with the signal significance graphic from [40] to the left in

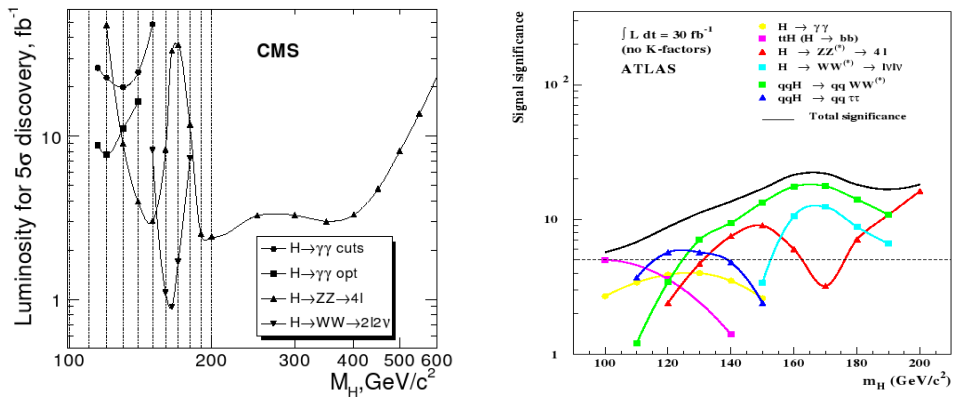


Fig. 9.3: Left: The integrated luminosity needed for the 5σ discovery of the inclusive Higgs boson production $pp \rightarrow H + X$ with the decay modes $H \rightarrow \gamma\gamma$ (gluon fusion), $H \rightarrow ZZ \rightarrow 4l$ and $H \rightarrow WW \rightarrow 2l2\nu$ [40]. Right: The signal significance of Higgs production channels at the LHC depending on the Higgs boson mass, assuming an integrated luminosity of 30 fb^{-1} [41].

fig. 9.3, an integrated luminosity of about 50 fb^{-1} will be needed for a 5σ discovery of a light Σ_0 (around $m_\Sigma \approx 130$ GeV) at the hadron collider. In the case of large mass corrections to the Σ_0 , it will be more difficult to find. In the SM vector boson fusion processes become dominant for a Higgs mass above $m_H = 150$ GeV. These channels are not present for the Σ_0 . Further

studies of allowed processes such as $\Sigma_0 \rightarrow \gamma\gamma$, $\Sigma_0 \rightarrow \tau\bar{\tau}$, $\Sigma_0 \rightarrow b\bar{b}$ and (for a very heavy Σ_0 scalar) $\Sigma_0 \rightarrow t\bar{t}$ would be required to make a prediction.

In the original representation of the third quark generation the suppression would have been with $1/3.5$ a bit stronger but of the same order. Apart from the slightly different suppression factor the same collider signature would be expected. However, the corresponding bottom quark would be in conflict with experiment due to the $Zb_l\bar{b}_l$ problem.

Conclusion

The precise mechanism of electroweak symmetry breaking is still an open question of elementary particle physics. Additional to the standard model, predicting a scalar Higgs field, there is a wide range of BSM models proposing alternative mechanisms. Models with a 5D warped background metric offer a completely new approach to EWSB. Abandoning the concept of a Higgs field, electroweak symmetry is broken by boundary conditions. The geometrical interpretation leads to new insights into parameters of the 4D theory such as masses and couplings.

In this work we have investigated a higgsless supersymmetric model, where supersymmetry breaking was systematically done on a separate IR brane. No additional fields are required. The number of model parameters is increased only by the additional fermion localization parameters α in the second AdS₅ slice. For the topics covered in this work, these parameters are of limited influence. On the other hand, we find additional restrictions on the SUSY spectrum, because the entire bulk symmetry is kept on the SUSY breaking brane.

We have implemented a realistic gauge and matter sector. Special attention was paid to the assignment of boundary conditions and a qualitative understanding of the mechanisms creating particle masses. We also have elaborated approximate analytical expressions. As first validity check for our model, we have investigated the electroweak precision observables S and T . It turned out that a brane kinetic term κ , originally introduced to split the masses within of the supersymmetric gauge spectrum, has a positive influence in that context. In particular, this term leads to a realistic S parameter without the need to delocalize the massless fermions towards the EWSB brane. We showed that realistic values of S and T are obtained for an appropriate choice of model parameters. Furthermore, we examined the $Zb_l\bar{b}_l$ problem. This problem arises as a consequence of the generic mechanism for fermion masses and has been addressed e.g. in [22, 30]. It can be solved extending the representation for the third quark generation in a way that the coupling is protected by custodial symmetry [31]. We find that in our setup this mechanism is to some extent more attractive than in [30], because in principle it could also be applied to the light quarks.

We also have investigated the neutralino as dark matter candidate. We find that the neutralino relic density is extremely sensitive to the neutralino mass and a realistic value requires $m_{\chi_0^0} = 80.426 \pm 0.004$ which translates in our setup into a localized Majorana mass parameter of $M_m = 955.7 \pm 0.3$. This is at one hand rather unattractive in comparison to [1], where a realistic neutralino relic density emerged for a wide neutralino mass range. On the other hand, it is a definite prediction which is easy to verify or contradict. Generally, one has to keep in mind that there are further potential dark matter particles, such as sneutralinos or gravitinos.

To conclude and as possible outlook, we discuss an interesting feature of the supersymmetric model namely the presence of a light scalar field Σ_0 . Since thousands of physicists are searching for the Higgs particle, the presence of a different light scalar field would be particularly interesting. The Higgs field and the scalar Σ_0 field in our model could experimentally be distinguished, for example by the absence of vector boson fusion and Higgsstrahlung processes.

A Notation, conventions and abbreviations

A.1 Notations and conventions

In this work the Minkowski metric in the “mostly -” convention is used where

$$\eta^{MN} = \text{diag}(+, -, -, -, -).$$

We use two coordinate systems, the proper distance coordinates and the conformal coordinates. A spacetime point in proper distance coordinates is specified by:

$$x^M = (x^\mu, y) \quad \text{with} \quad y \in [0, \pi] \quad (\text{A.1})$$

In conformal coordinates the notation is:

$$x^M = (x^\mu, z) \quad \text{with} \quad z \in \left[\frac{1}{k}, \frac{1}{\Lambda_{\text{IR}}} \right] \quad (\text{A.2})$$

Conformal coordinates have the advantage that the spacetime curvature is encoded in an overall factor. Thus, instead of $\mu, \nu = 0, 1, 2, 3$ and an explicit fifth component, one can use indices $M, N = 0, 1, 2, 3, 5$. The relation between the two coordinates is given through

$$z = \frac{e^{Rky}}{k} \quad \text{and} \quad \Lambda_{\text{IR}} = \frac{k}{e^{Rk\pi}}. \quad (\text{A.3})$$

The Randall-Sundrum metric in proper distance coordinates reads

$$g_{MN} = \begin{pmatrix} e^{-2Rky} & 0 & 0 & 0 & 0 \\ 0 & -e^{-2Rky} & 0 & 0 & 0 \\ 0 & 0 & -e^{-2Rky} & 0 & 0 \\ 0 & 0 & 0 & -e^{-2Rky} & 0 \\ 0 & 0 & 0 & 0 & -R^2 \end{pmatrix} \quad (\text{A.4})$$

or respectively

$$g_{MN} = \frac{1}{(kz)^2} \eta^{MN} \quad (\text{A.5})$$

in conformal coordinates.

Flat and curved ones vectors are connected by fünfbeins

$$V^\mu = e_a^{\mu,5} V^a,$$

where a, b explicitly refer to flat objects. The fünfbeins in proper distance coordinates are

$$e_\mu^a = e^{-Rky} \delta_\mu^a, \quad e_5^{\bar{5}} = R. \quad (\text{A.6})$$

In conformal coordinates the fünfbeins read

$$e_M^a = \frac{1}{(kz)} \delta_M^a. \quad (\text{A.7})$$

The flat Dirac matrices are given by

$$\gamma^\mu = - \begin{pmatrix} 0 & \sigma^\mu \\ \bar{\sigma}^\mu & 0 \end{pmatrix} \quad \gamma^5 = \begin{pmatrix} i\mathbb{1} & 0 \\ 0 & -i\mathbb{1} \end{pmatrix}, \quad (\text{A.8})$$

where $\sigma^0 = \bar{\sigma}^0 = -\mathbb{1}$ and $-\bar{\sigma}^i = \sigma^i$ are the Pauli matrices, satisfying $\sigma^i \sigma^j = \delta^{ij} + i\varepsilon^{ijk} \sigma^k$. Note that the fifth Dirac matrix in (A.8) is defined by $\gamma^5 = \gamma^0 \gamma^1 \gamma^2 \gamma^3$ in order to satisfy $\{\gamma^5, \gamma^5\} = \eta^{55} = -1$.

This is different to the usual definition [28] where an additional factor i appears: $\gamma^5 = i\gamma^0 \gamma^1 \gamma^2 \gamma^3$. The projectors, expressed in terms of γ^5 as defined in (A.8), then read:

$$P^+ = \frac{1}{2}(\mathbb{1} - i\gamma^5) \quad \text{and} \quad P^- = \frac{1}{2}(\mathbb{1} + i\gamma^5) \quad (\text{A.9})$$

For the Dirac spinors we write

$$\Psi = \begin{pmatrix} \eta_\alpha \\ \bar{\chi}^{\dot{\alpha}} \end{pmatrix} \quad \text{and} \quad \bar{\Psi} = \Psi^\dagger \gamma^0 = (\chi^\alpha, \bar{\eta}_{\dot{\alpha}}). \quad (\text{A.10})$$

The Dirac matrices in warped spacetime, denoted by a hat, read:

$$\left. \begin{aligned} \hat{\gamma}_\mu &= g_{\mu\nu} \hat{\gamma}^\nu = e^{-Rky} \gamma_\mu \\ \hat{\gamma}_5 &= -R^2 \hat{\gamma}^5 = R\gamma_5 \end{aligned} \right\} \quad \text{in proper distance coordinates} \quad (\text{A.11a})$$

$$\hat{\gamma}_M = g_{MN} \hat{\gamma}^N = \frac{1}{(kz)} \gamma_M \quad \text{in conformal coordinates} \quad (\text{A.11b})$$

Of course, in both coordinate systems the Dirac matrices satisfy the 5D Clifford algebra $\{\hat{\gamma}^M, \hat{\gamma}^N\} = 2g^{MN}$.

The model is extended to have an additional IR brane, where SUSY breaking is located. Therefore, we have two IR scales Λ_I and Λ_{II} . It is usually convenient to work in conformal coordinates. The fifth spacetime component z is:

$$z \in \left[\frac{1}{k}, \frac{1}{\Lambda_I} \right] \quad \text{or} \quad z \in \left[\frac{1}{k}, \frac{1}{\Lambda_{II}} \right]$$

in interval I in interval II

In proper distance coordinates, the size of the two extradimensional intervals is determined by

$$R_I = \frac{1}{k\pi} \ln \left(\frac{k}{\Lambda_I} \right) \quad \text{and} \quad R_{II} = \frac{1}{k\pi} \ln \left(\frac{k}{\Lambda_{II}} \right).$$

A.2 Definitions and abbreviations

The $SU(2)$ coupling constants are

$$g_5 = g_{5L} = g_{5R} \quad (\text{A.12a})$$

and the $U(1)$ coupling constant is g_{5X} . We abbreviate the ratio by

$$g_r = \frac{g_{5X}}{g_5}. \quad (\text{A.12b})$$

The expansion parameter x in the two brane setup is

$$x = \frac{1}{k\pi R}, \quad (\text{A.13a})$$

while in the three brane setup the expansions parameter x is given by

$$x = \frac{1}{k\pi(R_I + R_{II})}. \quad (\text{A.13b})$$

Further on we define the following abbreviations:

$$A_{0L} = \left(\frac{1 - (\frac{\Delta_I}{k})^{2\alpha_{LI}}}{\alpha_{LI}} + t_L^2 \frac{1 - (\frac{\Delta_{II}}{k})^{2\alpha_{LII}}}{\alpha_{LII}} \right)^{-1/2} \quad (\text{A.14a})$$

$$A_{0R} = \left(\frac{1 - (\frac{\Delta_I}{k})^{2\alpha_{RI}}}{\alpha_{RI}} + t_R^2 \frac{1 - (\frac{\Delta_{II}}{k})^{2\alpha_{RII}}}{\alpha_{RII}} \right)^{-1/2} \quad (\text{A.14b})$$

$$f_R = \frac{R_{II}}{R_I + R_{II}} \approx \frac{1}{2} \quad (\text{A.14c})$$

$$C_0 = \frac{1 + 2g_r^2}{1 + g_r^2} \quad (\text{A.14d})$$

$$C_\kappa = \frac{1 + g_r^2(2 + f_R \kappa)}{(1 + g_r^2)(1 + f_R \kappa)} \quad (\text{A.14e})$$

$$\alpha_{L_I, L_{II}} = c_{L_I, L_{II}} - \frac{1}{2} \quad (\text{A.14f})$$

$$\alpha_{R_I, R_{II}} = -c_{R_I, R_{II}} - \frac{1}{2} \quad (\text{A.14g})$$

B Fields

B.1 Overview

The fields in the supersymmetric higgsless model are elements of SUSY multiplets. The gauge multiplet consists of a vector multiplet

$$V = -\theta\sigma^\mu\bar{\theta}A_\mu - i\bar{\theta}\bar{\theta}\theta\lambda_1 + \theta\theta\bar{\theta}\bar{\lambda}_1 + \frac{1}{2}\theta\theta\bar{\theta}\bar{\theta}D, \quad (\text{B.1a})$$

and a chiral multiplet

$$\begin{aligned} \chi = & \frac{1}{\sqrt{2}}(\Sigma^a + iA_5) + \frac{i}{\sqrt{2}}\theta\sigma^\mu\bar{\theta}\partial_\mu(\Sigma + iA_5) - \frac{1}{4\sqrt{2}}\theta\theta\bar{\theta}\bar{\theta}\square(\Sigma + iA_5) \\ & + \sqrt{2}\theta\lambda_2 - \frac{i}{\sqrt{2}}\theta\theta\partial_\mu\lambda_2\sigma^\mu\bar{\theta} + \theta\theta F_\chi. \end{aligned} \quad (\text{B.1b})$$

The matter fields are part of the Hypermultiplet which contains

$$H = h + i\theta\sigma^\mu\bar{\theta}\partial_\mu h - \frac{1}{4}\theta\theta\bar{\theta}\bar{\theta}\square h + \sqrt{2}\theta\Psi - \frac{i}{\sqrt{2}}\theta\theta\partial_\mu\Psi\sigma^\mu\bar{\theta} + \theta\theta F \quad (\text{B.1c})$$

and

$$H^c = h^c + i\theta\sigma^\mu\bar{\theta}\partial_\mu h^c - \frac{1}{4}\theta\theta\bar{\theta}\bar{\theta}\square h^c + \sqrt{2}\theta\Psi^c - \frac{i}{\sqrt{2}}\theta\theta\partial_\mu\Psi^c\sigma^\mu\bar{\theta} + \theta\theta F^c. \quad (\text{B.1d})$$

D , F_χ , F and F^c are auxiliary fields which can be eliminated through their equations of motion. In order to obtain the proper units and canonical kinetic terms, we perform the following redefinitions of the fields from the SUSY multiplets

$$\begin{aligned} \psi &\longrightarrow e^{-\frac{1}{2}Rky}\psi & \psi^c &\longrightarrow e^{-\frac{1}{2}Rky}\psi^c \\ A_\mu &\longrightarrow 2gA_\mu & \lambda_1 &\longrightarrow 2ge^{-\frac{3}{2}Rky}\lambda_1 \\ A_5 &\longrightarrow 2gRA_5 & \lambda_2 &\longrightarrow -2igRe^{-\frac{1}{2}Rky}\lambda_2 & \Sigma &\longrightarrow 2gR\Sigma. \end{aligned} \quad (\text{B.2})$$

In tab. B.1, tab. B.2 and tab. B.3 the final field content after EWSB is displayed.

$SU(2)_L \times SU(2)_R \times U(1)_X$	after EWSB	name
$A_{L_1, L_2}^{(n)}, A_{R_1, R_2}^{(n)}$	$W^{\pm(n)}$	KK W -Boson
$A_{L_3}^{(n)}, A_{R_3}^{(n)}, A_X^{(n)}$	$\gamma^{(n)}, Z^{(n)}$	KK photon, KK Z -Boson
$A_{5, L_1, L_2}^{(n)}, A_{5, R_1, R_2}^{(n)}$	$A_5^{\pm(n)}$	would-be KK Goldstone
$A_{5, L_3}^{(n)}, A_{5, R_3}^{(n)}, A_{5, X}^{(n)}$	$A_5^{0(n)}$	would-be KK Goldstone
$\lambda_{L_1, L_2}^{1(n)}, \lambda_{R_1, R_2}^{1(n)}, \lambda_{L_1, L_2}^{2(n)}, \lambda_{R_1, R_2}^{2(n)}$	$\lambda^{\pm(n)}$	KK chargino
$\lambda_X^{1(n)}, \lambda_X^{2(n)}, \lambda_{L_3}^{1(n)}, \lambda_{R_3}^{1(n)}, \lambda_{L_3}^{2(n)}, \lambda_{R_3}^{2(n)}$	$\lambda_a^{0(n)}, \lambda_b^{0(n)}$	KK neutralino
$\Sigma_{L_1, L_2}^{(n)}, \Sigma_{R_1, R_2}^{(n)}$	$\Sigma^{\pm(n)}$	KK schargino
$\Sigma_{L_3}^{(n)}, \Sigma_{R_3}^{(n)}, \Sigma_X^{(n)}$	$\Sigma^{0(n)}$	KK sneutralino

Tab. B.1: The left column lists the component fields of the $SU(2)_L$, $SU(2)_R$ and $U(1)_X$ 5D gauge multiplet, where the fermionic fields are Weyl spinors. The middle column shows the particle content after the EWSB. In this notation $\lambda^{\pm(n)}$ is a Dirac spinor, while $\lambda_a^{0(n)}$ and $\lambda_b^{0(n)}$ are Majorana spinors.

$SU(3)_C$	name
$A^{a(n)}$	KK gluon
$A_5^{a(n)}$	would-be KK Goldstone
$\lambda_1^{a(n)}, \lambda_2^{a(n)}$	KK gluino
$\Sigma^{a(n)}$	KK sgluino

Tab. B.2: The left column lists the component fields of the $SU(3)_C$ 5D gauge multiplet. The fermionic fields in the left column are all Weyl spinors and the upper index denotes the $SU(3)$ gauge index. $\lambda_{(n)}^a$ is a Dirac spinor.

Ψ_L	Ψ_R	after EWSB
$\eta_L^u, \bar{\chi}_L^u$	$\eta_R^u, \bar{\chi}_R^u$	$u, c, t, \nu_e, \nu_\mu, \nu_\tau$
$\eta_L^d, \bar{\chi}_L^d$	$\eta_R^d, \bar{\chi}_R^d$	d, s, b, e, μ, τ
$h_L^u, h_L^{c u}$	$h_R^u, h_R^{c u}$	$\tilde{u}_i, \tilde{c}, \tilde{t}, \tilde{\nu}_e, \tilde{\nu}_\mu, \tilde{\nu}_\tau$
$h_L^d, h_L^{c d}$	$h_R^d, h_R^{c d}$	$\tilde{d}, \tilde{s}, \tilde{b}, \tilde{e}, \tilde{\mu}, \tilde{\tau}$

Tab. B.3: The left column lists the component fields of 5D hypermultiplet transforming under $SU(2)_L$ and $SU(2)_R$. The fermionic fields in the left column are Weyl spinors. The right column shows the particle content after EWSB. Here, we have suppressed KK indices. The quarks are represented as Dirac spinors and the neutrinos as Majorana spinors. The index i of the charged sleptons and squarks runs from 1 to 2.

The KK wave functions of the fields on the warped Randall-Sundrum background take the form

$$f(z) = (kz)^{(\text{exp})} [aJ_{(\text{order})}(mz) + bY_{(\text{order})}(mz)],$$

where we have suppressed the KK indices. In tab. B.4, we show the structure of the KK functions, abbreviated by $(kz)^{(\text{exp})}J_{(\text{order})}$, of the fields in our model before and after the redefinitions.

KK field	before redefinition	after redefinition
f_{A_μ}	$(kz)J_1$	
f_{A_5}	$(kz)^2J_0$	
f_Σ	$(kz)^2J_0$	
f_{λ_1}	$(kz)J_1$	$(kz)^{5/2}aJ_1$
f_{λ_2}	$(kz)^2J_0$	$(kz)^{5/2}J_0$
f_η	$(kz)^2J_{c+1/2}$	$(kz)^{5/2}J_{c+1/2}$
f_χ	$(kz)^2J_{c-1/2}$	$(kz)^{5/2}J_{c-1/2}$
f_h	$(kz)^2J_{c+1/2}$	
f_{h^c}	$(kz)^2J_{c-1/2}$	

Tab. B.4: Overview over the structure of KK fields before and after redefinition of the fields. Fields coupled by e.o.m. are not separated by horizontal lines.

B.2 Gauge bosons

For light modes with $m \ll \Lambda_I, \Lambda_{II}$ the bosonic KK wave functions can be approximated by:

$$f_i(z) \approx a_i + m^2 z^2 \left(b_i - \frac{a_i}{2} \log(zk) \right) + m^4 z^4 \left(-\frac{b_i}{8} - \frac{3a_i}{64} + \frac{a_i}{16} \log(zk) \right) + \mathcal{O}(m^6 z^6). \quad (\text{B.3})$$

The coefficients a_i, b_i are obtained by solving the system of coupled boundary conditions. The approximate coefficients in leading x order are listed below.

W^\pm coefficients

$$a_W \equiv a_{L^\pm}^I \quad (\text{B.4a})$$

T_{L^\pm} component:

$$\left. \begin{aligned} a_{L^\pm}^I &= 1 \\ a_{L^\pm}^{II} &= 1 \\ b_{L^\pm}^I &= \frac{1}{4} \left(-2 \frac{f_R}{x} (1 + \kappa) + 1 \right) \\ b_{L^\pm}^{II} &= \frac{1}{4} \left(+2 \frac{f_R}{x} (1 + \kappa) + 1 \right) \end{aligned} \right\} \cdot a_W + \mathcal{O}(x) \quad (\text{B.4b})$$

T_{R^\pm} component

$$\left. \begin{aligned} a_{R^\pm}^I &= 0 \\ a_{R^\pm}^{II} &= 0 \\ b_{R^\pm}^I &= \frac{1 + f_R \kappa}{2x} \\ b_{R^\pm}^{II} &= 0 \end{aligned} \right\} \cdot a_W + \mathcal{O}(x) \quad (\text{B.4c})$$

Z^0 coefficients

$$a_Z \equiv a_{L3}^I \quad (\text{B.5a})$$

 T_{3L} component

$$\left. \begin{aligned} a_{L3}^I &= 1 \\ a_{L3}^{II} &= 1 \\ b_{L3}^I &= \frac{1}{4} \left(-2 \frac{f_R}{x} (1 + \kappa) + 1 \right) \\ b_{L3}^{II} &= \frac{1}{4} \left(+2 \frac{f_R}{x} (1 + \kappa) + 1 \right) \end{aligned} \right\} \cdot a_Z + \mathcal{O}(x) \quad (\text{B.5b})$$

 T_{3R} component

$$\left. \begin{aligned} a_{R3}^I &= gr^2 \\ a_{R3}^{II} &= gr^2 \\ b_{R3}^I &= \frac{1}{4} \left(2 \frac{1 + f_R g_r^2}{x} - g_r^2 \right) \\ b_{R3}^{II} &= \frac{1}{4} g_r^2 \left(2 \frac{f_R}{x} - 1 \right) \end{aligned} \right\} \cdot -a_Z \cdot \frac{(1 + f_R \kappa)}{1 + g_r^2} + \mathcal{O}(x) \quad (\text{B.5c})$$

 $U(1)_X$ component

$$\left. \begin{aligned} a_X^I &= a_Z \\ a_X^{II} &= a_Z \\ b_X^I &= a_Z \cdot \frac{1}{4} \left(1 + 2 \frac{1 - f_R}{x} \right) \\ b_X^{II} &= a_Z \cdot \frac{1}{4} \left(1 + 2 \frac{f_R}{x} \right) \end{aligned} \right\} \cdot -\frac{gr(1 + f_R \kappa)}{1 + g_r^2} + \mathcal{O}(x) \quad (\text{B.5d})$$

C Boundary conditions

C.1 Boundary conditions for the two brane model

Gauge multiplet

The boundary conditions on the EWSB brane are

$$\begin{aligned} \begin{bmatrix} 1 & -1 \\ \partial_z & \partial_z \end{bmatrix} \begin{bmatrix} V^L \\ V^R \end{bmatrix} \Big|_{z=1/\Lambda_{\text{IR}}} &= 0 \\ \partial_z V^X \Big|_{z=1/\Lambda_{\text{IR}}} = 0, \quad \partial_z V^C \Big|_{z=1/\Lambda_{\text{IR}}} &= 0. \end{aligned} \quad (\text{C.1})$$

The corresponding twisted boundary conditions for the chiral multiplet are

$$\begin{aligned} \begin{bmatrix} \partial_z & -\partial_z \\ 1 & 1 \end{bmatrix} \left(\frac{1}{kz} \right)^2 \begin{bmatrix} \chi^L \\ \chi^R \end{bmatrix} \Big|_{z=1/\Lambda_{\text{IR}}} &= 0 \\ \chi^X \Big|_{z=1/\Lambda_{\text{IR}}} = 0, \quad \chi^C \Big|_{z=1/\Lambda_{\text{IR}}} &= 0 \end{aligned} \quad (\text{C.2})$$

The boundary conditions on the UV brane are given by

$$\begin{aligned} \begin{bmatrix} g_{5X} \partial_z & g_5 \partial_z \\ -g_5 & g_{5X} \end{bmatrix} \begin{bmatrix} V^{R_3} \\ V^X \end{bmatrix} \Big|_{z=1/k} &= 0 \\ \partial_z V^L \Big|_{z=1/k} = 0, \quad V^{R_1, R_2} \Big|_{z=1/k} = 0, \quad \partial_z V^C \Big|_{z=1/k} &= 0 \end{aligned}$$

and correspondingly for the chiral multiplet by

$$\begin{aligned} \begin{bmatrix} g_{5X} & g_5 \\ -g_5 \partial_z & g_{5X} \partial_z \end{bmatrix} \left(\frac{1}{kz} \right)^2 \begin{bmatrix} \chi^{R_3} \\ \chi^X \end{bmatrix} \Big|_{z=1/k} &= 0 \\ \chi^L \Big|_{z=1/k} = 0, \quad \partial_z \left(\frac{1}{kz} \right)^2 \chi^{R_1, R_2} \Big|_{z=1/k} = 0, \quad \chi^C \Big|_{z=1/k} &= 0. \end{aligned} \quad (\text{C.3})$$

Hypermultiplet

For the matter sector the boundary conditions on the IR brane are

$$\begin{aligned} \Psi_R - \frac{M_D}{\Lambda_1} \Psi_L \Big|_{z=1/\Lambda_{\text{IR}}} &= 0 \\ \Psi_L^c + \frac{M_D}{\Lambda_1} \Psi_R^c \Big|_{z=1/\Lambda_{\text{IR}}} &= 0. \end{aligned} \quad (\text{C.4})$$

On the UV brane the boundary conditions read:

- Quarks: The u- and d-type quarks are split introducing additional localized fermions which couple only to righthanded fermions. This term acts like a kinetic term proportional to ρ .

$$\begin{aligned} H_R - m_t \rho^2 H_R^c \Big|_{z=1/k} &= 0 \\ H_L^c \Big|_{z=1/k} &= 0 \end{aligned} \quad (\text{C.5})$$

- Leptons
Charged leptons:

$$\begin{aligned} H_R \Big|_{z=1/k} &= 0 \\ H_L^c \Big|_{z=1/k} &= 0 \end{aligned} \quad (\text{C.6})$$

Neutrinos:

$$\begin{aligned} H_R - \frac{M_M}{k} H_R^c \Big|_{z=1/\Lambda_1} &= 0 \\ H_L^c \Big|_{z=1/k} &= 0 \end{aligned} \quad (\text{C.7})$$

SUSY breaking

The SUSY breaking is done rather brutally on the UV brane. The scalars are removed from the spectrum by imposing the boundary conditions:

$$\begin{aligned} \Sigma^L(1/k) = \Sigma^R(1/k) = \Sigma^X(1/k) = \Sigma^C(1/k) &= 0 \\ h_L^i(1/k) = h_R^{c,i}(1/k) &= 0 \end{aligned} \quad (\text{C.8})$$

C.1.1 Boundary conditions for top and bottom quark in the enlarged representation

bulk field	SUSY brane $z_0 = \frac{1}{\Lambda_{\text{II}}}$	UV brane $z_0 = \frac{1}{k}$	EWSB brane (without $\mathcal{L}_{\text{Dirac}}$) $z_0 = \frac{1}{\Lambda_{\text{I}}}$	zero modes	EWSB brane (with $\mathcal{L}_{\text{Dirac}}$) $z_0 = \frac{1}{\Lambda_{\text{I}}}$
b_L	$\chi_L^{\text{II}b} _{z_0} = 0$	$\eta_L^{\text{II}b} - \eta_L^{\text{I}b} _{z_0} = 0$ $\chi_L^{\text{II}b} + \chi_L^{\text{I}b} _{z_0} = 0$	$\chi_L^{\text{I}b} _{z_0} = 0$	η_L^b	$\chi_L^{\text{I}b} + \frac{M_3}{\Lambda_{\text{I}}}\chi_R^{\text{I}b} _{z_0} = 0$
b_R	$\eta_R^{\text{II}b} _{z_0} = 0$	$\chi_R^{\text{II}b} - \chi_R^{\text{I}b} _{z_0} = 0$ $\eta_R^{\text{II}b} + \eta_R^{\text{I}b} _{z_0} = 0$	$\chi_L^{\text{I}b} _{z_0} = 0$	χ_R^b	$\eta_R^{\text{I}b} + \frac{M_3}{\Lambda_{\text{I}}}\eta_L^{\text{I}b} _{z_0} = 0$
t_L	$\chi_L^{\text{II}t} _{z_0} = 0$	$\eta_L^{\text{II}t} - \eta_L^{\text{I}t} _{z_0} = 0$ $\chi_L^{\text{II}t} + \chi_L^{\text{I}t} _{z_0} = 0$	$\chi_L^{\text{I}t} _{z_0} = 0$	η_L^t	$\chi_L^{\text{I}t} + \frac{1}{\sqrt{2}\Lambda_{\text{I}}}(M_3\chi_R^{\text{I}T} + M_1\chi_R^{\text{I}t}) _{z_0} = 0$
t_R	$\eta_R^{\text{II}t} _{z_0} = 0$	$\chi_R^{\text{II}t} - \chi_R^{\text{I}t} _{z_0} = 0$ $\eta_R^{\text{II}t} + \eta_R^{\text{I}t} _{z_0} = 0$	$\chi_L^{\text{I}t} _{z_0} = 0$	χ_R^t	$\eta_R^{\text{I}t} - \frac{M_1}{\sqrt{2}\Lambda_{\text{I}}}(\eta_L^{\text{I}t} - \eta_L^{\text{I}T}) _{z_0} = 0$
T_L	$\chi_L^{\text{II}T} _{z_0} = 0$	$\eta_L^{\text{II}T} _{z_0} = 0$ $\eta_L^{\text{I}T} _{z_0} = 0$	$\chi_L^{\text{I}T} _{z_0} = 0$	—	$\chi_L^{\text{I}T} + \frac{1}{\sqrt{2}\Lambda_{\text{I}}}(M_1\chi_R^{\text{I}t} - M_3\chi_R^{\text{I}T}) _{z_0} = 0$
T_R	$\eta_R^{\text{II}T} _{z_0} = 0$	$\chi_R^{\text{II}T} _{z_0} = 0$ $\chi_R^{\text{I}T} _{z_0} = 0$	$\chi_L^{\text{I}T} _{z_0} = 0$	—	$\eta_R^{\text{I}T} - \frac{M_3}{\sqrt{2}\Lambda_{\text{I}}}(\eta_L^{\text{I}t} + \eta_L^{\text{I}T}) _{z_0} = 0$
X_L	$\chi_L^{\text{II}X} _{z_0} = 0$	$\eta_L^{\text{II}X} _{z_0} = 0$ $\eta_L^{\text{I}X} _{z_0} = 0$	$\chi_L^{\text{I}T} _{z_0} = 0$	—	—
X_R	$\eta_R^{\text{II}X} _{z_0} = 0$	$\chi_R^{\text{II}X} _{z_0} = 0$ $\chi_R^{\text{I}X} _{z_0} = 0$	$\chi_L^{\text{I}X} _{z_0} = 0$	—	—

Tab. C.1: Boundary conditions in the enlarged representation. We choose continuous transition at the UV brane for $b_{L,R}$ and $t_{L,R}$. $X_{L,R}$ and $T_{L,R}$ receive $\ominus\ominus$ conditions at the Planck brane. Therefore, $X_{L,R}^{\text{II}}$ and $T_{L,R}^{\text{II}}$ in the SUSY interval decouple.

Bibliography

- [1] Alexander Knochel and Thorsten Ohl. Supersymmetric Extensions and Dark Matter in Models of Warped Higgsless EWSB. *Phys. Rev.*, D78:045016, 2008.
- [2] Csaba Csaki, Christophe Grojean, Luigi Pilo, and John Terning. Towards a realistic model of Higgsless electroweak symmetry breaking. *Phys. Rev. Lett.*, 92:101802, 2004.
- [3] Nima Arkani-Hamed, Savas Dimopoulos, and G. R. Dvali. The hierarchy problem and new dimensions at a millimeter. *Phys. Lett.*, B429:263–272, 1998.
- [4] Lisa Randall and Raman Sundrum. A large mass hierarchy from a small extra dimension. *Phys. Rev. Lett.*, 83:3370–3373, 1999.
- [5] N. Arkani-Hamed, A. G. Cohen, E. Katz, and A. E. Nelson. The littlest Higgs. *JHEP*, 07:034, 2002.
- [6] Roni Harnik, Graham D. Kribs, Daniel T. Larson, and Hitoshi Murayama. The minimal supersymmetric fat Higgs model. *Phys. Rev.*, D70:015002, 2004.
- [7] Markus A. Luty, John Terning, and Aaron K. Grant. Electroweak symmetry breaking by strong supersymmetric dynamics at the TeV scale. *Phys. Rev.*, D63:075001, 2001.
- [8] Rudolf Haag, Jan T. Lopuszanski, and Martin Sohnius. All Possible Generators of Supersymmetries of the s Matrix. *Nucl. Phys.*, B88:257, 1975.
- [9] Steven Weinberg. Implications of Dynamical Symmetry Breaking. *Phys. Rev.*, D13:974–996, 1976.
- [10] Savas Dimopoulos and John R. Ellis. Challenges for Extended Technicolor Theories. *Nucl. Phys.*, B182:505–528, 1982.
- [11] Csaba Csaki, Christophe Grojean, Hitoshi Murayama, Luigi Pilo, and John Terning. Gauge theories on an interval: Unitarity without a Higgs. *Phys. Rev.*, D69:055006, 2004.
- [12] Laslo Alexander Reichert. Signals of a Warped SUSY Higgsless Model at the LHC. Master’s thesis, Julius-Maximilians-Universität, Würzburg, Germany, June 2008.
- [13] Theodor Kaluza. On the Problem of Unity in Physics. *Sitzungsber. Preuss. Akad. Wiss. Berlin (Math. Phys.)*, 1921:966–972, 1921.
- [14] O. Klein. Quantum theory and five-dimensional theory of relativity. *Z. Phys.*, 37:895–906, 1926.
- [15] Alexander Karl Knochel. *Supersymmetry in a Sector of Higgsless Electroweak Symmetry Breaking*. PhD thesis, Julius-Maximilians-Universität, Würzburg, Germany, January 2009.
- [16] Juan Martin Maldacena. The large N limit of superconformal field theories and supergravity. *Adv. Theor. Math. Phys.*, 2:231–252, 1998.
- [17] J. Wess and J. Bagger. *Supersymmetry and supergravity*. Princeton University Press, 1992.

- [18] Nima Arkani-Hamed, Thomas Gregoire, and Jay G. Wacker. Higher dimensional supersymmetry in 4D superspace. *JHEP*, 03:055, 2002.
- [19] Lawrence J. Hall, Yasunori Nomura, Takemichi Okui, and Steven J. Oliver. Explicit supersymmetry breaking on boundaries of warped extra dimensions. *Nucl. Phys.*, B677:87–114, 2004.
- [20] Benjamin W. Lee, C. Quigg, and H. B. Thacker. Weak Interactions at Very High-Energies: The Role of the Higgs Boson Mass. *Phys. Rev.*, D16:1519, 1977.
- [21] Savas Dimopoulos, Shamit Kachru, Nemanja Kaloper, Albion E. Lawrence, and Eva Silverstein. Small numbers from tunneling between brane throats. *Phys. Rev.*, D64:121702, 2001.
- [22] Giacomo Cacciapaglia, Csaba Csaki, Christophe Grojean, Matthew Reece, and John Terning. Top and bottom: A brane of their own. *Phys. Rev.*, D72:095018, 2005.
- [23] C. Amsler et al. Review of particle physics. *Phys. Lett.*, B667:1, 2008.
- [24] Giacomo Cacciapaglia, Csaba Csáki, Christophe Grojean, and John Terning. Oblique corrections from Higgsless models in warped space. *Phys. Rev.*, D70:075014, 2004.
- [25] Csaba Csáki, Christophe Grojean, Jay Hubisz, Yuri Shirman, and John Terning. Fermions on an interval: Quark and lepton masses without a Higgs. *Phys. Rev.*, D70:015012, 2004.
- [26] Stephan J. Huber and Qaisar Shafi. Seesaw mechanism in warped geometry. *Phys. Lett.*, B583:293–303, 2004.
- [27] Michael Edward Peskin and Tatsu Takeuchi. Estimation of oblique electroweak corrections. *Phys. Rev.*, D46:381–409, 1992.
- [28] Michael E. Peskin and Daniel V. Schoeder. *An Introduction to Quantum field theory*. Westview Press, 1995.
- [29] Giacomo Cacciapaglia, Csaba Csáki, Christophe Grojean, and John Terning. Curing the ills of Higgsless models: The S parameter and unitarity. *Phys. Rev.*, D71:035015, 2005.
- [30] Giacomo Cacciapaglia, Csaba Csáki, Guido Marandella, and John Terning. A new custodian for a realistic Higgsless model. *Phys. Rev.*, D75:015003, 2007.
- [31] Kaustubh Agashe, Roberto Contino, Leandro Da Rold, and Alex Pomarol. A custodial symmetry for Z b anti-b. *Phys. Lett.*, B641:62–66, 2006.
- [32] T. Aaltonen and others (CDF collaboration). First Observation of Electroweak Single Top Quark Production. *arXiv:0903.0885v2 [hep-ex]*, 2009.
- [33] V.M. Abazov and others (DO collaboration). Observation of Single Top Quark Production. *arXiv:0903.0850v1 [hep-ex]*, 2009.
- [34] J. Dunkley et al. Five-Year Wilkinson Microwave Anisotropy Probe (WMAP) Observations: Likelihoods and Parameters from the WMAP data. *Astrophys. J. Suppl.*, 180:306–329, 2009.
- [35] Geraldine Servant and Tim M. P. Tait. Is the lightest Kaluza-Klein particle a viable dark matter candidate? *Nucl. Phys.*, B650:391–419, 2003.
- [36] Kyoungchul Kong and Konstantin T. Matchev. Precise calculation of the relic density of Kaluza-Klein dark matter in universal extra dimensions. *JHEP*, 01:038, 2006.

- [37] Edward W. Kolb and Michael W. Turner. *The early universe*. Addison-Wesley, 1990.
- [38] Alejandro Ibarra. Gravitino Dark Matter with Broken R-parity. 2007.
- [39] Abdelhak Djouadi. The Anatomy of electro-weak symmetry breaking. I: The Higgs boson in the standard model. *Phys. Rept.*, 457:1–216, 2008.
- [40] A de Roeck, Austin Ball, Michel Della Negra, L Foà, and Achille Petrilli. *CMS physics: Technical Design Report*. Technical Design Report CMS. CERN, Geneva, 2006. revised version submitted on 2006-09-22 17:44:47.
- [41] S. Asai et al. Prospects for the search for a standard model Higgs boson in ATLAS using vector boson fusion. *Eur. Phys. J.*, C32S2:19–54, 2004.

Danksagung

An dieser Stelle möchte ich mich bei allen bedanken, die mir im vergangenen Jahr geholfen, mich motiviert und fachlich oder moralisch unterstützt haben.

In erster Linie danke ich Prof. Dr. Thorsten Ohl dafür, mich in seiner Vorlesung für Theoretische Teilchenphysik fasziniert zu haben, für seine Betreuung und für seine Geduld und die Bereitschaft, auf Diskussionen und alle Fragen einzugehen.

Herzlichen Dank auch an Alexander Knochel für wertvolle Hilfe beim Verständnis von Extradimensionen, Denkanstösse und Hinweise auf besondere Tücken des Modells.

Ein grosses Dankeschön für sorgfältiges Korrekturlesen geht an Thorsten Ohl, Alex Knochel, Thomas Schutzmeier, Ines Weidle, Stefan Saftenberger und Matthias Bräuninger. Die unermüdliche Hilfe von Alex Schenkel, der für Satzzeichen hinter Formeln und viele inhaltliche Verbesserungen verantwortlich ist, soll an dieser Stelle besonders genannt werden.

Allen am Lehrstuhl, speziell der Verfügungsbau-Fraktion und meinen Zimmerkollegen Nadine und Daniel, möchte ich für eine angenehme und anspruchsvolle Atmosphäre und viele fachliche sowie fachfremde Diskussionen danken.

Meiner Familie danke ich für die Fernbetreuung durch Pakete und Briefe und für all ihre Unterstützung in jeglicher Hinsicht. Besonderer Dank geht an alle, die mich in den nervenaufreibenden Phasen "geerdet" haben: Benni, Stefan, Vroni, und ganz besonders Ines, die zu allen Nachtzeiten für mich da war. Danke an Tom für alles.

Erklärung

Hiermit erkläre ich, dass ich die vorliegende Arbeit selbständig verfasst und keine anderen als die angegebenen Hilfsmittel verwendet habe.

Würzburg, den 16. April 2009

Karoline Köpp